INVESTIGATING CHANGES IN FOREST GROWTH AND ATMOSPHERIC CIRCULATION IN THE HIMALAYAN REGION DURING THE PAST FOUR CENTURIES

A DISSERTATION SUBMITTED TO THE FACULTY OF
THE UNIVERSITY OF MINNESOTA
BY

Udya Kuwar Thapa

IN PARTIAL FULFILLMENT OF THE REQUIERMENTS FOR THE DEGREE OF
DOCTOR OF PHILOSOPHY
IN GEOGRAPHY

Dr. Scott St. George

July 2020

Acknowledgements

It has been a great experience of learning and growing since I joined the University of Minnesota in Fall 2014. This journey would not have been possible without the support and encouragement of my supervisor, Dr. Scott St. George. First of all, I sincerely thank Dr. St. George for accepting my request to serve as my academic advisor because of which I got admission into the graduate school. Scott gave expert advice and constructive feedback throughout my doctoral program. He also provided me tremendous opportunities for trainings and collaborations around the world. Coming to Minnesota from Nepal was a big change for me, and Scott was always thoughtful about my situation. I also thank my committee members, Drs. Dan Griffin, Emi Ito and Kathy Klink for being responsive and available whenever I wanted to meet them.

Many friends and colleagues have supported me during fieldworks in the remote mountains of Nepal. I thank Sanjaya, Sachin, Dilip, Bikash and Saroj for helping me out in coring samples in difficult environment and making the fieldwork fun and memorable with their jokes. I am also thankful to the local communities who provided accommodation, assisted in finding appropriate sites and helped core trees.

I express my sincere gratitude to the administrative team of the Department of Geography, Environment and Society. Glen, Sara and Cathy always answered my questions with patience from the point I started applying for the graduate school throughout the program. Finally, I acknowledge all internal and external funding agencies for supporting my research on forest ecology and paleoclimatology of the Himalayan regions.

Dedication

I dedicate my dissertation to my parents and my family. My mother is illiterate, and she values my education the most. My father did everything he could to make sure I continued my education. To my wife Sujata, I truly appreciate your support and patience throughout my dissertation process. You gave me the most beautiful present ever by giving birth to our son, Vivaan. Coming home tired and sometimes frustrated, I forget everything when I see both of you waiting for me.

Abstract

The Himalayan regions have experienced rapid changes in climate and hydrology in the recent decades. However, because weather and hydrological stations as well as radiosonde balloons across the Himalayas are sparsely located and relatively newly launched (1970s, on average), our understanding of the region's surface and upper atmospheric processes and their effects on climate as well as natural resources including forests are limited to only past few decades. My dissertation applies the field and laboratory methods of dendrochronology and combines observed and gridded climatic and atmospheric variables research to examine the climatic and human effects on Nepal's forest growth and to investigate the dynamics of the subtropical jet (STJ) over central Asia during the past four hundred years. I combined tree-ring chronologies across Nepal to produce a nation-wide index of forest growth spanning the past four hundred years, which showed that both short-term disturbances related to climate extremes such as volcanic eruptions as well as recent atmospheric warming can exert a lasting influence on the vigor of Nepal's forests. At a smaller scale, my study also showed that human use practices have overall negative impacts on the growth of pine forests in eastern Nepal's Koshi River watershed. Winter moisture is the primary limiting factor to the growth of Koshi pines, which suggests modeling future distribution of pine forests in eastern Nepal should consider winter precipitation even though summer is the wet season. These results indicate that it is important to include the competing effects of climate and humans on tree growth to achieve sustainable forest management in Nepal. My final dissertation chapter finds that, during the past four centuries, the 'Himalayan jet' (the latitudinal position of the STJ over the Himalayas during spring) has become more variable and experienced the highest number of poleward excursions since the 1950s. During these

poleward excursions, most parts of central Asia experienced heat waves and droughts, which suggests that incorporating the latitudinal position of the jet into forecasting models may improve the accuracy of dry season weather predictions in the Himalayan regions. This four-century long tree-ring record of the Himalayan jet provides crucial datasets to validate model simulations required to detect the role of internal variability and climate change in the unique behavior of the Himalayan jet.

Table of Contents

List of Figures

List of Tables

CHAPTER 1: INTRODUCTION

1.1 Background

The Himalaya is the highest mountain range in the world that stretches nearly 3000 km from Myanmar in the east to Afghanistan in the west (Mani, 1974). Because of its steep altitudinal gradient (more than 8 km over less than 300 km north-south transect), the Himalaya has diverse climatic regimes spanning from hot and humid tropical type near the southern plains and cold and dry tundra type above 4000 m in the north (Karki et al., 2015). Climate of the Himalaya is dominated by the south Asian monsoon (SAM) during summer (Bollasina et al., 2011) and by the westerly subtropical jet (STJ, a band of high-speed winds in the upper troposphere) during non-summer months (Koteswaram, 1953; Koteswaram and Parathasarathy, 1954). About 80% of the total annual precipitation in central and eastern Himalayas comes from the Indian Ocean and is delivered by the summer SAM (Shrestha et al., 2000). During winter and spring, the STJ acts to guide the mid-tropospheric storms developed over the Mediterraneans, which deliver snow and rain to the Himalayan regions (Dimri et al., 2015). These storms contribute more than half of all total annual precipitation in the western Himalaya and a smaller fraction of annual moisture in the eastern Himalayas (Madhura et al., 2014). Snow delivered by the SAM and STJ-embedded storms contribute to the Himalayan glacial mass, which are the primary source of water to more than one billion people in south Asia and also are crucial sources for agriculture and energy production during the dry season (Mall et al., 2006; Ojha et al., 2014; Mölg et al., 2014; Biemans et al., 2019).

The diversity in topography and climate makes the Himalaya one of the global biodiversity hotspots (Mani, 1974; Myers et al., 2000). Despite making up only 0.1% of

the global land mass, the central Himalaya of Nepal hosts 3.2% and 1.1% of global flora and fauna respectively (Government of Nepal, 2014). There are more than 18 ecosystem types and 35 forest types in central Himalaya (Stainton, 1972; Government of Nepal, 2014). Forests in the mountainous region help mitigate climate change, reduce soil erosion, and stabilize slopes (Birch et al., 2014; Lamsal et al., 2018). More importantly, the montane forests in central Asia provide timber, firewood, fodder for cattle, resins, medicines and other non-timber products crucial to the livelihood of rural communities (Thoms, 2008; Sharma et al., 2018).

1.2 Statement of the problem

1.2.1 Changing climate in the Himalayas

Climate and hydrology in the Himalayan region have changed drastically over the recent decades. The average annual temperature in central Himalayas of Nepal has increased by more than 1.5 °C since the 1970s (Shrestha et al., 1999; Shrestha and Aryal, 2011). Comparable magnitudes of temperature changes have also been observed in western and eastern Himalayas (Bhutiyani et al., 2010; Bocchiola and Diolaiuti, 2013; Hoy et al., 2016). During the last century, the SAM has weakened and average monsoon precipitation in the lowland Indian sub-continent has declined (Duan et al., 2006; Bollasina et al., 2011). However, in the high mountain Asia, precipitation has become sporadic, and the region has experienced extreme dry and wet spells (Karki et al., 2017; Shrestha et al., 2017a). The frequency and strength of dry season storms have also increased during the recent decades (Madhura et al., 2014; Cannon et al., 2014). Himalayan glaciers are retreating at an alarming rate in response to elevated warming at higher altitudes (Shrestha and Aryal, 2011; Mahagaonkar et al., 2017). Over the past 15

years, the Himalaya has lost ice at the rate of 0.43 meters of water equivalent per year, doubling the rate of ice loss during 1975-2000 (Maurer et al., 2019). With rapid glacier retreat, the size and number of glacier lakes have spawned, increasing the risks of glacier lake outburst floods (Nie et al., 2017; Veh et al., 2020). The waterflow in the glacier-fed rivers has increased particularly during spring and winter seasons with increased contribution from rapid snowmelt (Gautam and Acharya, 2012). Extreme devastating floods have also become frequent recently (Dixit, 2009; Shreevastav et al., 2019).

Studies have predicted abrupt changes in climate and hydrology across the Himalaya with continued emissions of anthropogenic greenhouse gases. The average annual temperature is expected to rise by 3-4 °C across the entire Himalayan range by the end of 21st century (Kulkarni et al., 2013). Nepal's average annual temperature is expected to rise by 2.5-5 °C with the doubling of atmospheric carbon dioxide (Shrestha et al, 2016; Rajbhandari et al., 2018). Though variable, annual average precipitation is also projected to increase by 20-40% in most parts of the Himalaya (Kulkarni et al., 2013; Mishra et al., 2018; Rajbhandari et al., 2018). Both temperature and precipitation extremes are projected to intensify by 2100 (Rajbhandari et al., 2017). Glaciers are also expected to melt rapidly in the near future. For example, the Mount Everest region may lose 70-99% of its glaciers by 2100 (Shea et al., 2015). Because of the accelerated rate of glacial retreat, flood events are likely to become more common during the next 50 years (Lutz et al., 2014). Water flow in the glacier-fed rivers is projected to increase initially (Mishra et al., 2018), but is expected to decline due to shrinking glaciers by the end of this century (Akhtar et al., 2008; Gautam and Acharya, 2012; Miller et al., 2012; Immerzeel et al., 2012; Beldrin and Vokso, 2012).

Climate change has drastic implications on hydrology, agriculture, biodiversity and economy, affecting the livelihood of the Himalayan and downstream communities. Shrinking glaciers have direct negative effects on water availability as glacier melt during spring is the primary source of water for human consumption, crops and energy production during the dry season (Xu et al., 2009; Immerzeel et al., 2010; Immerzeel and Bierkens, 2012). Mountain biodiversity and ecosystems functions are also expected to be affected by future climate change (Xu et al., 2009; Shrestha and Shrestha, 2019). Warming temperature and reduced water supply will negatively affect endemic species and predator-prey dynamics, ultimately declining biodiversity in the Himalayas (Xu et al., 2009). The high-altitude trees are shifting their vertical distributional limit upwards, reducing wildlife habitat in the high Himalayan ecotones (Gaire et al., 2014; Immerzeel et al., 2010; Shrestha et al., 2014; Mainali et al., 2020). Habitat shrinking and shifts in habitat suitability and climatic niche have been predicted for several Himalayan endemic tree species under continued warming (Hamid et al., 2019; He et al., 2019). Climate change and related hazards are also likely to harm the tourism industry, which is the major source of local employment and national revenue for the Himalayan nations, particularly Bhutan and Nepal (Maddison, 2001; Nyaupane and Chhetri, 2009; KC and Thapa Parajuli, 2014).

1.2.2 Brief perspectives on climate and forest-climate interactions

Instrumental records of climate and hydrology in high Asia are limited to only the past few decades, which is too brief to gauge the trends, magnitudes and drivers of recent changes. The majority of the weather and river gauge records in the Himalayan region go back to only 1970s (Shrestha et al., 1999; Hannah et al., 2005; Bhutiyani et al., 2010;

Hoy et al, 2016). In addition, these stations are few in number and sparsely distributed in the high-altitude areas (Shrestha et al., 2000). Discontinuity in operations of weather stations, missing observations and errors due to manual recording are other challenges in accurately gauging the changes in regional climate (Hannah et al., 2005; Shrestha et al., 2000). Longer and reliable records of climate and hydrology are required to provide perspective to the recent changes and investigate the roles of natural variability and man-made climate change in the climate system, which in turn helps better anticipate future changes. The climate of the Himalayan region is also influenced by atmospheric circulations and synoptic scale storms, but because of the lack of radiosonde measurements prior to the 1940s, it is difficult to assess how these systems are being influenced by modern climate change. Because of the short history of observations, our understanding on climate change and its impacts on forest resources of the Himalayas are limited to only the past few decades. Long-term perspectives on forest-climate interactions are needed to detect the response of forests to different climatic conditions that helps better predict future distribution of forests and prepare conservation measures in the changing climate.

1.3 Dendroclimatic studies in the Himalayas

Information preserved in natural proxies including ice cores, pollens, cave deposits, lake sediments and tree rings have been used to reconstruct past climate and environmental changes across the Himalaya (Duan and Yao, 2004; Hoorn et al., 2000; Glaser and Zech, 2005, Cook et al., 2003; Joshi et al., 2017). Because of their widespread distribution and annual (and sometimes sub-annual) resolution, tree rings remain the dominant proxy used to reconstruct several aspects of climate in the Himalayan region (Bhattacharyya and

Shah, 2009, Gaire et al, 2012; Ahmed and Zafar, 2014). Tree rings in the region were first applied to measure forest health including growth rates and wood productivity in India during the early 20th century (Bhattacharyya and Shah, 2009). Dendroclimatic potential of several tree species were explored later during the 1980s in the western Himalayas of Pakistan and India (Bhattacharyya and Shah, 2009; Ahmed and Zafar, 2014). First collections in the central Himalaya were made in late 1970s under the leadership of Fritz Schweingruber (Bhattacharyya et al., 1992), but the earliest comprehensive network of tree-ring width chronologies was established by Ed Cook and Paul Krusic in the late 1990s (Cook et al., 2003). Tree-ring studies in the eastern Himalayas of India and Bhutan started much later (Shah et al., 2014; Dukpa et al., 2018). As of present, tree-ring records have been produced from hundreds of sites across the Himalayas, which are the primary source of high-resolution climatic information in the region spanning the past millennium. Tree rings have been widely applied to produce surrogate estimates of surface climate and hydrology including temperature, precipitation, drought indices and river flow across the Himalayas (Esper et al., 2002; Sano et al., 2011; Cook et al., 2013b; Thapa et al., 2015; Shah et al., 2014; Gaire et al., 2017a, Bhandari et al., 2019; Krusic et al., 2015). The Himalayan climate during winter and spring is dominated by the STJ and the embedded storms, but there remains no study to reconstruct the variability in this aspect of atmospheric circulation in central Asia. Tree rings have also been used to investigate forest-climate relationships and to assess vegetation dynamics in response to atmospheric warming (Dukpa et al., 2018; Gaire et al., 2014), but the majority of such studies have been focused at high altitude (> 3000 m) forests. Low-altitude (< 3000 m) forests, which are relatively at proximity to

communities, provide important resources for livelihood of rural populations, but there remains a knowledge gap on the effects of climate and human use on these forests.

1.4 Dissertation research

In my dissertation, I applied the field and laboratory methods of tree-ring science and combined observed and gridded climatic and atmospheric variables to examine forest-climate-human interactions and to investigate the dynamics of atmospheric circulation in the Himalayan region at different spatial scales covering the period of past four hundred years.

In my first paper published in *Progress in Physical Geography* (Thapa et al., 2017, CHAPTER 2), I evaluated the quality of tree-ring width chronologies in Nepal as climate proxies and examined climatic effects on nation-wide forest growth during the past four centuries. Because respective individual studies used different approaches in removing non-climatic age trends in tree growth to produce site chronologies, it is difficult to compare one record against the other as a climate proxy. I accessed 55 tree-ring chronologies across Nepal and evaluated their fundamental characteristics, including the quality of the common signal shared amongst all trees at a given site, the variability in strength of that signal through time and the presence of shared growth anomalies including locally absent rings. Next, I applied the same method of age-size standardization to all tree-ring records and combined them to produce a four-century-long growth index of mean radial tree growth across Nepalese forests.

Because my first dissertation chapter suggested that low-elevation pine forests growing in the dry river valleys could be used as hydroclimatic proxy, I led two field trips in summer of 2016 and 2017 and collected more than 600 tree-ring core samples

from ten different pine forests in the dry valleys of eastern Nepal to reconstruct river discharge for the Koshi River. Cross-dating one of the pine tree species, *Pinus roxburghii* from the Koshi basin was particularly challenging due to frequent presence of false ring-bands and indeterminate ring boundaries. Out of the total collections, I was able to cross-date and produce annual ring-width measurements from six sites. After conducting preliminary assessment on these measurements and river discharge data, I learned that pine trees in eastern Nepal are not sensitive to hydrological flow and therefore could not be used as predictors for the Koshi River discharge. For my second paper published in *Forest Ecology and Management* (Thapa and St. George, 2019, CHAPTER 3), I used the tree-ring width chronologies produced from these collections to determine the primary climatic variable that drives the growth of Koshi pine forests. Until my research, it was not clear what climatic variable primary controlled the growth of pine forests in eastern Nepal. Because the Koshi forests are relatively accessible to local communities and are subject to human use, I also examined the influence of human activities on pine growth during their life spans.

In my final paper (Thapa et al., submitted to *Geophysical Research Letters*; CHAPTER 4), I examined the interannual variability of the STJ in central Asia during the modern and extended time periods. I used the upper tropospheric wind speed from a reanalysis database to examine the variability in the position of the jet in the Himalayan corridor during spring (Himalayan jet, hereafter) by locating the position of the jet core as the latitude corresponding to the maximum speed. To provide a longer-term perspective to the modern behavior of the jet in central Asia, I produced a four-century long tree-ring record of the Himalayan jet using tree-ring chronologies from Pakistan, India, Nepal and

Bhutan, the regions where climate is influenced by the STJ. I also examined effects of the Himalayan jet variability on regional climate.

1.5 Conclusions

1.5.1 Major findings and conclusions

In sum, my dissertation research provides multi-century perspectives on forest-climate interactions, history of human impacts on forest health, and the dynamics of atmospheric circulation and its effect on climate in the Himalayan region where climate is rapidly changing and our understanding of climate variability and its impacts on natural resources are limited to only past few decades.

Tree-ring width network across Nepal provides a four-century long perspective on tree-growth trends across the Nepal Himalaya and allows us to evaluate how forests across Nepal have been affected by recent and past environmental changes. The nation-wide forest growth index exhibited two major events: i) prolonged suppression during 1809-1822, which coincides with the two volcanic eruptions and ii) the high-accelerated growth trends since 2000, primarily by high-elevation (> 3000 m) Himalayan fir, that is in line with faster rate of warming at higher altitudes in Nepal. These results show that short-term climatic episodes such as volcanoes and long-term warming can have prolonged effect on the vigor of forests in central Himalayas and suggest that studies should consider such extreme events to accurately model distribution of forests. Based on the synthesis of ring-width characteristics of all Nepalese records, it is apparent that ring-width chronologies from pines have stronger between-tree agreement, and pines also form locally-absent rings more commonly, suggesting Nepalese pines could serve as proxies for drought or streamflow.

My second chapter focused on climate-human-forest interactions in eastern Nepal's Koshi River watershed shows that both climate and human factors have discernible effects on the growth of pine forests across the basin. The pine chronologies spanned only 100 years on average and had relatively weak between-tree agreements indicating presence of intensive human use in these forests. Reconstruction of past disturbance events as growth releases and suppressions suggested that pine forests in eastern Nepal have been mediated by humans. The frequency of suppression events was greater than releases, suggesting human use practices have negative effects on the health of Koshi pine forests. I hope this knowledge will help stakeholders evaluate their current approaches of forest management and make better-informed future decisions for effective conservation. Because the growth of pine forests in eastern Nepal is primarily limited by moisture availability during winter, it may be important to consider winter moisture to more accurately model future growth and distribution of Koshi pine trees in the warming world.

In my final chapter, I show that the spring Himalayan subtropical jet typically strikes near the Himalayan foothills, but it also moved far poleward to pass over Kyrgyzstan and north-west China in1956, 1971, 1984 and 1999. Tree-ring reconstruction (1625-2003) of the jet demonstrated that the Himalayan jet had made poleward excursions even during the pre-modern period, but such displacements have become more frequent since the 1950s. In contrast to the observed poleward trends in global STJs, the Himalayan jet did not show any significant trend over the past four hundred years. This difference, which might be due to land-ocean distribution and orographic effects (Held et al., 2002), suggests that the Himalayan jet is unique from the global and

other regional STJs. In the years of extreme northerly positions of the jet during both modern and reconstructed time periods, the Himalayan region experienced heat waves and drought during spring lasting until summer. Weather forecasting in the Himalayan region has primarily relied on meteorological and radiosonde observations including wind, temperature, relative humidity and wind speed (Moore and Semple, 2004; Das, 2005; Joshi et al., 2017). Our results suggest that accuracy of spring weather predictions in the Himalayas can be improved by including the location of the jet into the forecasting models. That job, however, could be further challenging due to enhanced interannual variability in the mean position of the Himalayan jet since 1950. The four-century long tree-ring record will help validate model simulations in order to determine the role of internal variability and external forcings in the behavior of the Himalayan jet.

1.5.2 Future directions

Assessment of Nepal-wide tree-ring chronologies demonstrated that trees in central Himalaya have volcanic signals, but the effects of eruptions in ring widths persisted for multiple years due to multi-year needle retention and carbon storage by trees (Pallardy, 2010; Matalas, 1962). Temperature reconstructions based on ring widths elsewhere and in Nepal have displayed delayed and underestimated volcanic cooling (Cook et al., 2003; Esper et al., 2018). If the aim is to examine post-volcanic effects on surface air temperature, ring widths therefore may not be the ideal proxy to target (Esper et al., 2015). Generating new tree-ring density records, in which biological persistence is less of an issue, will help more precisely gauge the magnitude of cooling caused by eruptions in the early 1800s in the Himalayan region (St. George and Esper, 2019).

Tree species growing at timberline limits (3500-4000m) in Nepal exhibited accelerated growth since 2000. But the collections of tree-core samples from near the upper treeline sites are few and predominantly from a single species of Himalayan fir. New collections from the upper treeline limits from several species including fir, birch and pine across the Himalayan corridor is required to better map the dynamics of treeline ecotones in central Asia in response to warming. Because the apparent enhanced growth of the Himalayan fir in recent years is also, in part, sensitive to the choice of detrending approach in removing biological growth trends in ring widths, extra caution is advised in interpreting such outcomes (Klippel et al., 2020). It is also recommended to further evaluate tree-ring based vegetation dynamics with other ground or remotely sensed methods.

Dendroecological studies across the Himalaya including my dissertation research conclude that moisture availability during winter and spring is the primary factor limiting the growth of the majority of woody tree species across the Himalayas, even though summer is the wet season. Such knowledge is important to accurately predict future distribution of trees under climate change (He et al., 2019; Hamid et al., 2019), but these ring-width chronologies may not be suitable proxies to reconstruct aspects of hydroclimate including streamflow associated with summer monsoon precipitation at least in the central Himalayas. If the aim is to study the dynamics of summer precipitation or river discharge, I recommend producing measurements of water isotopes in tree rings because they reflect the isotopic signature of source water (McCarroll and Loader, 2004). From my dissertation collections in eastern Nepal, I produced oxygen isotope measurements from a few (six) pine trees to test whether oxygen isotopes could serve as

a better proxy than ring widths for hydroclimatic reconstruction. Because I generated isotope measurements from the samples that were challenging to cross-date due to frequent presence of false and indeterminate ring boundaries, I was not able to produce an accurately dated oxygen-isotope chronology. Based on this experience, I advise to target the trees growing at high-elevation (> 3000 m) sites in the Himalayan regions where difficulty in developing chronology has not been reported and isotopes measurements have summer monsoon signal (Sano et al., 2011; Sano et al., 2013).

Human interventions have discernible negative effects on the health of pine forests in eastern Nepal. Prior to my field trips to eastern Nepal's Koshi River basin, I did not have appreciation of human impacts on pine forests. Majority of the middle-mountain (1000-3000m) forests of Nepal are community managed and therefore subject to human use. Future research with appropriate characterization of the affected and unaffected trees would provide a more complete picture of human disturbances on forests. For example, collection of samples from only resin-tapped trees will help precisely quantify the effects of resin tapping on the growth of pine forests. In addition, structured survey questions to the local community forest user groups and the district forest offices would help produce quantitative information on management practices and resource exploitation specific to each site and enable researchers to better isolate human influences on tree growth.

My research also shows that the Himalayan jet exhibited increased variability since 1950, but the factors driving that change are unknown. Modelling studies are required to perform attribution and detection experiments to identify the factors responsible for the increased poleward excursions and enhanced variance of the jet (Fallah et al., 2016). The model simulations of the Himalayan jet latitudes will provide

the opportunity to explore the physical drivers of the interannual variability of the jet, as well as to determine the possible role of anthropogenic climate change and natural climate 'forcing factors' such as volcanic eruptions or changes in solar irradiance in altering those drivers (Stevenson et al., 2018).

1.6 Dissertation outline

My dissertation consists of four chapters. In CHAPTER 1, I describe the motivation for my dissertation, summarize specific research and their key findings, discuss the major conclusions and highlight the priorities for future research. In the subsequent CHAPTERS: 2, 3 and 4, I present my three dissertation papers in detail. In CHAPTER 2, I evaluated tree rings as climate proxies across Nepal and investigated climatic effects on nation-wide forest growth during the past four hundred years. CHAPTER 3 describes detection of climatic and human influences on the growth of pine forests in the dry valleys of eastern Nepal's Koshi River basin. The final CHAPTER 4 examines the variability of the Himalayan STJ and its impacts on the regional climate over the past four centuries.

CHAPTER 2: TREE GROWTH ACROSS THE NEPAL HIMALAYA DURING THE LAST FOUR CENTURIES[1]

2.1 Synopsis

The climate of Nepal has changed rapidly over the recent decades, but most instrumental records of weather and hydrology only extend back to the 1980s. Tree rings can provide a longer perspective on recent environmental changes, and since the early 2000s, a new round of field initiatives by international researchers and Nepali scientists have more than doubled the size of the country's tree-ring network. In this paper, we present a comprehensive analysis of the current tree-ring width network for Nepal and use this network to estimate changes in forest growth nation-wide during the last four centuries. Ring-width chronologies in Nepal have been developed from 11 tree species, and half of the records span at least 290 years. The Nepal tree-ring width network provides a robust estimate of annual forest growth over roughly the last four centuries, but prior to this point, our mean ring-width composite fluctuates wildly due to low sample replication. Over the last four centuries, two major events are prominent in the all-Nepal composite: (i) a prolonged and widespread growth suppression during the early 1800s; and (ii) heightened growth during the most recent decade. The early 19th century decline in tree growth coincides with two major Indonesian eruptions, which suggests that short-term disturbances related to climate extremes can exert a lasting influence on the vigor of Nepal's forests. Growth increases since AD 2000 are mainly apparent in high-elevation

[1] UK Thapa, S St. George, DK Kharal and NP Gaire (2017) Tree growth across the Nepal Himalaya during the last four centuries. *Progress in Physical Geography*, 41 (4): 478-495. https://doi.org/10.1177/0309133317714247

fir, which may be a consequence of the observed trend towards warmer temperatures, particularly during winter. This synthesis effort should be useful to establish baselines for tree-ring data in Nepal and provide a broader context to evaluate the sensitivity or behavior of this proxy in the central Himalayas.

2.2 Introduction

Nepal's climate has changed significantly over the recent decades. The Nepal Himalaya has warmed rapidly since the 1970s, with the increase in temperature being even more pronounced at higher elevations (Shrestha and Aryal, 2011; Shrestha et al., 1999; Stocker et al., 2013). Over the same interval, precipitation has become both more intense and sporadic, with the region experiencing fewer rainy days on average (Karki et al., 2017; Shrestha et al., 2000, 2017). During the past three decades, roughly a third of the country's rivers produced increased flow during spring and winter seasons, likely reflecting the enhanced contribution from snowmelt due to warming (Gautam and Acharya, 2012). But most climate observations in Nepal are available only back to the 1980s, and this brief perspective makes it more difficult to gauge both the rate and potential causes of recent changes.

To address this deficiency, several biological or geological proxies have been used to reconstruct Holocene climates in the Nepal Himalaya, including pollen (e.g. Schlutz and Zech, 2004), glacial moraines (Gayer et al., 2006; Owen, 2009), lake sediments (Fujii and Sakai, 2002), and tree rings (e.g. Cook et al., 2003; Sano et al., 2005; Thapa et al., 2015). Tree-ring data from Nepal have been used as surrogates to reconstruct seasonal temperatures at local (Sano et al., 2005; Thapa et al., 2015), regional (Cook et al., 2003; Cook and Krusic, 2008), and subcontinental to continental scales

(Cook et al., 2008, 2010, 2013a), as well as local summer drought severity (Sano et al., 2011) and spring precipitation (Gaire et al., 2017a). Dendrochronological methods have also been applied to assess treeline shifts in response to warming temperatures in central Nepal (Gaire et al., 2014, 2017) and to date archeological sites in the Mustang region (Schmidt, 1993; Schmidt et al., 1999). Cook et al. (2003) conducted a comprehensive sampling campaign in the 1990s to collect tree-ring specimens from sites across the country, but, since that time, a new round of field initiatives by international researchers (e.g. Bräuning, 2004; Liang et al., 2014) and Nepali scientists (e.g. Dawadi et al., 2013; Kharal et al., 2017; Thapa et al., 2013) have more than doubled the size of the country's tree-ring network. But because these recent studies have adopted a variety of different approaches to remove age-size trends from ring-width data and compile stand-level composites (called 'chronologies'; Fritts, 1976), it is not appropriate to combine those published series to yield a reliable estimate of past variations in tree growth across Nepal. Gaire et al. (2013) recently reviewed the history of dendrochronology in Nepal and summarized the current status of the national tree-ring network, but their summary only reported the number of collections obtained from particular tree species or geographic regions and did not include a reanalysis of the original tree-ring data.

In this paper, we present a comprehensive analysis of the current tree-ring width network for Nepal and use this network to estimate mean changes in forest growth across the country during the past four centuries. First, we summarize the development of tree-ring width collections from Nepal, and describe their distribution by tree genera, elevation, and region. Second, we evaluate the fundamental characteristics of common signal in Nepalese tree-ring chronologies, including the quality of the common signal

shared amongst all trees at a given site, the variability in strength of that signal through time and the presence of shared growth anomalies including locally absent rings. Third, after applying the same method of age-size standardization to all records, we develop a four-century-long growth index of mean tree-ring widths across Nepalese forest and report two major growth excursions during that interval. Because we apply the same pre-processing to all tree-ring width data in our network, we are better able to evaluate long-term growth trends without the conflating influence of inconsistent standardization methods. Finally, we conclude by highlighting the potential applications of dendrochronology to studies of environmental change in Nepal.

2.3 Development and structure of the Nepalese tree-ring width network

Based on our survey of the literature and public databases, we estimate the Nepalese tree-ring width network currently includes more than 80 individual records (ring-width measurements made on core samples from dozens of trees or more at a single location; Figure 1.1). The network is primarily the result of three major pulses of field collections in the late 1970s, the 1990s, and the recent decade (Figure 2.2(a)). The first collections were made by Rudolf Zuber in 1979–1980 while working under the direction of Fritz Schweingruber from the Swiss Forest Research Center in Birmensdorf. Zuber collected 13 records from central and western Nepal, with the tree-ring measurements for these samples being generated later by Amalava Bhattacharyya, Edward Cook, and Paul Krusic (Bhattacharyya et al., 1992; Cook et al., 2003). In the early 1980s, Eizi Suzuki from Japan's Kagoshima University developed three records from western Nepal (Suzuki, 1990). Following Suzuki's collections, no sampling was conducted in Nepal for the next decade until Edward Cook and Paul Krusic from Columbia University made several trips

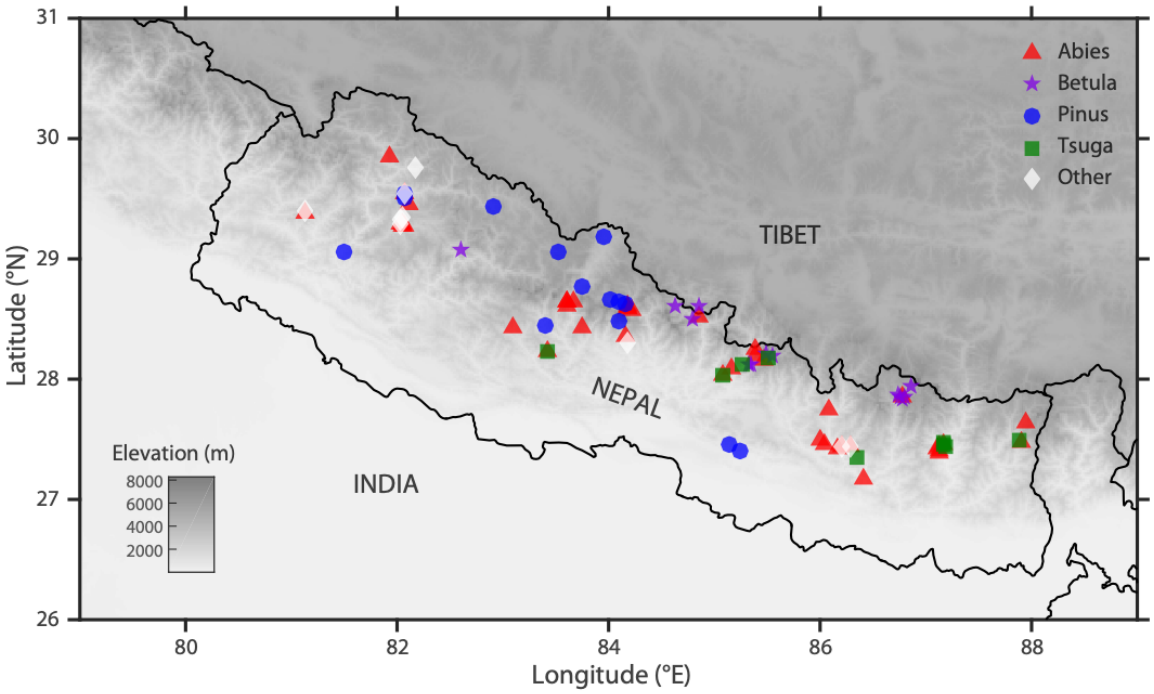

Figure 2.1 The current network of known tree-ring width data from Nepal, classified by tree genera. This compilation includes data archived at the International Tree Ring Data Bank (Zhao et al., 2019) and privately held records reported in the published literature.

over six consecutive years collecting tree-core samples during the 1990s (Cook et al., 2003). During the same period several non-Nepalese investigators, including Burghart Schmidt, Achim Bräuning, and Masaki Sano, also developed records from Nepal (Bräuning, 2004; Sano et al., 2005; Schmidt, 1993; Schmidt et al., 1999). By the end of the 20th century, roughly half of the current network was in place. Finally, due in part to the establishment of the first tree-ring laboratory in Nepal at the Nepal Academy of Science and Technology in Kathmandu, the latest round of tree-ring collections has been led by scientists of Nepalese origin, either based domestically (e.g. Gaire et al., 2013) or working abroad (e.g. Dawadi et al., 2013).

The spatial distribution of the Nepalese tree-ring width network is fairly homogenous along the country's east–west dimension (Figure 1.1). Nearly half (41) of the records are located in central Nepal between 83^0 and 86^0 E. In the central region, most collections have been made in Langtang National Park, Manaslu Conservation Area, and the Annapurna Conservation Area (Bhattacharyya et al., 1992; Cook et al., 2003; Dawadi et al., 2013; Gaire et al., 2014; Liang et al., 2014), likely due to these regions' proximity to Kathmandu and their relatively gentle topography as compared to other parts of the country. The Nepalese records span an elevation range of nearly three kilometers between 1320 m and 4150 m (Figure 2.3), with most collections having been made between 2500 and 3800 m. This elevation range matches the distribution of most of the conifer species including pine, fir, hemlock, and spruce at this elevation along east–west Nepal. A few high-elevation records have been established near the elevational limit of tree growth in Nepal (3900–4200 m) to study treeline dynamics (Gaire et al., 2014) or the climate relationships of treeline species (Liang et al., 2014). Only 10 ring-width records

Table 2.1 Length of longest ring-width chronology for each tree species within the Nepalese tree-ring network.

Species	Span (years)	Earliest year (AD)	Most recent year (AD)	Reference
Tsuga dumosa	1141	856	1996	Cook et al. (2003)
Pinus wallichaina	694	1303	1996	Cook et al. (2003)
Abies spectabilis	603	603	1997	Cook et al. (2003)
Juniperus recurva	582	1417	1998	Cook et al. (2003)
Betula utilis	458	1552	2009	Dawadi et al. (2013)
Ulmus wallichaina	432	1566	1977	Cook et al. (2003)
Picea smithiana	422	1591	2012	Thapa et al. (2015)
Abies pindrow	363	1650	2012	Thapa et al. (2013)
Pinus roxburghii	297	1683	1979	Bhattacharyya et al. (1992)
Cedrus deodara	265	1714	1978	Bhattacharyya et al. (1992)
Populus sp.	171	1824	1994	Cook et al. (2003)

have been developed at sites below 2500 m, and most of those collections have been made from *Pinus*, which is the most widely distributed conifer genus at lower elevations (Stainton, 1972). Prior dendrochronological investigations of pines, particularly *P. roxburghii* (Bhattacharyya et al., 1992; Cook et al., 2003) have reported that this genus frequently forms false rings (Fritts, 1976), which might pose another obstacle to the development of ring-width records from these particular trees. The only broadleaved tree species collected below 2500 m is *Populus ciliata*, and only one record has been established from this species.

Overall, ring-width chronologies in Nepal have been developed from nine genera and 11 tree species (Table 2.1). Nearly half of the total records were collected from *Abies spectabilis* due to its wide east–west distribution across Nepal (Stainton, 1972). Other common species include *Betula utilis, Tsuga dumosa*, and *Pinus wallichiana*. Half of the Nepalese records span at least 292 years, and there are 22 records scattered across the country that predate AD 1600 (Figure 2.2(d)). The longest Nepalese tree-ring width record, which extends back to AD 856, was built from a mid-elevation stand of *Tsuga dumosa* from eastern Nepal (Cook et al., 2003). The exceptional length of that chronology is evidence that the forests of Nepal offer at least some opportunities to construct long, millennial-length records from living trees, instead of being only restricted to long sequences pieced together from historical or subfossil wood.

2.4 Synthesis of the Nepal Himalayan tree-ring network

Following our survey of the published literature, we obtained tree-ring width measurements for 55 locations in Nepal (Table 2.2), drawing upon data from the public archive maintained by the International Tree-Ring Data Bank (ITRDB, Zhao et al., 2019),

Table 2.2 Metadata table outlining the general characteristics of tree-ring width records assembled from the public archive (International Tree Ring Data Bank; Zhao et al., 2019) and the respective investigators. Records are ordered by longitude from east to west. Unless noted by a specific citation, records were obtained from the World Data Center for Paleoclimatology (WDC-Paleo).

Site code	Species	Site name	Lat (^{0}N)	Lon (^{0}E)	Elevation (m)	Reference
nepa021	ABSB	Ghunsa	27.63	87.95	3740	WDC-Paleo
nepa027	ABSB	Lamite Bhajyung	27.48	87.9	3267	WDC-Paleo
nepa042	TSDU	Yalung khola	27.5	87.88	3033	WDC-Paleo
nepa004	TSDU	Above hatiya	27.43	87.18	2940	Cook et al. 2003
nepa012	TSDU	Budorouke	27.45	87.17	2970	Cook et al. 2003
nepa030	ABSB	Budorouke	27.45	87.17	2970	Cook et al. 2003
nepa011	TSDU	Lukuchi Khola	27.47	87.17	2880	Cook et al. 2003
nepa026	ABSB	Kauma Karka	27.38	87.13	2900	Cook et al. 2003
nepa036	ABSB	Rachel's Death	27.43	87.12	3630	Cook et al. 2003
nepa032	ABSB	Mumbuk	27.4	87.12	3200	Cook et al. 2003
nepa034	ABSB	Nehe Karka	27.42	87.1	3250	Cook et al. 2003
bhw032	BEUT	Sagarmatha	27.95	86.85	4100	Gaire et al. 2016
bhw033	ABSB	Sagarmatha	27.85	86.78	4100	Gaire et al. 2016
nepa013	ABSB	Chardung	27.17	86.42	3300	Cook et al. 2003
nepa041	TSDU	Tragdobuk	27.35	86.35	2950	Cook et al. 2003
nepa009	ABSB	Bhulepokhari	27.43	86.28	3600	Cook et al. 2003
nepa010	JURE	Bhulepokhari	27.43	86.28	3600	Cook et al. 2003
nepa018	JURE	Dobini Danda	27.43	86.2	3500	Cook et al. 2003
nepa017	ABSB	Dobini Danda	27.43	86.2	3500	Cook et al. 2003
nepa014	ABSB	Chardung Danda	27.42	86.17	3000	Cook et al. 2003
nepa002	ABSB	Kalinchowk	27.75	86.08	3720	WDC-Paleo
nepa022	ABSB	Kalinchowk	27.45	86.05	3720	Bhattacharyya et al., (1992)
nepa028	ABSB	Lamjura	27.5	86	3020	WDC-Paleo
bhw008	ABSB	Langtang NP	28.25	85.38	2729	Gaire et al., (2011)
nepa029	TSDU	Langtang	28.12	85.27	2670	Cook et al., (2003)
nepa007	PIRO	Bhaktapur	27.4	85.25	1320	WDC-Paleo
nepa033	PIRO	Nagarjun	27.45	85.15	1420	WDC-Paleo

Site code	Species	Site name	Lat (^{0}N)	Lon (^{0}E)	Elevation (m)	Reference
nepa039	ABSB	Banal-Salme	28.03	85.07	3115	Cook et al., (2003)
nepa038	TSDU	Banal-Salme	28.03	85.07	2910	Cook et al., (2003)
bhw011	ABSB	Manaslu	28.52	84.86	3690	Gaire et al., (2014)
bhw027	ABSB	Manang	28.60	84.18	3175	Kharal et al., (2016)
nepa006	PPSP	Bagarchap	28.3	84.18	2270	WDC-Paleo
bhw028	ABSB	Manang	28.60	84.17	3375	Kharal et al., (2016)
bhw029	ABSB	Manang	28.59	84.17	3575	Kharal et al., (2016)
nepa031	ABSB	Marsyangdi khola	28.35	84.15	2900	Bhattacharyya et al., (1992)
nepa008	PIWA	Bhratang	28.48	84.1	3095	Cook et al., (2003)
nepa001	ABSB	Ghorepani pass,	28.42	83.75	3220	Bhattacharyya et al., (1992)
bhw025	ABSB	Mustang, Pangu Khark	28.65	83.66	3100	Kharal et al., (2014)
bhw026	ABSB	Mustang, Lete upper	28.61	83.61	3300	Kharal et al., (2014)
bhw024	ABSB	Mustang, Titi upper	28.64	83.61	2900	Kharal et al., (2014)
bhw023	ABSB	Mustang,Titi lower	28.65	83.61	2700	Kharal et al., (2014)
nepa016	TSDU	Deorali	28.23	83.42	1830	Cook et al., (2003)
nepa015	ABSB	Deorali	28.23	83.42	1830	Cook et al., (2003)
nepa005	PIWA	Alu bari	28.45	83.4	3000	WDC-Paleo
nepa035	ABSB	Pun Hill	28.43	83.1	2950	WDC-Paleo
nepa019	ABSB	GhurchiLehk Recollection	29.28	82.07	3330	Cook et al., (2003)
nepa020	ABSB	GhurchiLehk	29.3	82.05	3450	Bhattacharyya et al., (1992)
nepa037	ABSB	Above Gheri	29.28	82.05	3450	Cook et al., (2003)
nepa037	PCSM	Rara Goan	29.35	82.05	3000	WDC-Paleo
nepa024	PCSM	KatyaKhola-3	29.3	82.02	3480	Cook et al., (2003)
nepa023	ABSB	Katyakhola-2	29.3	82.02	3330	Cook et al., (2003)
nepa025	ULWA	KatyaKhola	29.32	82.02	2760	Cook et al., (2003)
nepa040	PIRO	TilaNala	29.05	81.5	2080	Bhattacharyya et al., (1992)
bhw009	ABPI	Khaptad	29.38	81.13	3000	Thapa et al., (2013)
bhw010	PCSM	Khaptad	29.4	81.13	2700	Thapa et al., (2015)

Note: ABPI: *Abies pindrow*; ABSB: *Abie spectabilis*; BEUT: *Betula utilis*; JURE: *Juniperus recurva*; PCSM: *Picea smithiana*; PIRO: *Pinus roxburghi*; PIWA: *Pinus walichiana*; TSDU: *Tsuga dumosa* (D.Don) Eichl; ULWA: *Ulmus wallichiana*; PPCI: *Populus ciliata*

and new records produced by Nepalese scientists (Gaire et al., 2011, 2014; Kharal et al., 2017; Thapa et al., 2015). The remainder of the Nepal tree-ring width network described earlier in Section II is held privately by individual investigators, and we were not able to include those data in our analysis.

Each set of ring-width measurements was evaluated using the COFECHA software package (Holmes, 1983) to confirm cross-dating accuracy (Fritts, 1976) and to identify cases of locally absent ('missing') rings (Schulman, 1941; St. George et al., 2013). We generated site-level composites (chronologies) via the RCSigFree (courtesy of Dr Edward Cook, Columbia University), and used the signal-free standardization method (Melvin and Briffa, 2008) with age-dependent smoothing (Melvin et al., 2007) to estimate and remove long-term trends related to tree age or size from individual ring-width measurements. The signal-free method uses an iterative approach to produce detrending curves that are 'free' of growth patterns common across the entire set of ring-width measurements at a given location, and is intended to preserve more variance at medium and low frequencies relative to traditional detrending approaches (Melvin and Briffa, 2008).

2.5 Fundamental characteristics of Nepalese tree-ring width records

In this section, we summarize the fundamental characteristics of tree-ring width data from Nepal, beginning by outlining the quality of common signal inherent to individual sets of ring-width measurements. Neighboring trees exhibit similar year-to-year patterns in tree- ring widths because their growth is influenced by common external environmental forcings, which can include climate, disturbance, and competition (Cook, 1987). The clarity of that shared environmental signal is most often estimated by

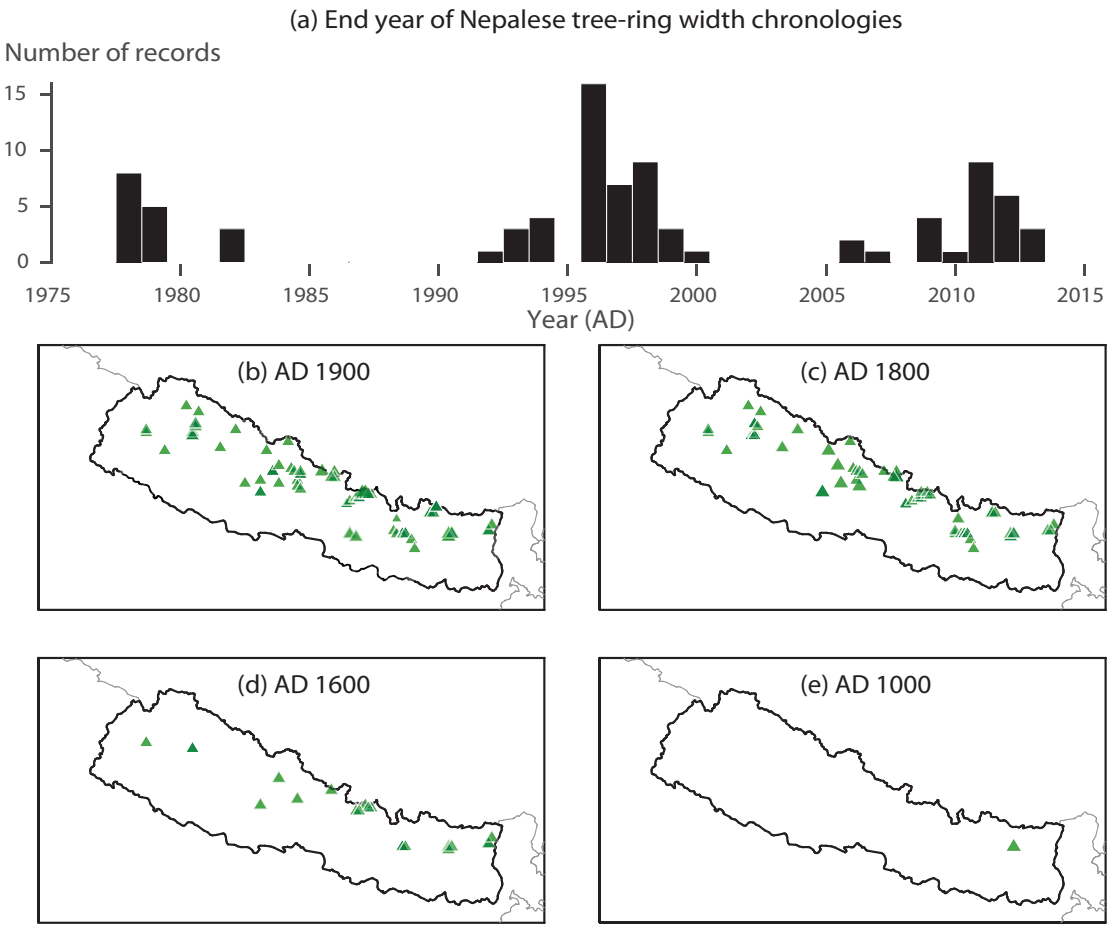

Figure 2.2 (a) Histogram showing the year of collection for tree-ring width records in Nepal, and maps showing the distribution of tree-ring records (triangles) that extend back to (b) AD 1900, (c) AD 1800, (d) AD 1600, and (e) AD 1000. These plots are based on all 86 tree-ring records established across the nation to date.

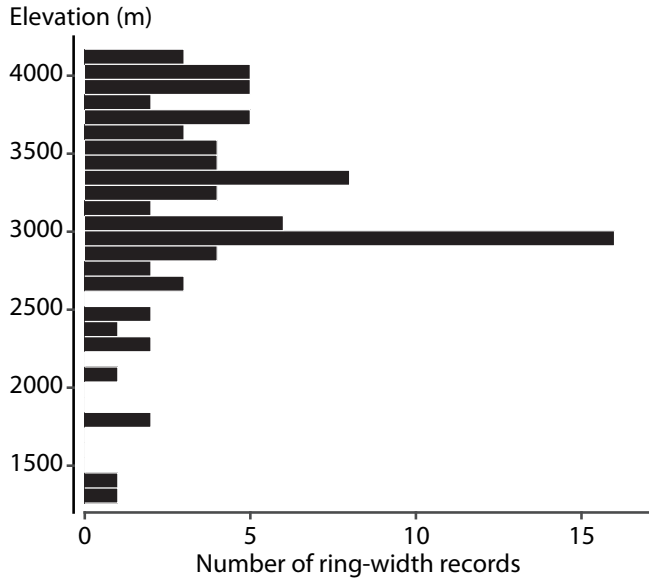

Figure 2.3 Histogram showing the distribution of all Nepalese tree-ring width records by elevation established to date.

computing the mean correlation between all possible pairs of tree-ring width measurements within the stand (RBAR; Wigley et al., 1984). Over the entire Northern Hemisphere tree-ring width network, the median value of RBAR is 0.4, but for some records, mainly those in the arid American Southwest, this metric may exceed 0.8 or 0.9 (St. George, 2014). The median value of RBAR for the Nepal tree-ring network is 0.35, which is lower than the hemispheric standard but does match the level of agreement reported for other collections from the broader region, including those in the neighboring Himalayas and the Tibetan Plateau (St. George, 2014). There is not any clear spatial pattern in RBAR across the country (Figure 2.4), but tree-ring width data derived from *Pinus roxburghii* and *P. wallichiana* generally exhibit a stronger common signal than the other major tree species. The five pine chronologies have a median RBAR of 0.43, and two of the five highest RBAR values are associated with *P. wallichiana* from mid-elevation (3000 m) sites in central Nepal. Because in many cases those ring-width records with strong between-tree agreement are also the most skillful predictors for climate reconstruction, this result indicates *Pinus* species from Nepal's lower to mid-elevation forests may be particularly well-suited to be potential paleoclimatic proxies.

In terms of temporal coverage, the Nepal tree-ring width network provides a robust estimate of annual forest growth over roughly the past four centuries. Six chronologies maintain an Expressed Population Signal (EPS; Wigley et al., 1984) greater than 0.85 back to AD 1600 (Fig 5(b)). Earlier in the 16th century, five chronologies or fewer satisfy this criterion, and the mean ring-width index (computed as the average of all chronologies; Figure 2.5(a)) and mean RBAR values (Figure 2.5(b)) both fluctuate wildly, which suggests that such a restricted network is not a reliable indicator of tree

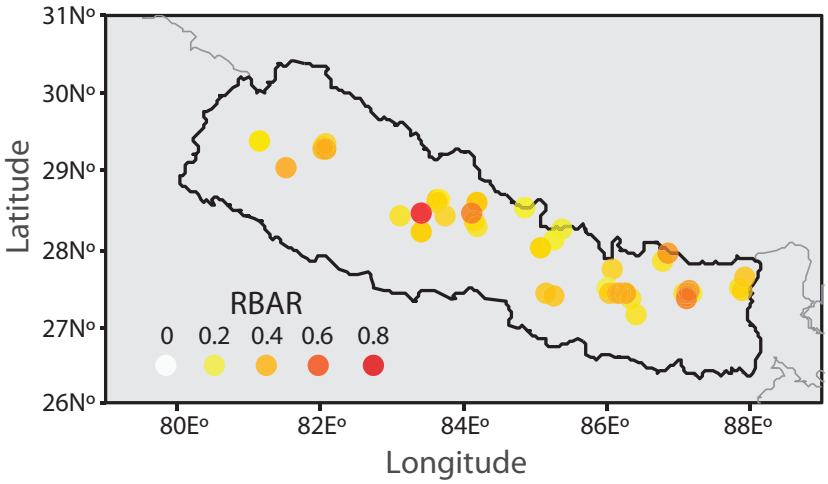

Figure 2.4 Map showing the strength of common growth signals shared across the forest stand (as measured by the mean between tree correlation, RBAR; Wigley et al., 1984) for each tree-ring width chronology.

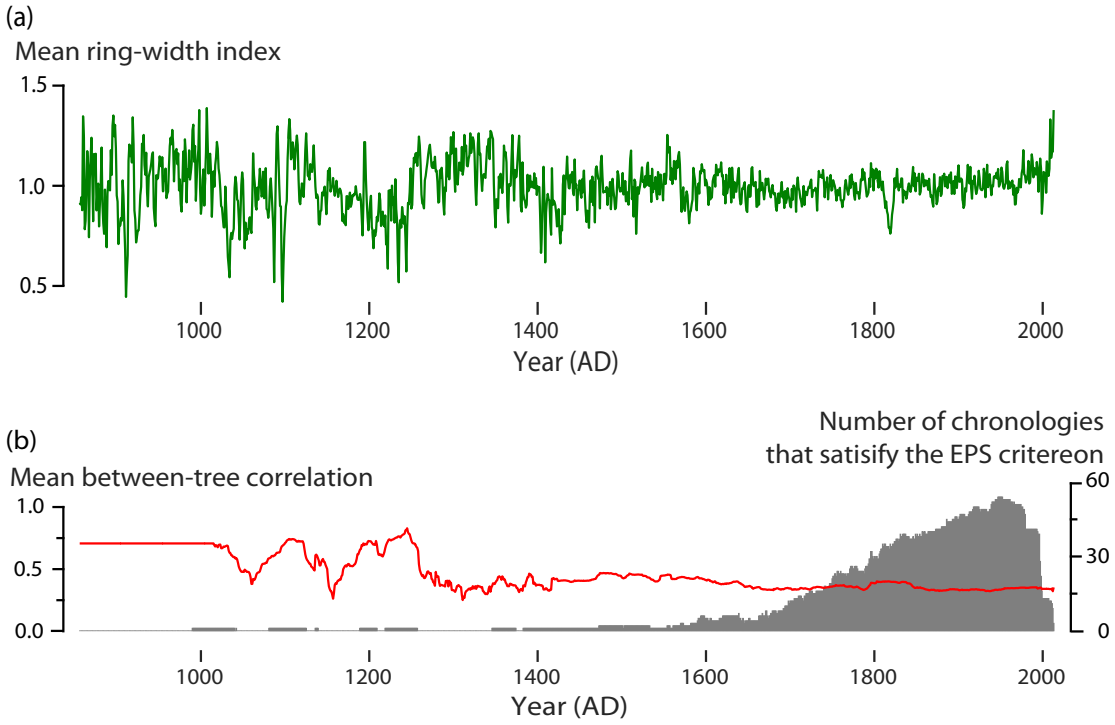

Figure 2.5 (a) The composite (median) ring-width chronology constructed by combining all 55 tree-ring chronologies from Nepal. (b) The total number of site chronologies that preserve an adequate estimate of the stand-wide signal (grey bars, as measured by the Expressed Population Signal, EPS; Wigley et al., 1984), and time-varying between-tree correlations, RBAR (red line).

growth across the country. As a result, we restrict our subsequent analysis to the portion of the Nepal network that spans the period between AD 1600 and 2013. That interval predates by more than a century the country's unification by Prithvi Narayan Shah in AD 1768 (Pradhan, 2009), and encompasses the Rana dynasty, the return of the Shah family to power, and the modern initiation of the Federal Democratic Republic of Nepal in 2008 (Sharma, 2012).

In addition to evaluating the signal quality of tree-ring width chronologies across Nepal, we also identified all occurrences of locally absent rings within the national network. As a consequence of severe environmental stress, often related to drought, wildfire, or insect infestation, trees will occasionally form a discontinuous layer of wood around their stem (Fritts et al., 1965; Glock and Pearson, 1937; Schulman, 1941). All the tree-ring data in our synthesis followed the 'Tucson Decadal Format' standard, which uses the number zero to represent locally absent rings (Holmes, 1994). For each site, we computed the total number of absent rings as a percentage of all rings included in that set of measurements. We also calculated the frequency of absent rings for each year by dividing the total number of absent rings across the network by the total number of rings. Across the entire Nepal tree-ring network, the median frequency of absent rings was 0.12% and ranged between 0 (no absent rings present in the record) to 0.55%. There is no obvious spatial pattern in the distribution of absent rings across the country (Figure 2.6(a)), but these features occur most frequently in low-elevation pines and high-elevation fir (Figure 2.6(b)). During the past four centuries, absent rings were most common in 1999 (1.6% of all rings), AD 1657 (1.2%), and during the period between AD 1817 and 1820 (1.1–1.4%). Globally, by far the most common cause of geographically

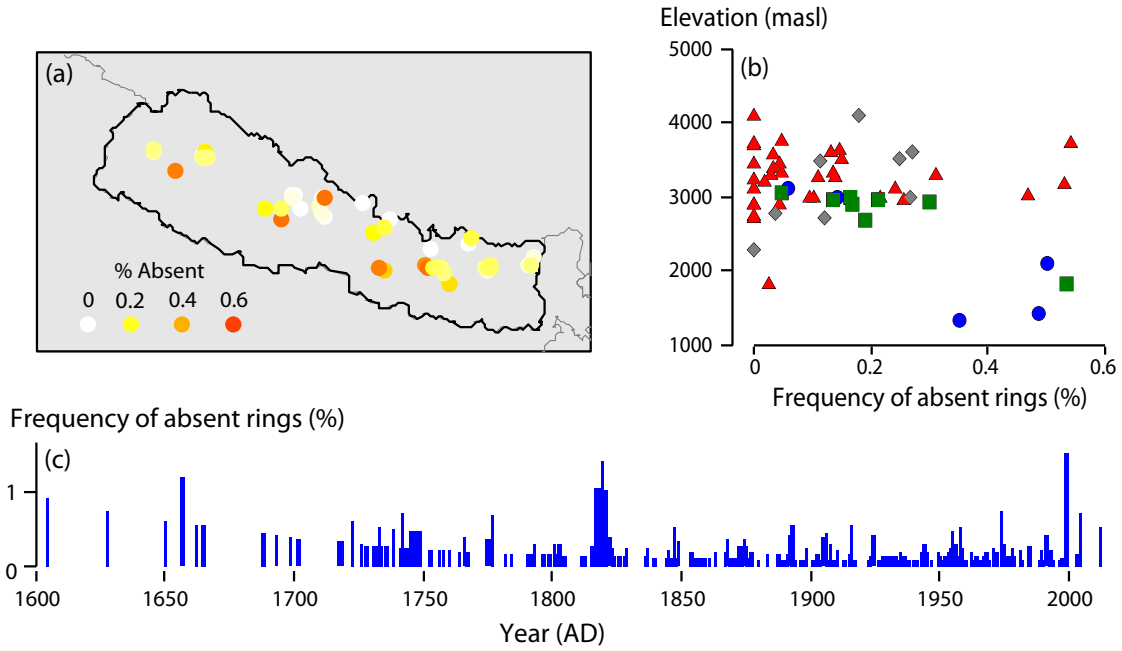

Figure 2.6 (a) Map showing percentage of locally absent rings within each site chronology across Nepal. (b) Scatterplot comparing the percentage of absent rings (sorted by genera) plotted against elevation. The symbols match the genera described in Figure 1.1 (c) Percentage of locally absent rings (total number of absent rings divided by the total number of rings) in the Nepalese ring-width network by year.

widespread absent rings (cases where they occur simultaneously at several locations) is severe moisture stress (St. George et al., 2013; Novak et al., 2016). The high frequency of absent rings in AD 1999 coincides with a record drought in that year across the country (Sigdel and Ikeda, 2010), which suggests that in Nepal locally absent rings might be evidence of shortfalls in moisture supply during the growing season.

2.6 Four centuries of tree growth in the Nepal Himalaya

In order to provide a long-term view of tree growth across the country, we constructed an all-Nepal tree-ring composite by computing the median of the entire set of ring-width chronologies through time (Figure 2.7(a)). It would also be possible to aggregate tree-ring chronologies by region (Briffa et al., 1998; Yang et al., 2014) or via principal components analysis (Cook et al., 2013a; Liang et al. 2014), but we chose to compute a simple average in order to provide a general overview of growth across the network that was not limited by the length of the shortest series. Across the network, the median between-chronology correlation is 0.17, and the agreement is somewhat stronger in the eastern part of the network (Figure 2.8), likely because more collections have been made in the areas between Langtang and Kanchenjunga. To avoid the influence of segments with low sample replication and signal quality, each individual chronology was truncated at the year where its EPS value fell below the 0.85 threshold (Wigley et al., 1984) prior to being combined into the all-Nepal median.

Over the past four centuries, two major events are prominent in the all-Nepal composite: (i) a prolonged and widespread growth suppression during the early 1800s; and (ii) heightened growth during the most recent decade. The median ring-width index was below one for each year between AD 1811 and AD 1822, with the lowest growth

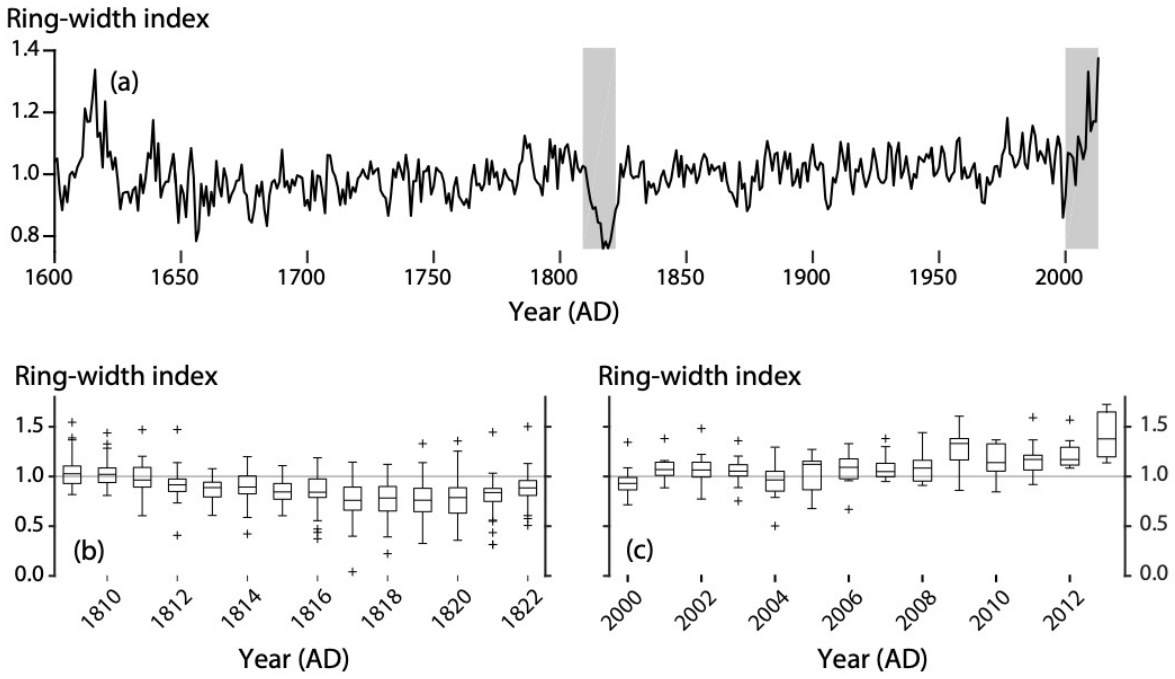

Figure 2.7 (a) Median ring-width chronology across the Nepal tree-ring network since AD 1600. Box plots illustrating the distribution of tree-ring width indices across all available sites during (b) the early 1800s and (c) the early 21st century.

during this interval occurring in AD 1817 (Figure 2.7(b)). This extended downturn in tree growth is evident in chronologies from all major tree genera and at all elevations within the network. This period coincides with two major eruptions of Indonesian volcanoes, including the unknown eruption of AD 1809 (Cole-Dai et al., 1997) and the AD 1815 Tambora eruption (Stothers, 1984). The latter event was the third-largest eruption of the past 1500 years (Gao et al., 2008; Oppenheimer, 2003) and was responsible for the abnormally cold weather observed across much of the Northern Hemisphere during AD 1816 (Cole-Dai et al., 2009). Recent studies have argued that major tropical eruptions can cause the Asian monsoon to fail two or three years after the triggering event (Anchukaitis et al., 2010), and drought estimates based on tree rings show dry conditions extending over much of the region during the AD 1809 to 1822 period (Cook et al., 2010; Figure 2.9). But because the influence of eruptions on monsoon precipitation is not thought to persist for several consecutive years, even after the very largest events (Anchukaitis et al., 2010), it may be that the early 1800s slowdown in forest growth was the combined product of two or more dry years caused by explosive volcanism that was subsequently amplified and extended by legacy effects imposed by tree physiology (Anderegg et al., 2015). But regardless of the specific cause, the early 1800s growth suppression is influence on the vigor of Nepal's forests. More optimistically, because there have not yet been any reports of increased tree recruitment following this slowdown in tree-line forests (Gaire et al., 2014, 2017b), this event may not have been sufficiently severe to cause widespread tree mortality.

Our all-Nepal tree-ring index suggests that tree growth has been above average in almost every year since AD 2000 (Figure 2.7(c)). This apparent trend towards higher

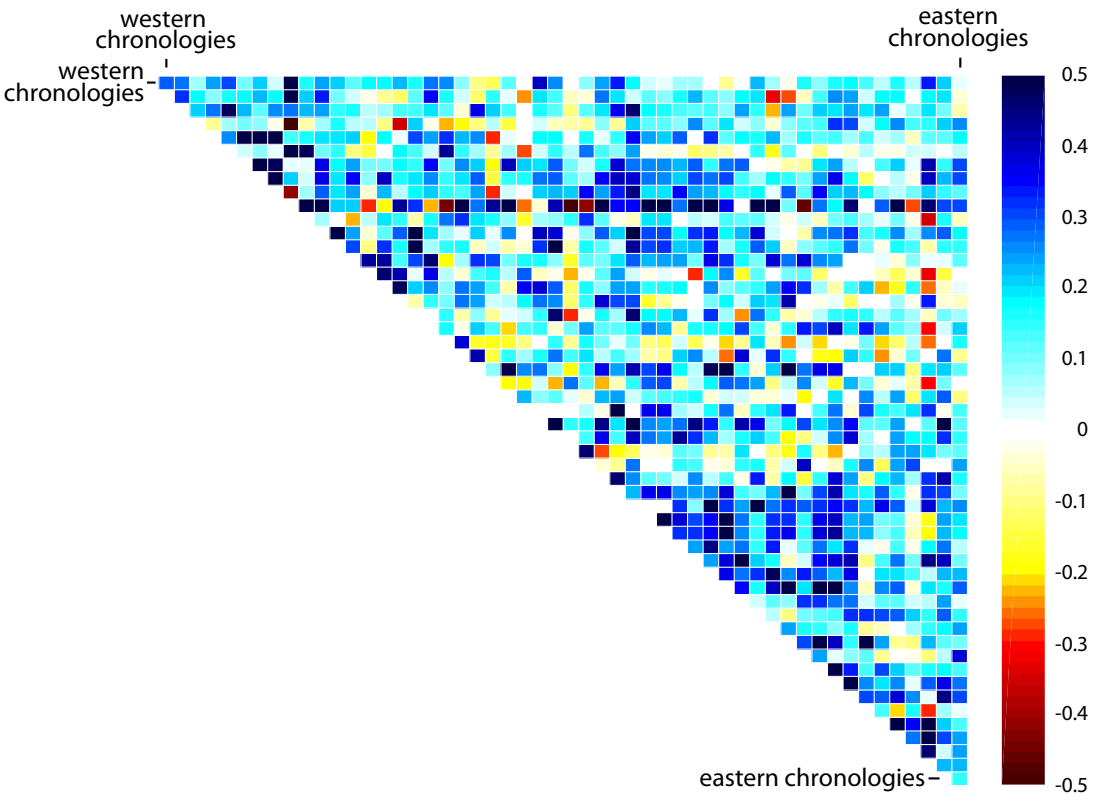

Figure 2.8 Matrix of between-chronology correlations for all pairs of records within the Nepal tree-ring network. Correlations are calculated for the maximum period of overlap between each pair of chronologies. The portion of each chronology that did not meet the EPS criterion (0.85) was not included in this analysis.

ring-widths has coincided with widespread and substantial warming in Nepal's alpine environments (Shrestha and Aryal, 2011; Shrestha et al., 1999), and a concomitant increase in the upper limit of *Abies* (Gaire et al., 2014). Other age–size standardization methods (specifically, negative exponential curves and 30-year cubic smoothing splines) also produced all-Nepal ring-width indices with marked post-2000 growth increases, but examining the tree-ring width measurements (not detrended) for the 11 *Abies* collections shows only four sites with enhanced growth over the most recent decade (Figure 2.10). Because this recent spurt of high growth could perhaps be an artifact of our chronology construction, we recommend other methods be applied to evaluate potential enhancement of *Abies* growth at high-elevation sites, such as the installation of dendrometer bands (Deslauriers et al., 2007; McMahon and Parker, 2015) or applying either satellite or ground-based methods to estimate tree biomass and productivity of Himalayan fir (Chave et al., 2014; Donoghue et al., 2007; Popescu, 2007).

2.7 Priorities for future tree-ring work in Nepal

Our synthesis of the current Nepalese tree-ring width network demonstrates that these data provide a reliable estimate of tree-growth across the country back to approximately AD 1600. Earlier on, there are not a sufficient number of tree-ring records to estimate regional tree growth or serve as paleoclimate surrogates. Longer records are needed to test, for example, whether the warm and dry period that occurred in many parts of the world during AD 900–1400 (Chen et al., 2015; Cook et al., 2004; Goosse et al., 2012; Mann et al., 2009) had any manifestation in Nepal. Those few chronologies that predate AD 1500 demonstrate that old growth forests are still present in Nepal, and samples obtained from archeological sites could also be very useful to extend chronologies back

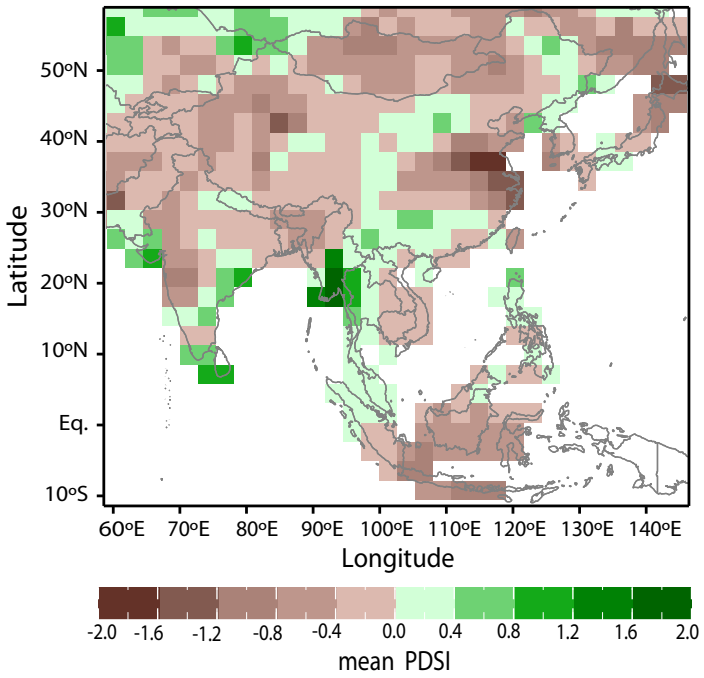

Figure 2.9 The spatial pattern of Palmer Drought Severity Index (PDSI; Palmer, 1965) across monsoon Asia during the period AD 1809 to 1822. The PDSI values are reconstructed from a large network of moisture-sensitive tree-ring records from the region (Cook et al., 2010), which includes some of the Nepalese records incorporated into our current analysis.

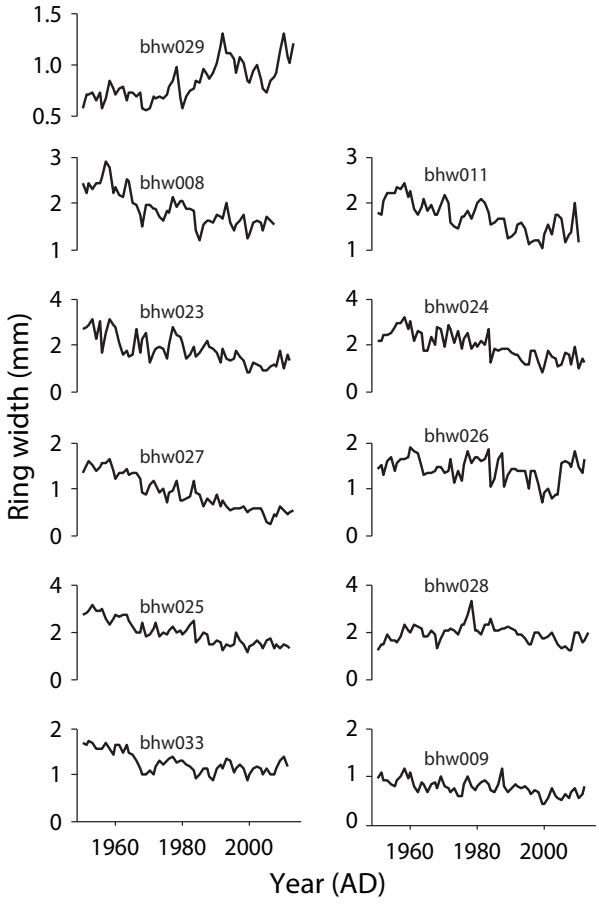

Figure 2.10 Mean 'raw' ring-width composites for those 11 *Abies* records that post-date AD 2000. In contrast to our other analysis, these chronologies were produced without any standardization to remove trends due to age or size.

in time. So far, the sole attempt to date archeological timbers in Nepal using tree rings was conducted by the Nepalese Department of Archeology and the German Research Foundation in the early 1990s (Schmidt et al., 1999). That project, which was conducted in the Mustang Valley of central Nepal, began with the collection of wooden artifacts from caves in the Muktinath and southern Mustang valleys, and expanded to include samples from several houses and ruins between Marpha and Dzakot. This suite of archeological specimens from three tree species (*Pinus wallichiana, Abies spectabilis,* and *Picea smithania*) yielded a master chronology that extended between AD 1997 and AD 1324. Obtaining timbers from archeological sources like these may be key to the development of longer tree-ring sequences for use in paleoclimatology or paleoecology.

Based on our survey, it is apparent that tree-ring width chronologies from pines have stronger between-tree agreement than other species, and pines also form locally absent rings more commonly. Because these two characteristics are often associated with sensitivity to moisture, this behavior might be evidence that Nepalese pines could serve as proxies for drought or streamflow. Cook et al. (2003) suggested that *P. wallichiana* are primarily moisture-limited and for that reason did not include records from those species within their nation-wide temperature reconstruction. Pines have been successfully used to reconstruct rainfall and streamflow in the adjoining regions, including India (Singh et al., 2009), China (Liu et al., 2005), Pakistan (Cook et al., 2013b), and Mongolia (Liu et al., 2009), but in Nepal, no attempt has been made to reconstruct past hydroclimate using tree rings.

Our study confirms that the high-elevation fir has grown rapidly during the recent-most decade. However, only 11 *Abies* chronologies post-date AD 2000, and these

records were mostly developed from central Nepal. Additional *Abies* collections from treeline forests in the far-western and far-eastern regions of the country are needed to make a robust argument about the recent growth trends of this species. Further collections from other high-elevation species such as hemlock and birch as well as low-elevation pines would also be helpful to determine if the Himalayan fir is currently growing faster than any other species. If we were able to gauge more accurately the rate and causes of the recent growth of Nepalese high-elevation forests, then that would help develop strategies such as assisted migration and restoration (Gray and Hamann, 2013) to conserve these systems that are critical for livestock grazing, wildlife habitat, and tourism (Nepal, 2000; Stevans, 2003).

2.8 Conclusions

Nearly four decades have passed since Rudolf Zuber collected the first tree-ring samples from Nepal, but in many respects the country remains a frontier area for dendrochronology and its various subdisciplines (Bhuju, 2016; Cherubini, 2015). Even today, most of the country's tree-ring data have been developed by international scientists, with the pioneering efforts of Ed Cook and Paul Krusic (Cook et al., 2003) making up the largest single contribution to the network. But over the last 10 years most tree-ring studies have been led by foresters and environmental scientists from Nepal, and that work has expanded considerably the geographic coverage and the variety of tree species and forest biomes within the network. The Nepal tree-ring network now encompasses an altitudinal range of nearly 3 kilometers, extending from lower temperate forests near Kathmandu to treeline forests in Sagarmatha (Mt. Everest) National Park, and includes data from nine genera and 11 species. Even though forests in Nepal are an

important local resource for timber and fuel (Pandit and Bevilacqua, 2011), half of all tree-ring chronologies in the network extend back at 292 years and 22 records span the past four centuries (and earlier). Taken together, these data provide a much longer perspective on tree-growth trends across the Nepal Himalaya and allow us to evaluate how Nepalese forests have been affected by recent and past environmental changes.

In order to assess tree growth across Nepal, we obtained data for 55 tree-ring width records out of the 86 records we estimate have been collected from the country. After averaging together those chronologies to construct an all-Nepal ring-width index spanning the past four centuries, we identified two prominent and long-lasting growth excursions. The first, which occurred in the early 19th century, shows that forests across Nepal experienced a prolonged downturn in growth that began in 1811 and extended until 1822. This widespread growth suppression, which is evident in all major tree genera and across the entire elevational range of the network, may be the result of one or more volcanically induced monsoon failures (Anchukaitis et al., 2010) whose detrimental influence on tree growth was subsequently amplified by strong legacy effects due to tree physiology (Anderegg et al., 2015). The other prominent growth anomaly is an apparent trend towards wider rings since AD 2000 in high-elevation forests, most of which are located in central Nepal. Although this recent growth spurt does coincide with widespread and substantial warming in Nepal's alpine environments, the techniques used to remove age–size trends from ring-width data can sometimes artificially inflate tree-ring indices near the recent end of the series (Melvin and Briffa, 2008). For that reason, we suggest that in-situ or remotely sensed methods be applied to either corroborate or refute tree-ring evidence for enhanced tree growth in Nepal's highest-elevation forests.

The Nepal tree-ring width network has been used to extend back the temperature record from Kathmandu (Cook et al., 2003) and these data have also been incorporated into efforts to reconstruct drought in Monsoon Asia (Cook et al., 2010) and summer temperatures in East Asia (Cook et al., 2013a). We anticipate that this synthesis will aid the identification of priority targets (both geographic areas and tree species) for future tree-ring collections in Nepal and provide a broader context to evaluate the characteristics of newly developed tree-ring data. And more broadly, we hope this new assessment will highlight the substantial recent progress made by Nepali scientists and their international collaborators to produce a robust dataset for paleoclimate reconstruction drawn from the forests of the Nepal Himalaya.

2.9 Acknowledgements

This research was supported by a Herbert E. Wright, Jr., Quaternary Paleoecology Fellowship to U.K. Thapa and a Talle Faculty Research Award to S. St. George.

CHAPTER 3: DETECTING THE INFLUENCE OF CLIMATE AND HUMANS ON PINE FORESTS ACROSS THE DRY VALLEYS OF EASTERN NEPAL'S KOSHI RIVER BASIN[2]

3.1 Summary

Pine forests provide goods and services crucial to more than ten million people living in the middle-mountains (600–4000 m) of Nepal. These critically important forests are already often overexploited and could be at risk from future climate change. In order to investigate the combined effects of climate and human disturbances on the growth of pine forests, we established a new network of tree-ring sites in six *Pinus wallichiana* and four *P. roxburghii* forests across the dry inner valleys of eastern Nepal's Koshi River watershed. We produced measurements of total annual ring widths, and detrended individual tree-ring series with 67% cubic splines to produce site-level chronologies. The Koshi tree-ring chronologies were compared against local records of mean monthly temperature and total monthly rainfall to identify the main climatic factor(s) limiting pine growth. We also employed a relative growth change method to estimate growth releases and suppressions in ring-width series as indicators of disturbances. At all sites, trees are relatively young (median age was 102 years) and variations in ring-width provide estimates of tree growth over only the past century. Ring-width chronologies from the Koshi have a weak common signal strength in comparison to trees from the same species obtained from sites in the central Himalaya, and the climate-growth response of Koshi pines appears to be governed primarily by moisture balance during winter. Disturbance

[2] UK Thapa and S St. George (2019). Detecting the influence of climate and humans on pine forests across the dry valleys of eastern Nepal's Koshi River basin. *Forest Ecology and Management,* 440: 12-22. https://doi.org/10.1016/j.foreco.2019.03.013

events evident in pine ring-width data are largely asynchronous, which suggests these forests have been historically perturbed by human influences rather than large-scale climatic or ecological influences. The sacred forest at Sikri contained the oldest living trees (118 years), had the lowest number of disturbance events, and preserved a stronger common signal, which provided additional evidence of the effects of humans on other pine forests in the Koshi basin. Based on our findings, we suggest that modeling the future growth and distribution of pine trees in eastern Nepal should consider winter moisture. Furthermore, management strategies to better conserve pine forests in eastern Nepal should incorporate the two competing influences of climate and human activities on tree growth.

3.2 Introduction

Pine forests provide key ecosystem services and resources to more than ten million people living in the middle mountains (600-4000 m) of Nepal (Central Bureau of Statistics, 2012; Shrestha et al., 2007). These mid-mountain forests help mitigate climate change, reduce soil erosion and stabilize slopes (Schreier et al., 1994; Lammeranner et al., 2005; Baral et al., 2009; Shrestha et al., 2013; Dhital et al., 2013; Pandey et al., 2014; Birch et al., 2014), and serve as important sources of timber and firewood for local people (Adhikari et al., 2004; Thoms, 2008). Furthermore, non-timber forest products such as pine resins are important sources of income generation for rural communities (Kanel and Niraula, 2004; KC and Stainback, 2012). The pines also have medicinal values and local people use them as stimulants and anti-pathogens (Kaushik et al., 2013; Sharma et al., 2018). Most pine forests in Nepal are categorized as community forests where thinning, pruning, regulated cattle grazing and controlled harvesting of forest

products primarily timber, fuelwood and fodder are practiced (Department of Forest Research and Survery, 2006; cited in Dangal et al., 2017), but these pine forests are often overexploited. In addition, due to observed and anticipated future change in mean and extreme climates (Agarwal et al., 2014, 2016; Karki et al., 2017; Shrestha et al., 2017a; Rajbhandari et al., 2017, 2018; Talchabhadel et al., 2018), the pine forests growing in the relatively dry river valleys of Nepal might be negatively affected (Allen et al., 2010; Williams et al., 2012).

Most studies of pine forests in Nepal have focused on estimating biomass and carbon sequestration (Applegate and Gilmour, 1988; Shrestha et al., 2013; Dangal et al., 2017; Luintel et al., 2018), the economic value of forest products (Birch et al., 2014; Chand et al., 2015; Gauli and Hauser, 2011), and the extent of human disturbances (Mahat et al., 1987; Panta et al., 2008). Little is known about climate's influence on the growth of pine trees in Nepal, but understanding the principal climatic factor that limits tree growth is key to appropriately model the future growth and distribution of any tree species (Pearson and Dawson, 2003; Austin and Van Niel, 2011; Elsen and Tingley, 2015; Moran-Ordonez et al., 2017). So far, only tree-ring analysis has been applied to investigate the tree-climate relationships in Nepal, and many of the extant dendroclimatic studies are focused on high elevation (> 3000 m) tree species such as *Abies spectabilis*, *Picea smithiana* and *Betula utilis* (Suzuki, 1990; Bhattacharyya et al., 1992; Cook et al., 2003; Bräuning 2004; Sano et al., 2005; Dawadi et al., 2013; Thapa et al., 2013; Liang et al., 2014; Gaire et al., 2017a; Kharal et al., 2017; Panthi et al., 2017; Rayback et al., 2017; Tiwari et al., 2017; Sigdel et al., 2018b). Two studies have specifically targeted low elevation (< 3000 m) *P. roxburghii* forests but these analyses were based on single

sites in western and central Nepal (Aryal et al., 2018; Sigdel et al., 2018a). A few studies have also evaluated the influence of climate on the growth of *P. wallichiana* at higher elevations in western Nepal (Bräuning, 2004; Gaire et al., 2019), but it is not known what climatic factors affect this species' growth at lower elevations. Furthermore, the growth of relatively accessible pine forests might also be affected by human activities, but earlier studies have not attempted to estimate human effects on the growth of pine forests. Quantifying the effects of human disturbance on tree growth may help evaluate the impacts of current and past human actions on forest growth, which would help guide forest managers in the country to develop sustainable forest conservation plans.

Because varying patterns of wide and narrow rings reflect the climatic conditions under which trees grow and disturbances they experience over their life spans (Fritts, 1976; Cook, 1987), tree-ring measurements can provide baseline data to study the combined effects of climate and humans on forest growth (Druckenbrod et al., 2013; Rydval et al., 2016; Trotsiuk et al., 2018). In this study, we present a new network of pine tree-ring sites across the dry valleys of eastern Nepal's Koshi River watershed to examine the influence of climate and human activities on the growth of *P. wallichiana* and *P. roxburghii* forests. Because the inner valleys of the Koshi River catchment are dry compared to central and western Nepal, we test whether it is possible to apply tree-ring analysis to determine the principal climatic factor limiting growth of pine trees under relatively adverse environmental conditions. Furthermore, because low-elevation pines in the Koshi basin are subject to human management and exploitation, we also examine growth releases and suppression to evaluate the effects of human disturbance on the dry forests of eastern Nepal.

3.3 Materials and methods

3.3.1 Study area, tree distribution, and sampling sites

The current study was carried out amongst the inner valleys of Koshi River watershed, which is the easternmost river basin in Nepal (Figure 3.1). The Koshi River originates from the Tibetan Plateau in the north, flows down the Himalayas, and then finally merges into the Ganges in the south. The river occupies the largest watershed in Nepal and is the third largest tributary of the Ganges River. With most of its population distributed in rural areas, the Koshi watershed is heavily populated in the plains and middle mountains and scattered in the higher mountains (Central Bureau of Statistics, 2012). Having an extreme elevational gradient of more than 8 km (Shrestha et al., 2017a), the Koshi basin hosts a wide range of bioclimatic zones ranging from tropical in the southern plains to alpine and tundra in the northern high altitudes (Karki et al., 2015). As a whole, the climate of Nepal, including the Koshi basin, is heavily influenced by the South Asian monsoon during summer, which delivers roughly 80% of total annual rainfall (Nayava, 1980).

The inner valleys of the Koshi River and its major tributaries are particularly dry, and so provide suitable habitat for *P. roxburghii* and *P. wallichiana* forests (Stainton, 1972; Ohsawa et al., 1986). Within the basin, *P. roxburghii* is most common on dry, south-facing slopes in the river valleys of Tamor, Arun, and Dudhkoshi rivers (major tributaries of the Koshi River), whereas P. wallichiana are concentrated in the Solukhumbu-Everest region (Stainton, 1972; Ohsawa et al., 1986). Across Nepal, the vertical distribution ranges of *P. roxburghii* and *P. wallichiana* are 800–2500 m and 1800–4000 m respectively (Stainton, 1972). We collected tree-ring samples from ten forest sites in eight districts in the middle-mountains of the Koshi River watershed (Figure 3.1, Table 3.1). The elevation of these forest sites ranged from 825 m (at

Hattisude) to 3090 m (at Junbesi). The six *P. roxburghi*i sites were located at relatively low elevations (average altitude, 1140m) with subtropical climates while the *P. wallichaina* sites were located at relatively high elevations (average altitude, 2400 m) in warm temperate climates. The *P. roxburghii* sites were monodominant stands, but the *P. wallichiana* forests, except for Sikri, had several other coexisting species including *Tsuga dumosa* and *Rhododendron* spp. Our field team trekked for one to two days after traveling an equal number of days by Jeep from Kathmandu to reach the sampling sites. All sampled forests are natural (not plantations), close to human settlements, and community managed. At all *P. roxburghii* sites, we noted trees with peeled bark to extract resins. Sites also served as grazing lands for cattle (goats and buffaloes), which were particularly common in *P. wallichiana* forests. We also saw evidence of cut stumps and stacks of logged trees at most sites as pine timber is a common construction material here and elsewhere in Nepal.

3.3.2 Sample collection, ring-width measurement, and chronology development

We collected 641 core samples from six *Pinus roxburghii* and four *P. wallichiana* forests across the Koshi watershed during the summers of 2016 and 2017 (Table 3.1, Figure 3.1). Haglöfs AB increment borers were used to extract core samples at breast height, and attempts were made to collect two cores from a tree at opposite directions. In those few instances when rugged terrain did not allow us to extract the second core, only one core was collected. The core samples were transferred to the laboratory where they were air dried and then sanded with progressively finer grit sandpapers for clear visualization of ring boundaries under the microscope (Stokes and Smiley, 1968).

For each ring, the calendar year of formation was determined by comparing the

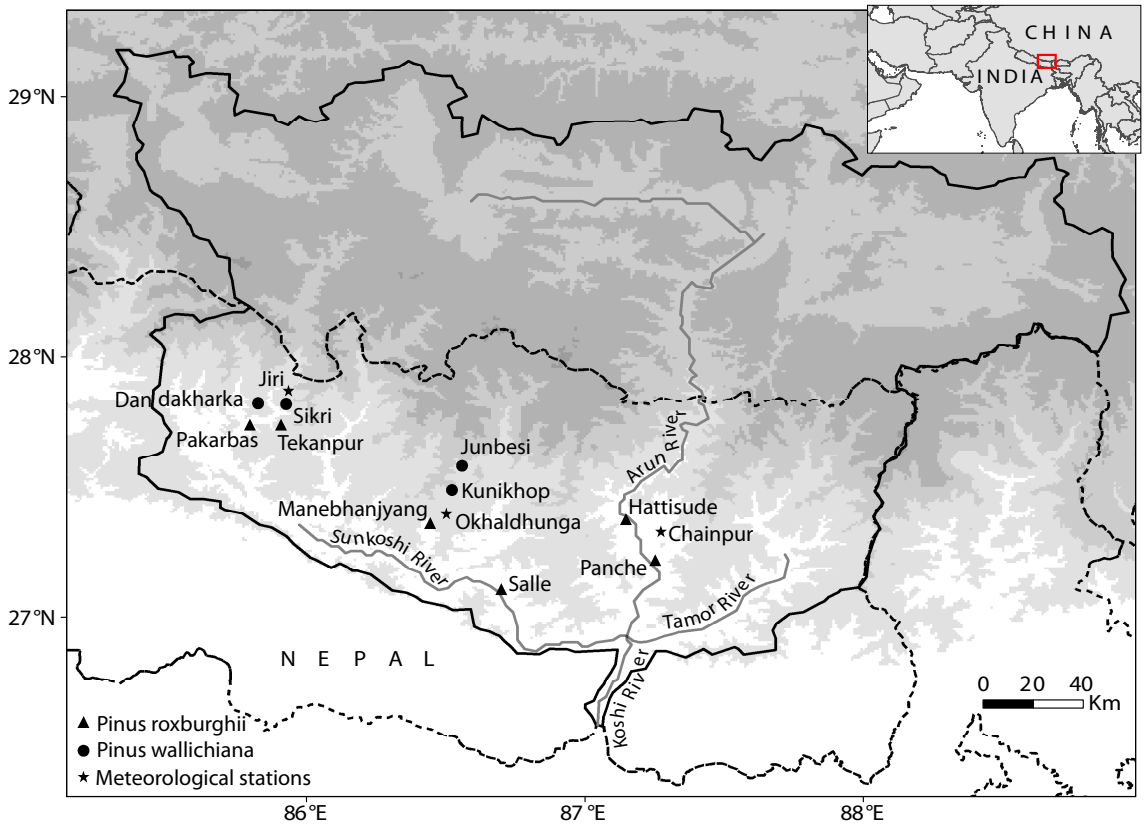

Figure 3.1 Map of the Koshi River watershed showing the locations of *Pinus roxburghii* (triangles) and *Pinus wallichiana* (circles) tree-ring sites and meteorological stations (stars) used to examine tree-climate relationships. The solid line represents the catchment boundary of the Koshi River, the dashed-dot line represents Nepal's borders, and the gray lines represent the major river tributaries of the Koshi River.

patterns of wide and narrow rings across all samples within a site using skeleton plots (Stokes and Smiley, 1968). Ring-width measurements were then generated using a Velmex measurement system. After measurements were produced, the accuracy of cross dating was tested using the computer program COFECHA (Holmes, 1983). To remove the growth trend from each tree-ring width series, we fit a 67% cubic spline and computed ring-width index (the ratio of ring width to spline value; Cook and Peters, 1981). Standardizing ring-width measurements in this manner removes the age-size related growth trend and maximize common signal in the final chronology (Cook and Peters, 1981). For closed-canopy forests like the Koshi pines, spline detrending is recommended over other methods because of its improved ability to estimate and remove competition effects (Cook and Kairiukstis, 1990). All detrended series from each site were averaged to develop a site-level chronology. The standardization procedure and site average chronology building were performed using program ARSTAN (Cook et al., 2017). ARSTAN also computes several common statistical measures to describe the characteristics of tree growth including the all-series correlation (Rbar), the Expressed Population Signal (EPS), and the Signal to Noise Ratio (SNR) (Fritts, 1976; Wigley et al., 1984).

3.3.3 Detecting climate signals in the Koshi pine chronologies

In order to detect the primary climate variable that limits the growth of pine trees, we computed Pearson correlation coefficients between each ring-width chronology and climate data from weather stations close to the respective forest site (Table 3.2). Meteorological stations in Nepal are sparse and were established only recently compared to those in western countries. Because climate data in Nepal are not freely available, we

Table 3.1 Metadata table describing the details of tree-ring sampling sites in eastern Nepal's Koshi River watershed. Forest sites are ordered by longitude from west to east.

Site name	Species	Location	No of trees (cores)	Lat (^{0}N)	Lon (^{0}E)	Elevation (m)	Slope	Aspect
Pakarbas (pkw)	*Pinus roxburghii*	Ramechhap	40 (80)	27.24	85.79	1210	20	N
Dandakharka (ddk)	*P. wallichiana*	Dolakha	32 (64)	27.50	86.02	1820	22	SW
Tekanpur (tkp)	*P. roxburghii*	Ramechhap	30 (60)	27.40	86.09	1130	22	N
Sikri (skr)	*P. wallichiana*	Dolakha	16 (32)	27.43	86.23	1750	10	NE
Manebhanjyang (mbj)	*P. roxburghii*	Okhaldhunga	34 (69)	27.22	86.44	1513	55	SW
Kunikhop (kkp)	*P. wallichiana*	Solukhumbu	30 (60)	27.49	86.52	2950	35	NW
Junbesi (jbs)	*P. wallichiana*	Solukhumbu	30 (60)	27.58	86.56	3090	25	W
Salle (sal)	*P. roxburghii*	Udaypur	36 (72)	26.97	86.70	1330	57	SW
Hattisude (hsd)	*P. roxburghii*	Sankhuwasabha	35 (70)	27.14	87.14	825	18	NW
Panche (pnc)	*P. roxburghii*	Dhankuta	37 (74)	27.10	87.25	834	35	N

purchased mean monthly temperature and total monthly rainfall data from 14 stations close to the sampling sites from the Nepal Government's Department of Hydrology and Meteorology in Kathmandu. Climate records that were shorter than 31 years were not used even if the corresponding stations were nearby to the sampling sites. Our analysis gave emphasis to rainfall data from Jiri (spanning the period 1961 to 2016), Okhaldhunga (1948 to 2016) and Chainpur (1947 to 2016), and temperature data from Jiri (1965 to 2016) and Okhaldhunga (1977 to 2016). There were a small number of years with missing values (0–6% of total measurements), which we filled with the monthly means of the entire period for each station (Battipaglia et al., 2008). According to the modified Koppen-Geiger climate classification, the sampled forest sites fall under temperate climates with dry winters and hot/warm summers (Karki et al., 2015). The median monthly rainfall is less than 25mm during November-January and about 600mm during rainy season (June-September) across the stations (Figure 3.2). June-August are the hottest months with temperature measuring between 20 and 25 degrees C while January is the coldest month with mild temperatures between 6 and 11 degrees C (Figure 3.2)**.** Correlation coefficients between tree growth and local climate were computed using the program SEASCORR (Meko et al., 2011). This program performs both monthly as well as seasonal correlation tests by computing simple and partial correlation coefficients between a tree-ring chronology and monthly temperature and precipitation. Significance levels are estimated by Monte Carlo simulations of synthetic tree-ring chronologies. Because the sampled forests were located in the dry valleys of the Koshi basin, we assumed moisture would be the likely dominant factor and therefore chose precipitation as the primary climate variable and temperature as the secondary climate variable. We

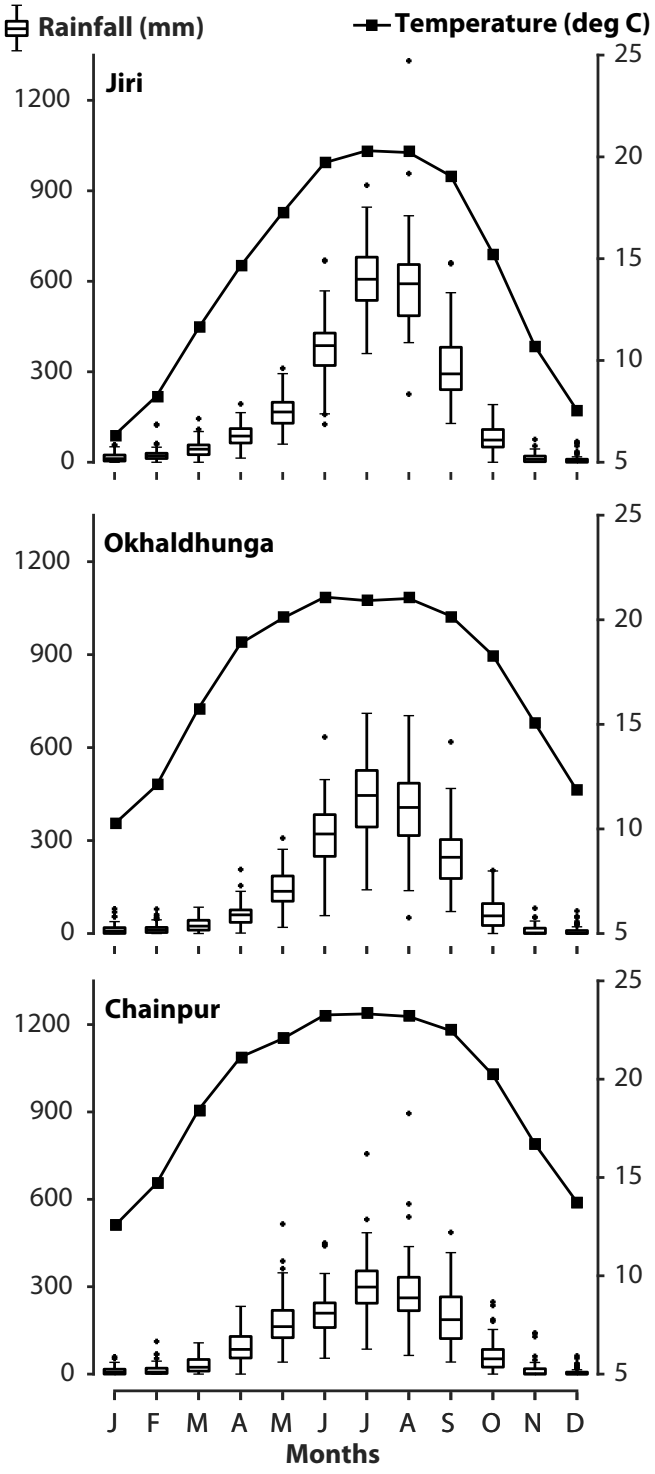

Figure 3.2 Climate diagrams demonstrating the total monthly precipitation and mean monthly temperature from meteorological stations at Jiri, Okhaldhunga, and Chainpur used to detect climate signals in tree-ring chronologies.

compared tree growth with climate records from September of the previous year to October of the growth year. The periods of comparison between tree-ring and climate data were short, which might have affected the results as it is difficult to get reliable correlations when the overlapping periods between the two types of data are relatively brief.

3.3.4 Detecting disturbance events in the Koshi pine forests

Because the sampled forests are affected by management practices and exploited for resources, it is plausible that tree growth might be influenced by those disturbances. We estimated the occurrence of disturbance events within the Koshi pine forests using the radial-growth averaging method (Lorimer and Frelich, 1989; Nowacki and Abrams, 1997). In this approach, disturbances are identified as a relative growth change between the preceding and the subsequent 10-year means of ring widths in every tree-ring series. Nowacki and Abrams (1997) defined moderate (major) disturbance as growth change greater than 25% (50%) between two consecutive 10-year running means for five continuous years. Positive and negative growth changes that met the criteria above were considered to be releases or suppressions, respectively. This relative growth change technique has been widely used to detect growth releases and suppression in each series as indicators of human disturbances in different forest types and tree species globally (Brienen and Zuidema, 2006; Camarero et al., 2011; Schongart et al., 2015; Bretfeld et al., 2015; Omelko et al., 2016; Vitali et al., 2016; Piraino et al., 2017; Camarero et al., 2018). Averaging all cores for each tree might affect the result but we employed the common practice of detecting growth releases and suppressions at the core level. We

Table 3.2 Metadata table outlining the general characteristics of climate records from weather stations close to tree-ring sampling sites in the Koshi River basin. All climate data were purchased from Nepal's Department of Hydrology and Meteorology in Kathmandu.

Station name	Climate variable	First year	Last year	Span (years)	Lat (DD)	Lon (DD)	Elevation (m)	Corresponding tree-ring site(s)
Jiri	Precipitation	1961	2016	56	27.63	86.23	2003	ddk, skr
	Temperature	1965	2016	52				ddk, skr, sal
Okhaldhunga	Precipitation	1948	2016	69	27.32	86.05	1720	jbs, kkp, sal
	Temperature	1977	2016	40				jbs, kkp, hsd
Chainpur	Precipitation	1947	2016	70	27.28	87.03	1329	hsd
	Temperature	1987	2016	30				

used TRADER, an R package, to estimate percentage growth change and identify release events in each ring-width series across all sites (Altman et al., 2014). Because the program is designed to detect only release events, we wrote MATLAB code to identify suppression events using the same percentage growth change estimated by TRADER. A disturbance event, for the purpose of this study, was defined as any major suppression or release event that exceeds the 50% growth change criteria.

3.4 Results

3.4.1 Cross dating and characteristics of the Koshi pine tree-ring widths

Out of the ten sampled forest sites, we were able to successfully cross-date specimens from all four *P. wallichiana* sites and two of six *P. roxburghii* sites (Table 3.3). The *P. roxburghii* samples were particularly challenging to cross-date due to the frequent occurrence of false and indeterminate ring boundaries (Figure 3.3). Under normal conditions, conifer trees produce distinct light-colored earlywood cells during the early growing season and dark-colored latewood cells at the end of the growing season, making clear boundaries between the rings of consecutive years (Figure 3.3a, Fritts, 1976). When climate conditions during the growing season becomes stressful, trees produce latewood-like cells, called false latewood, that have an indistinct boundary, as opposed to true latewood bands that have sharp boundaries with the following year's earlywood cells (Figure 3.3b,c; Copenheaver et al., 2006; De Micco et al., 2016; Fritts, 1976; Hoffer and Tardif, 2009). These false rings were more frequent and inconsistent between neighboring trees at four *P. roxburghii* sites (Pakarbas, Tekanpur, Manebhanjyang and Panche), which created major challenges to differentiate between true and false ring boundaries (Figure 3.3c). Several samples also had indeterminate boundaries which

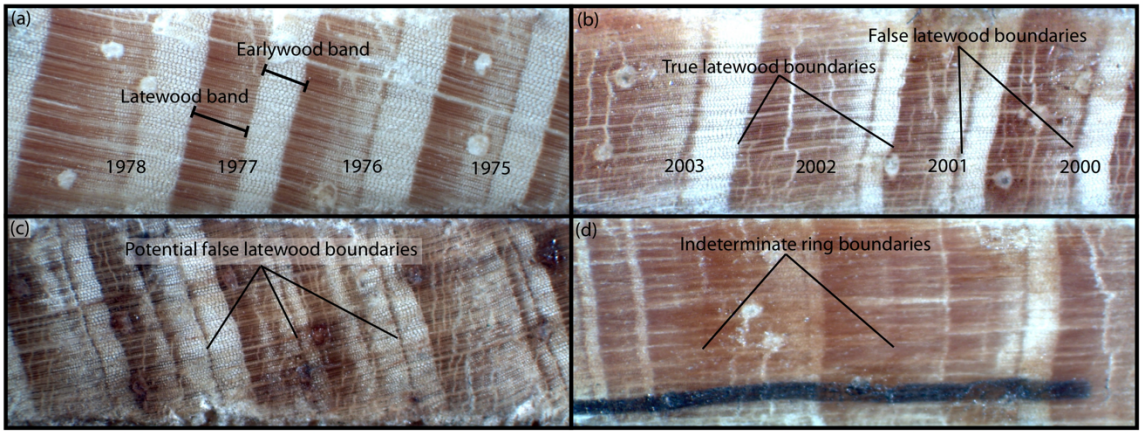

Figure 3.3 Wood sections of *P. roxburghii* showing clear and complete earlywood and latewood bands (a), identified false ring boundaries (b), challenging potential false latewood boundaries (c) and indeterminate ring boundaries (d).

created extra difficulties in the dating of *P. roxburghii* sites (Figure 3.3d). Because of these challenges, we were not able to cross- date samples from those four sites, and therefore did not incorporate them in further analyses. Two *P. roxburghii* sites (Salle and Hattisude) had relatively few and consistent patterns of false latewood bands, so we were able to cross-date specimens from those two sites (Figure 3.3b). False-ring boundaries were much less common in samples from *P. wallichiana* sites, so the dating of that species was much more effective. On average, even at the dateable sites we were forced to discard about 13% of collected series due to these challenges.

We measured total tree-ring widths for only those six dated sites. The median value of mean interseries correlation, which explains the degree of coherence across the samples in a stand, was 0.45 with highest value observed at Sikri (Table 3.3). We also made additional tests of our assigned dating by making cross-comparisons between all six Koshi chronologies as well as five pine chronologies collected previously (nepa040, nepa005, nepa008, nepa033, nepa007) from central and western Nepal (Cook et al., 2003). We were able to cross-date samples from neighboring sites only if they were less than 10 km apart (Figure 3.4). For example, the paired chronologies at Dandakharka and Sikri and Junbesi and Kunikhop exhibited positive and significant correlations ($r = 0.39$ & 0.42, $p < 0.01$). Similarly, a pair of previously collected *P. roxburghii* chronologies (nepa007 and nepa033) from the hills surrounding Kathmandu also correlate well with each other ($r = 0.4$, $p < 0.01$). There were a very few years where reduced tree growth was common to most of the Koshi sites, and those marker years were used to cross-date individual series within each stand (Figure 3.5). For example, all four chronologies of *P. wallichiana* had narrow rings in 1950, 1955, 1964, 1972, and 1985. In addition, the

narrowest ring-width indices in all *P. wallichiana* sites were during 1999–2001. The two *P. roxburghii* chronologies at Salle and Hattisude had narrow rings only in 1955, with no other marker years in common with each other or any *P. wallichiana* chronology.

The median length of the Koshi pine chronologies is 102 years, with the oldest tree located at Sikri and spanning 118 years (Table 3.3; Figure 3.5). All six chronologies exceeded the EPS threshold criteria of 0.85, which helps determine whether the number of core samples is adequate to describe the shared common signal at the stand level (Wigley et al., 1984). The average annual growth rate ranged from 0.34 to 0.41 mm/ year, with a median growth rate of 0.37 mm/year across the sites. The median Rbar, which explains the strength of common environmental signal shared across all series, is 0.19. The two *P. wallichiana* sites (Dandakharka and Sikri) had Rbar values equal to 0.22, while rest of the sites were below 0.18 (Table 3.3). The SNR, which indicates the strength of common signal, ranged from 5.8 at Sikri to 12.9 at Dandakharka.

3.4.2 Climate signals in the Koshi pine chronologies

At most sites, monthly and seasonal correlation analyses showed that pine tree-ring chronologies had significant and positive correlations with rainfall, and significant negative correlations with temperature during winter months (Figure 3.6). Ring-width chronologies at each site had a significant positive correlation with at least one 3-month season of rainfall ending between the previous October and current February. There were, however, differences in the magnitude, sign, and specific months of significant correlations between tree growth and precipitation across the sites. In addition, tree growth at Dandakharka, Sikri, and Salle also had significant negative correlations with monthly rainfall in May, August and October. Similarly, tree growth at Dandakharka and

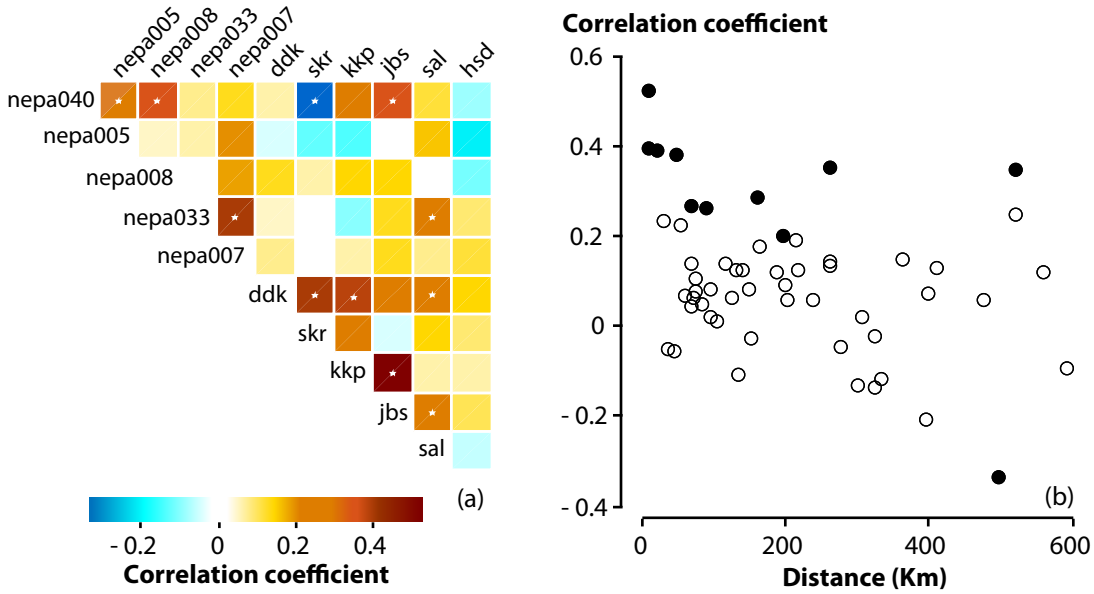

Figure 3.4 (a) Matrix of between-chronology correlations for all pairs of pine records including the current Koshi chronologies and previous collections from elsewhere across Nepal. Left and top (right and bottom) sides of the matrix represent chronologies from western (eastern) Nepal. Correlations are calculated for the maximum period of overlap between each pair of chronologies. (b) Scatterplot showing the fading coherence among the pine chronologies with increasing distance. White stars in panel (a) and filled circles in panel (b) represent significant correlation coefficients at the 0.01 level.

Table 3.3 Table summarizing the ring-width characteristics of *Pinus roxburghii* (PIRO) and *P. wallichiana* (PIWA) chronologies developed from the Koshi River watershed.

	Sites					
	Dandakharka (ddk)	Sikri (skr)	Kunikhop (kkp)	Junbesi (jbs)	Salle (sal)	Hattisude (hsd)
Species	PIWA	PIWA	PIWA	PIWA	PIRO	PIRO
Chronology span (years)	1917-2015 (99)	1898-2015 (118)	1936-2016 (81)	1913-2016 (104)	1910-2015 (106)	1925-2015 (91)
Number of cores (trees)	59 (32)	26 (14)	31 (18)	50 (30)	61 (33)	58 (34)
Average ring-width	0.416	0.334	0.409	0.379	0.367	0.341
Series intercorrelation	0.461	0.493	0.44	0.441	0.461	0.447
Common period analysis	1977-2012	1953-2012	1963-2015	1948-2015	1968-2015	1965-2011
Correlation within trees	0.509	0.505	0.365	0.29	0.439	0.499
Correlation between trees	0.214	0.209	0.143	0.155	0.18	0.173
Correlation among all series (Rbar)	0.22	0.225	0.148	0.157	0.184	0.178
EPS	0.928	0.853	0.862	0.87	0.925	0.909
SNR	12.943	5.801	6.237	7.716	12.381	9.964

Kunikhop were also correlated negatively with spring and summer rainfall. Three out of six chronologies (Sikri, Kunikhop and Salle) had significant negative correlations with winter temperatures. Like precipitation, there were some differences in the particular months or seasons of significant correlations between tree growth and temperature across all sites. For example, Junbesi and Salle chronologies correlated negatively with March temperature while Sikri and Salle chronologies correlated negatively with spring and summer temperatures.

3.4.3 Disturbances in the Koshi pine forests

We estimated growth releases and suppressions in tree-ring width measurements as indicators of disturbance events for all six forest sites across the Koshi basin (Figure 3.7). Disturbance events (releases or suppressions) occurred almost all over the entire span of each chronology. The P. roxburghii forest at Hattisude and P. wallichiana forest at Sikri respectively had highest (35) and lowest (18) number of total disturbance events. Except for Junbesi and Hattisude, most chronologies exhibited more suppression events than release events over their entire lengths. The occurrence of continuous release events over multiple years was rare across all sites, with only Hattisude showing growth releases for five continuous years during 1982–1986. In contrast, continuous suppression events for multiple years were much more common. For example, Dandakharka, Salle and Hattisude showed suppression events that lasted for five or more years during 1989–1995, 1986–1993 and 1993–1997 respectively. Except for a very few cases, neither suppression nor release events were synchronized in time across the six sites. Overall, less than 15% of trees were affected either negatively or positively in any one year with few exceptions. For example, 20.6% and 33.3% of trees at Kunikhop and Salle

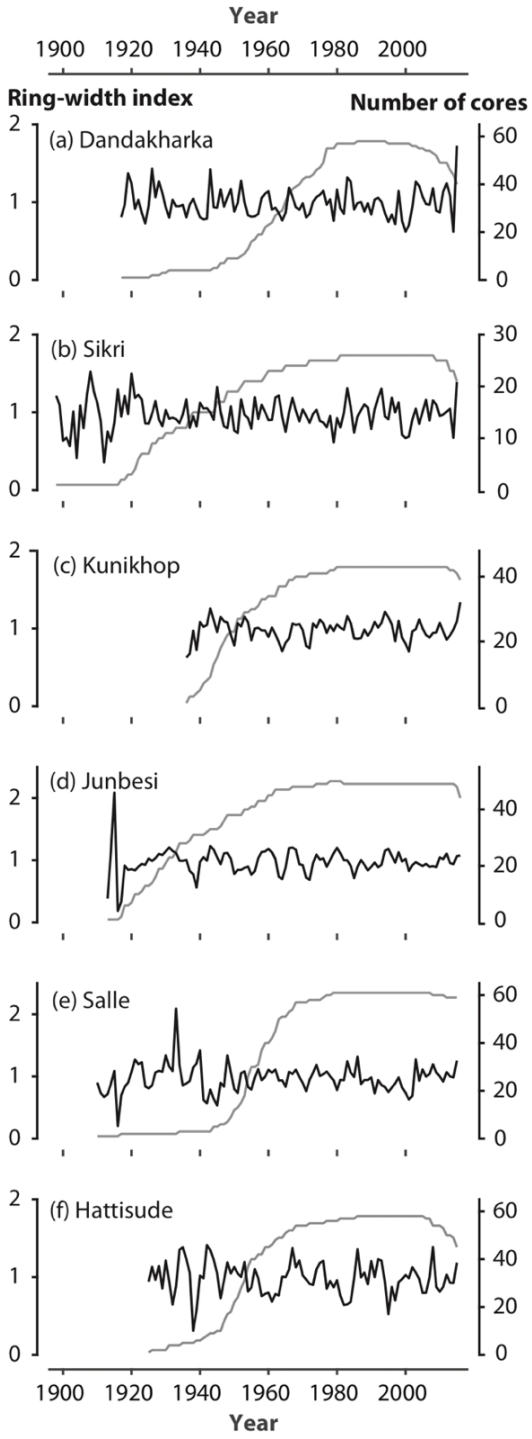

Figure 3.5 Tree-ring width chronologies (black lines) and the corresponding number of core samples (grey lines) of P. wallichiana (a-d) and Pinus roxburghii (e-f) developed at six sites in the Koshi River watershed.

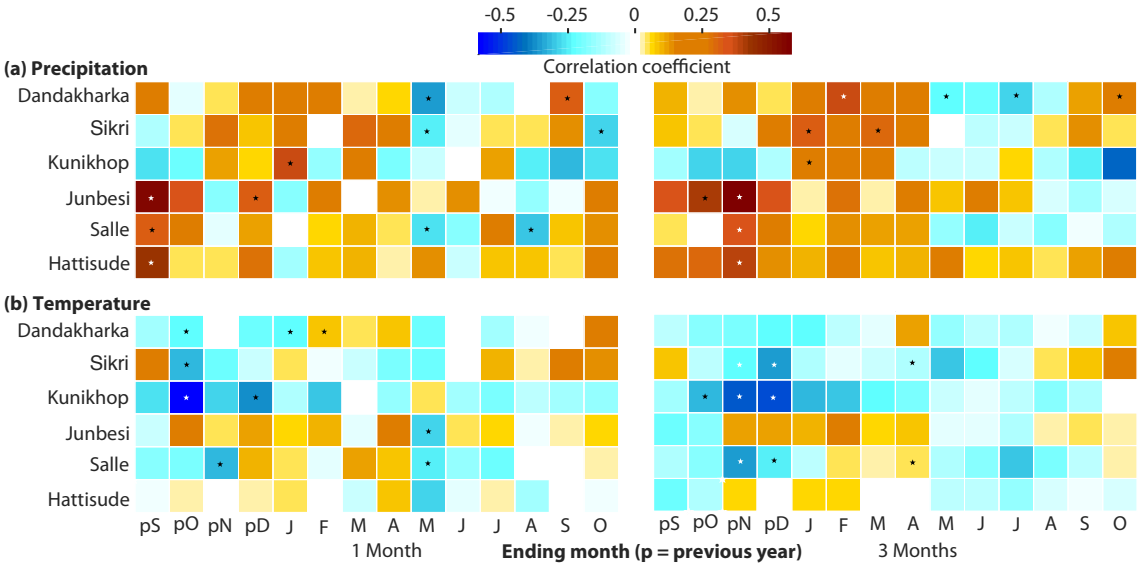

Figure 3.6 Color diagram illustrating correlation coefficients between tree-ring width chronologies and local records of climate across the Koshi River watershed. The top panels represent simple correlation coefficients between tree-ring widths and rainfall while the bottom panels represent partial correlations between tree-ring widths and temperature. The left and right panels respectively demonstrate monthly and seasonal (3 months, ending month) correlations. White (black) stars indicate correlation coefficients significant at the 0.01 (0.05) level.

experienced peak suppression events in 1962 and 1937 respectively. In addition, 100% of samples at Sikri showed release in 1913, but that extreme value is due to the fact that only one tree is old enough to include that year.

3.5 Discussion

3.5.1 Cross dating and ring-width characteristics of the Koshi pine chronologies

From our cross-dating procedures, we learned it is difficult but possible to develop ring-width chronologies of pine trees growing in dry river valleys of the Koshi watershed. Assigning exact dates to the growth rings from *P. roxburghii* trees was particularly challenging due to the frequent occurrence of false and indeterminate ring boundaries. Individual series within each stand matched against each other for all four *P. wallichiana* and two *P. roxburghii* sites. There were several years of reduced growth common across *P. wallichina* forests but marker years were not common between the two *P. roxburghii* sites or between two species. Several pairs of nearby chronologies did match against each other, but poor matches between more distant chronologies indicates the challenges inherent to the large-scale dating of these species in eastern Nepal. This lack of synchrony among the chronologies over short distances might be due to the strong spatial heterogeneity in climate. For example, based on monthly rainfall data from 14 stations across the middle mountains of the Koshi basin, we found that winter precipitation changes quickly as a function of distance in the study area (Figure 3.8).

The Koshi ring-width chronologies provided robust estimates of forest growth and common variance over the past century, as indicated by EPS value greater than 0.85 for all sites (Wigley et al., 1984). All Koshi pine forests are young and have weak common signals compared to those of pines and other species elsewhere in Nepal (Bhattacharyya

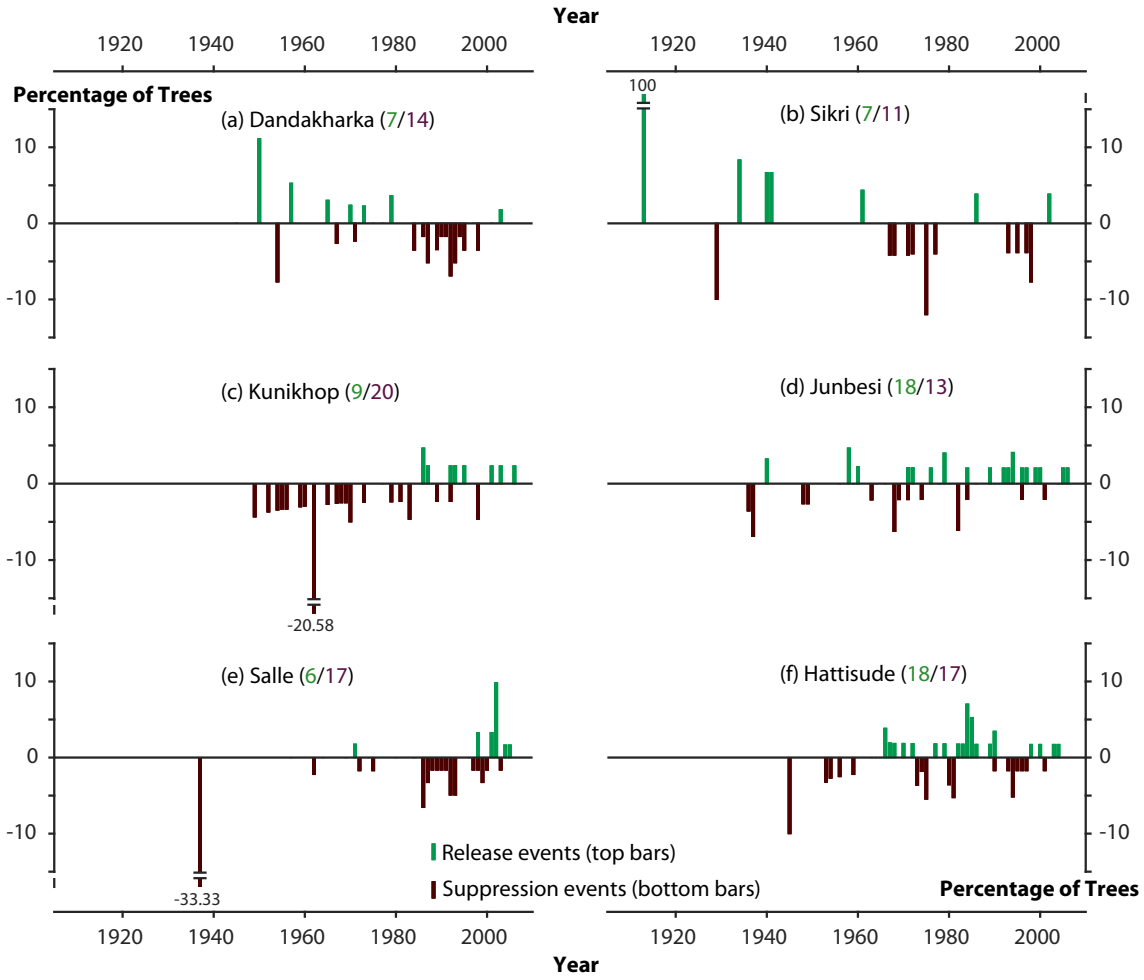

Figure 3.7 Bar diagrams showing percentage of trees that experienced disturbances expressed as either growth release or suppression events over time in the forests of Pinus wallichiana (a-d) and Pinus roxburghii (e-f) across the Koshi River basin. The top green bars represent release events and the bottom brown bars represent suppression events.

et al., 1992; Thapa et al., 2017; Aryal et al., 2018; Sigdel et al., 2018a; Gaire et al., 2019), which we interpret as evidence of the strong human use of these forests. Sikri, which is a religiously protected forest, has the oldest living trees and relatively high values of Rbar compared to the other sites. The SNR is low but comparable to several other studies across the central Himalayas (Thapa et al., 2013; Kharal et al., 2017; Gaire et al., 2017b). As part of the forest management practices, community forests in Nepal are regularly thinned by cutting old-appearing trees for improved growth of the rest of the trees as well as to meet local timber demand (Dangal et al., 2017; Rana et al., 2017). Furthermore, the annual growth rate of both pine species is very low compared to pine trees in central and western Nepal (Aryal et al., 2018; Sigdel et al., 2018a) as well as other species across the country with much greater ages (Kharal et al., 2017; Panthi et al., 2017), which suggest these Koshi trees are growing under stress conditions created by climate, humans, or a combination of both factors.

3.5.2 Climatic influences in the growth of Koshi pine trees

Despite subtle differences in climate signals between the sites, overall, moisture supply during winter is the primary factor limiting growth of pine trees at most of the sites in the Koshi River basin as indicated by common positive correlations with winter rainfall and negative correlations with winter temperatures. Because winter is the driest season (Figure 3.2), which contributes only 2% of total annual rainfall in the region, small variations in winter moisture supply could be a crucial resource for the overall growth of these pine trees. In other forests, winter rainfall is known to replenish soil moisture balance that can be used by plants during the early growing season (Fritts, 1976; Cleaveland et al., 2003; St. George and Ault, 2014). Rainfall prior to growing season can

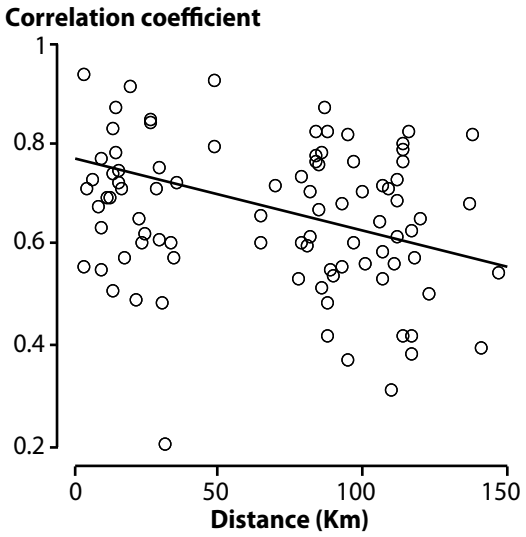

Figure 3.8 Distance-correlation plot showing decreasing coherence in winter precipitation with increasing distance among the fourteen meteorological stations at mid-altitudes of the Koshi River watershed. All correlation coefficient values are significant at 0.01 level.

control the growth of trees in places where temperatures are warm throughout the year for photosynthesis to occur for much longer time in evergreen needles (Fritts, 1976; D'Arrigo and Jacoby, 1991; Cleaveland et al., 2003). The mean winter temperatures in the study area (Figure 3.2) never drops below the minimum threshold of 6 degrees C required for trees to enter dormancy (Körner and Paulsen, 2004; Alvarez-Uria and Körner, 2007). A warmer winter could enable the early onset of the growing season, but we lack information on cambial activity of pines in the region to confirm that effect. The differences in climate signals we observe across our network might be due to differences in topography, altitude, slope, aspect and microclimate (Dittmar et al., 2003; Babst et al., 2013; Gaire et al., 2017b). Such differences could also be due to rapidly changing rainfall pattern over short distance (Figure 3.8) also discussed earlier as one of the challenges in cross-dating pine chronologies. Because the correlation analyses in this study are based on relatively short periods of overlap between tree-ring chronologies and climate records, we emphasize it is difficult to achieve significant results. Furthermore, human activities might also cause neighboring trees to grow differently irrespective of common climatic control across the stand resulting in weaker correlations with climate.

Our result generally agrees with several studies focused on pine trees across the central Himalaya. Moisture during winter and spring has been reported to limit the growth of *P. roxburghii* in western Nepal (Sigdel et al., 2018a) while only spring moisture was found to be primarily influencing the growth of same species in central Nepal (Aryal et al., 2018). Gaire et al., (2019) also concluded that moisture balance during winter and spring is crucial for the growth of *P. wallichiana*, even though their analysis was based on data from higher elevations compared to the Koshi sites. The

climate response of Koshi pine forests is clearly distinct from those of high-altitude tree species including fir, spruce and birch where growth is primarily limited by spring moisture (Dawadi et al., 2013; Thapa et al., 2013; Liang et al., 2014; Gaire et al., 2017a; Panthi et al., 2017; Shrestha et al., 2017b). In addition, compared to other parts of the nation the climate of eastern Nepal remains dry in winter as the westerlies, which deliver cool-season moisture, are confined largely to western Nepal (Shrestha, 2000; Rajbhandari et al., 2018).

3.5.3 Human disturbances in the Koshi pine forests

Our analysis of release and suppression events during the past hundred years suggests the growths of pine trees in the Koshi River watershed have been historically influenced by human activities. The lack of synchrony in disturbance events, even among close sites, and the overall lower proportion of affected trees compared to the forests elsewhere affected by ecological or climatic agents suggest the identified events are the results of episodic human disturbances specific to each site. Large-scale ecological or climatic disturbances such as insect outbreaks and hurricanes (Büntgen et al., 2009; Fernandes et al., 2018; Trotsiuk et al., 2018) usually affect the growth of a larger proportion of trees within an affected forest. We lack quantitative information on forest exploitation in the Koshi such as number of logged trees, amount of resin tapped, or number of grazing livestock, but during our fieldwork did observe several instances of logging, cattle grazing and resin tapping across the forests. These activities might cause neighboring trees to grow differently, and as a consequence the ring-width chronologies to have weaker common signals. Even though the number of disturbance events depends on the nature of human interventions specific to each forest, both the frequency and intensity of

disturbances in this study are fairly comparable to other global studies over similarly long chronologies (Brienen and Zuidema, 2006; Druckenbrod et al., 2013; Parobeková et al., 2016; Rydval et al., 2016; Petritan et al., 2017; Lemus-Lauzon et al., 2018). Sikri, the only religiously protected forest, had the least number of disturbance events, which suggests humans have a discernible effect on the growth of pine forests elsewhere in the Koshi basin.

Growth releases are indicators of canopy openings (Brienen and Zuidema, 2006; Smith and Brennan, 2006; Zhang et al., 2006), which in the case of Koshi pine forests, might be the result of logging. Forest gaps created by intensive logging increases light availability that can enhance the growth of remaining trees at proximity (Figueira et al., 2008). The occurrence of growth suppressions in *P. roxburghii* sites might be due to the combined effects of bark peelings to tap resins (Papadopoulos, 2013; Genova et al., 2014; Chen et al., 2015) and soil compaction by intensive cattle grazing, while growth reductions in the *P. wallichiana* forests might be a consequence of cattle-induced soil compaction (Jones, 2000; Pulido et al., 2018). Growth reductions following resin extractions might be a result of the increased investment of carbohydrates in the production of resins at the expense of tree growth (van der Maaten et al., 2017). Although its effect depends on soil type and tree species, in general, compaction increases soil's strength (bulk density) and decreases the volume of macropores, which limits ability of roots to effectively transport nutrient and water, as a consequence trees might have reduced growth (Corns, 1988).

It is likely that not all disturbance events evident in these data are caused solely by human activities and some events might be a result of climatic change or combined

effects of climate and humans (Abiyu et al., 2018). For example, growth indices were lowest during 1999–2001 across all four *P. wallichiana* sites, which coincides with a nation-wide record drought year of 1999 (Sigdel and Ikeda, 2010). Furthermore, based on our analysis of rainfall data from 14 weather stations (not shown), we found that 1998–2001 was one of the driest winter periods in the past five decades across the middle altitudes in the Koshi basin. But, in the same interval, two *P. wallichiana* forests (Kunikhop and Junbesi) experienced growth releases while both *P. roxburghii* forests (Salle and Hattisude) experienced growth suppressions.

3.6 Conclusions

Pine forests are the primary sources of timber, firewood, and resins to more than three million people living in the middle mountains of eastern Nepal's Koshi River watershed. Based on our analysis of a new network of pine tree-ring width chronologies, we suggest that both climate and human factors have discernible effects on the growth of *Pinus roxburghii* and *P. wallichiana* forests across the Koshi basin. Even though *P. roxburghii* from the Koshi was particularly challenging to cross-date, it is possible to develop annually resolved tree-ring chronologies from both species. Pine forests across the watershed are young and have weak common signals indicating presence of intensive human use in these forests.

Estimation of growth release and suppression events suggested that pine forests across the Koshi watershed have been historically intervened by humans. The higher frequency of single and continuous multiple suppression events than release events, as well as, low annual growth rates of trees indicate that, overall, human activities have negative effects on the growth of the pine forests in the Koshi basin. We hope this

knowledge will help stakeholders evaluate their current approaches of forest management and conservation and make better-informed future decisions. In addition, future research that specifically discriminates between affected and unaffected trees could provide a more complete picture of human disturbances on forests. For example, collection of samples from only resin-tapped trees is recommended to quantify the effects of resin tapping on the growth of *P. roxburghii*. Structured survey questions to the local community forest user groups and the district forest offices would help produce quantitative information on management practices and resource exploitation specific to each site and enable researchers to better isolate human influences on tree growth.

The growth of pine trees across the Koshi River basin is limited by moisture availability during winter. Because the ring-width chronology at the protected forest at Sikri has a similar climate signal compared to the rest of the sites, we are more confident that winter moisture is important to the growth of Koshi pine forests. This information may be helpful to understand future growth and distribution of pine trees under a changing climate, which could contribute to evidence-based conservation strategies to protect pine forests in eastern Nepal. So far, no attempt has been made to model potential tree distribution movements with climate change in Nepal but studies elsewhere, including the Tibetan Plateau and the Alps (Song et al., 2004; Austin and Van Niel, 2011; Dullinger et al., 2012), have primarily linked tree distribution to summer precipitation. Even though summer is the wettest season in Nepal, it may be important to consider winter moisture to more accurately model future growth and distribution of Koshi pine trees. It is not certain whether rainfall in the watershed will increase or decrease in the coming decades, but the Koshi basin will experience significant warming, particularly

during winter in the near future (Agarwal et al., 2014, 2016; Rajbhandari et al., 2017, 2018). This projected rise in winter temperature is likely to enhance winter drought through increased evapotranspiration (Vicente-Serrano et al., 2010; Trenberth et al., 2014). The growth of these critically important pine forests might therefore be further suppressed by future winter drought affecting eastern Nepal.

3.7 Acknowledgements

We express our gratitude to the Nepal Government's Department of Forests, District Forest Offices and the local community forestry user groups for granting permission to collect samples from pine forests across the Koshi basin. UK Thapa received support from the Department of Geography, Environment and Society and Dr. St. George received a Talle Family Research Award from the College of Liberal Arts at the University of Minnesota to support field work in Nepal. This work would not have been possible without untiring assistance from several graduate and undergraduate students as well as local assistants during field collections. At last, we thank Mr. Paul Krusic (University of Cambridge) and an anonymous reviewer for their constructive feedback that helped improve the quality of this paper substantially.

CHAPTER 4: INCREASINGLY FREQUENT POLEWARD EXCURSIONS BY THE HIMALAYAN SUBTROPICAL JET[3]

4.1 Digest

Since the 1980s, the subtropical jet stream has generally moved poleward, but its behavior varies strongly by region and season. Here we examine the interannual variability and trends in the latitudinal position of the spring subtropical jet over the Himalayas. During the modern period (1948 to 2018), the jet is typically anchored immediately south of the Himalayas, but in four springs (1956, 1971, 1984 and 1999), it moved poleward to pass over Kyrgyzstan and north-west China. A tree-ring-based reconstruction of the interannual variability in spring Himalayan jet latitude indicates that, relative to the past four centuries, such poleward excursions have been more common in the latter half of the 20th century. These new insights into the behavior of the Himalayan subtropical jet can improve spring weather forecasts for the region and provide a real-world target for climate simulations to test whether recent excursions can be attributed to anthropogenic warming.

4.2 Introduction

The subtropical jet (STJ) is a band of high-speed westerly winds located near the tropopause and poleward of the Hadley Cell in both hemispheres (Archer & Caldeira, 2008). Since the 1980s, the STJs in both hemispheres have moved poleward (Archer & Caldeira, 2008; Fu et al., 2006; Maher et al., 2020; Manney & Hegglin, 2018; Pena-Ortiz et al., 2013; Strong & Davis, 2007) and these poleward shifts have largely been attributed

[3] UK Thapa, S St. George and V Trouet. Increasingly frequent poleward excursions by the Himalayan subtropical jet. *Geophysical Research Letters*. Submitted.

to differential tropospheric warming and stratospheric cooling induced by anthropogenic climate change (Fu & Lin, 2011; Wilcox et al., 2012). With continued emissions of anthropogenic greenhouse gases, the STJs are projected to move further poleward in the future (Lu et al., 2007; Seidel et al., 2007). In addition to this general poleward movement, the structure and behavior of the STJs is known to vary strongly by region and season, and those nuances cannot be represented by global or hemispheric annual means (Maher et al., 2020; Manney & Hegglin, 2018; Strong & Davis, 2007).

In regions of high jet speed, synoptic-scale storms tend to form and changes in the behavior of the jet therefore affect their distribution, frequency and intensity (Whitney, 1977). In central Asia, a westerly STJ occurs in all seasons except summer and sits generally between 27° to 30° N (Koteswaram, 1953; Koteswaram et al., 1953; Koteswaram & Parthasarathy, 1954). The STJ acts as an important control on the region's climate during boreal winter and spring by steering the trajectory of the mid-tropospheric storms, commonly known as western disturbances (Dimri et al., 2015). Poleward movements of the STJ in Central Asia allow for the northerly displacement of storms and advection of warm tropical air to higher latitudes (Hunt et al., 2018; Wang et al., 2013; Yin, 2005). Most studies on atmospheric circulation over central Asian have primarily focused on investigating changes in the behavior of western disturbances (Cannon et al., 2016, 2017; Madhura et al., 2014). The dynamics of the STJ have been examined for East Asia (Kuang & Zhang, 2005; Schiemann et al., 2009; Wang et al., 2013; Zhongda & Riyu, 2005), but the behavior of the STJ over central Asia has not received the same attention.

We examine the interannual variability and trend in the 'latitudinal position of the spring STJ over central Asia and over the Himalayas in particular (Himalayan Jet Latitude or HJL, hereafter) over modern and pre-instrumental periods. The HJL influences the distribution of western disturbances (Hunt et al., 2018), which are important contributions to the mass balance of Himalayan glaciers (Cannon et al., 2014; Lang & Barros, 2004). Better understanding of variability of the HJL may help predict its future position, which in turn can improve the accuracy of dry season weather forecasts (Hunt et al., 2018). We show that, although the spring HJL is typically anchored south of the Himalayas, during the last six decades it has on occasions moved northward and adopted a route passing over Kyrgyzstan and north-west China. In other regions, including east Asia, the North Atlantic, and the North Pacific, tree-ring-based reconstructions of jetstream latitude have been used to place recent behavior in a multi-century context (Trouet et al., 2018; Wahl et al., 2019; Wright et al., 2015). In order to determine whether the recent poleward shifts of the Himalayan jet are unusual, we produce a new proxy estimate of its spring latitudinal position that spans the past four centuries (C.E. 1625 to 2003; hereafter all dates will be referred as Common Era, C.E.). We also investigate the impacts of extreme northerly positions of the Himalayan jet on regional climate during both modern and pre-instrumental periods.

4.3 Data and methods

4.3.1 Himalayan jet latitude calculation

In the Northern Hemisphere, the spring STJ moves generally in an eastward direction. It exits North Africa and passes through the Middle East to encounter the southern edge of the Himalayas (at approximately 29° N) before entering into East Asia and the Pacific

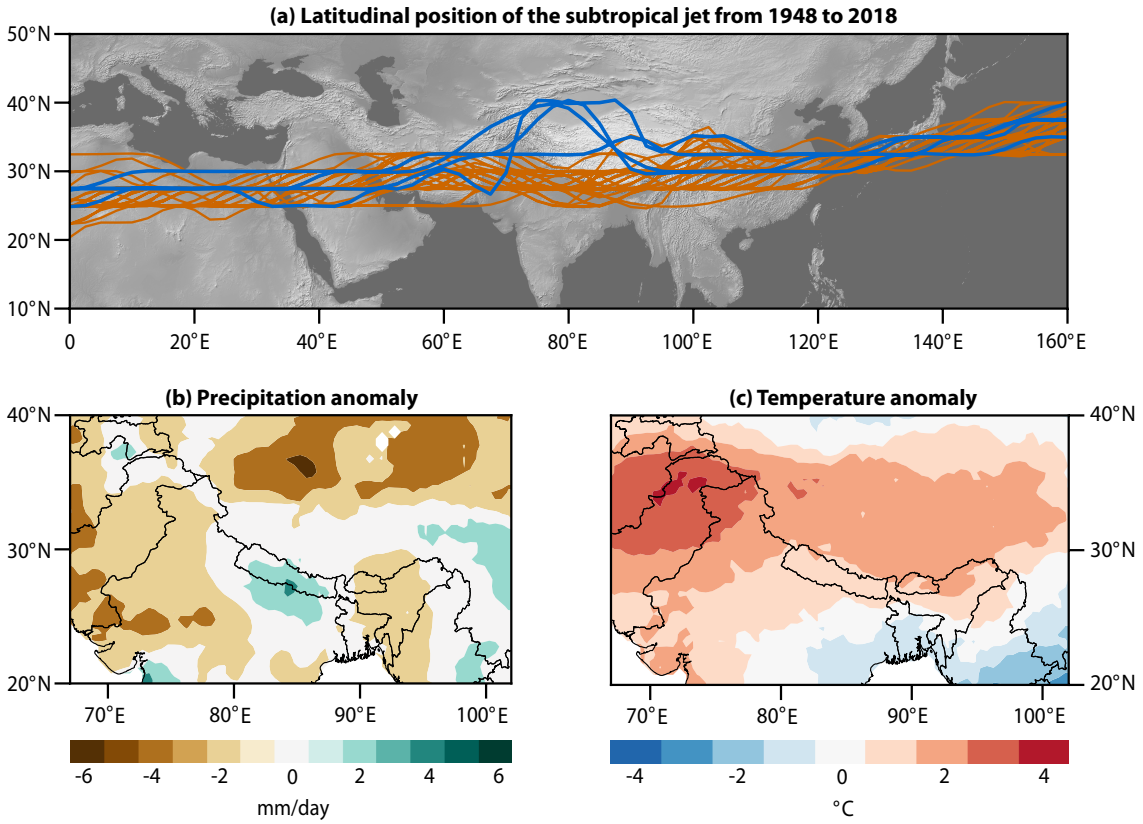

Figure 4.1 (a) Latitudinal position of the spring (March-May) subtropical jet (STJ) for each year from 1948 to 2018 over the window that extends from north Africa to the Pacific. The blue lines represent the four years (1956, 1971, 1984 and 1999) when the STJ moved poleward to a position over central Asia, while the orange lines show the jet's position for all other years. The latitude of the STJ was calculated by locating the position of the maximum March-May wind speed at 200 mb for every 2.5° of longitude using NCEP/NCAR reanalysis data (Kalnay et al., 1996). Composites of spring (b) precipitation (mm/day) and (c) temperature (°C) for the four years when the Himalayan jet was positioned anomalously poleward. Composites are based on the CRU TS 4.03 gridded climate data (1901-2018; Harris et al., 2014).

(Hunt et al., 2018; Koteswaram & Parthasarathy, 1954). Because the STJ typically passes just southward of the Himalayas, we created an index of the latitudinal position of the spring STJ that encompasses the Himalayan region (70 to 95° E; 20 to 40° N). That index, which we describe as the Himalayan jet latitude (HJL), is calculated using the NCEP/NCAR gridded (2.5° × 2.5°) monthly scalar wind (m/s) at 200 mb for the period of 1948 to 2018 (Kalnay et al., 1996; Text S1). For each longitudinal grid cell, the position of the Himalayan jet was defined as the latitude corresponding to the maximum average spring wind speed (Barton & Ellis, 2009; Koch et al., 2006; Trouet et al., 2018). We also identified cases where the central position of the STJ in the Himalaya region moved substantially (two or more standard deviations above or below the mean) north or southward, which we describe as "poleward" or "equatorward" excursions, respectively. To examine the relationship between Himalayan jet position and the region's climate, we used gridded (0.5° × 0.5°) CRU TS 4.03 average monthly temperature and total monthly precipitation (Harris et al., 2014).

4.3.2 Tree-ring reconstruction of the Himalayan jet latitude

Prior to the 1960s, when radiosonde stations were introduced over the Himalayas, estimates of the HJL rely strongly on stations over the Indian sub-continent and southern China (Durre et al., 2006, 2018). The time series of direct observations of atmospheric circulation over the Himalayas is therefore limited in length and we extended the instrumental HJL time series using regional tree- ring chronologies. For this purpose, we selected 23 tree-ring width chronologies located in the Himalayan regions of Pakistan, India, Nepal and Bhutan that (i) are sensitive to the same aspects of spring climate that are influenced by the HJL (i.e. positively correlated with regional spring precipitation

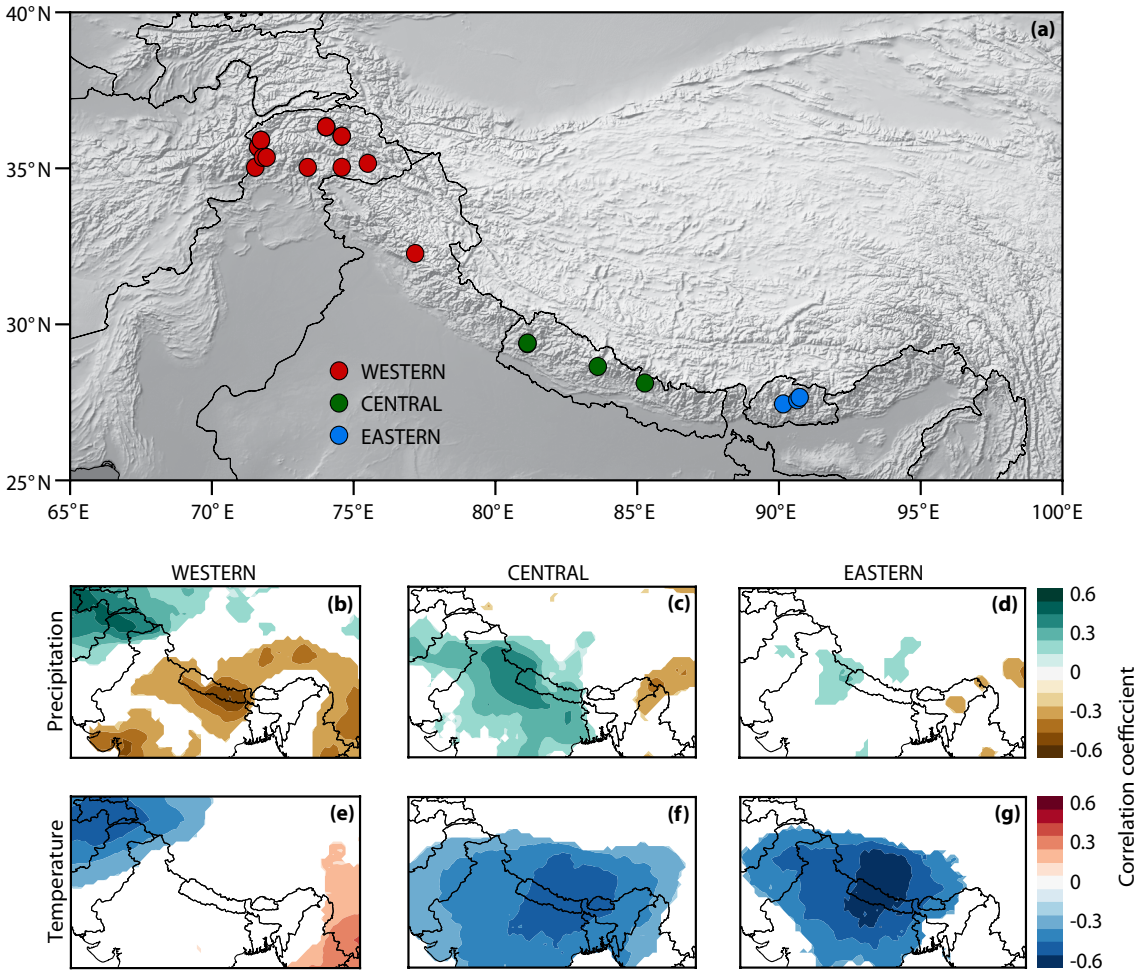

Figure 4.2 (a) Locations of 23 tree-ring chronologies from Pakistan, Indian, Nepal and Bhutan used as predictors for our Himalayan jet latitude reconstruction. The red, blue, and green dots represent the tree-ring records clustered into WESTERN, CENTRAL, and EASTERN regional composite chronologies, respectively. Maps showing the correlation between each regional composite chronology and spring precipitation (b-d) and temperature (e-g) over the 1901 to 2003 period. Only those values significant at 0.05 level are shaded.

and/or negatively correlated with spring temperature), and (ii) correlated significantly with the HJL (Figure 4.2a-g, see Appendix A: Text S2 and Table S1). Based on their locations and degree of coherence (see Appendix A: Figure S7), we combined the 23 tree-ring records in three regional composite chronologies (Figure 4.2a, see Appendix A: Text S3) representing Pakistan and India (WESTERN), Nepal (CENTRAL), and Bhutan (EASTERN). Each composite chronology was developed by combining all individual ring-width series from each contributing site chronology within that region (Figure 4.3; Alfaro-Sánchez et al., 2018; Trouet, 2014).

To reconstruct the spring HJL prior to the modern period, we performed a stepwise linear regression of the modern HJL against the three regional chronologies, but only WESTERN and EASTERN composite chronologies were retained for reconstruction. We used a split calibration-verification method to test the reconstruction skill of the regression model over two sub-periods: (1948-1977 and 1978-2003). The calibration and verification sub-periods were then switched to 1974-2003 and 1948-1973. Commonly used statistics such as explained variance over the calibration period, and reduction of error (RE) and coefficient of efficiency (CE) over the verification period were used to evaluate the model's fidelity (Cook et al., 1999). We estimated uncertainty in the reconstruction using the standard error of the regression model.

4.3.3 Himalayan jet latitude variance and trend estimation

We examined HJL variability over time by calculating the coefficient of variance as well as the number of jet excursions over a moving 31-year window. We performed Mann-Kendall (M-K) tests (Hamed & Rao, 1998) to check the presence of significant

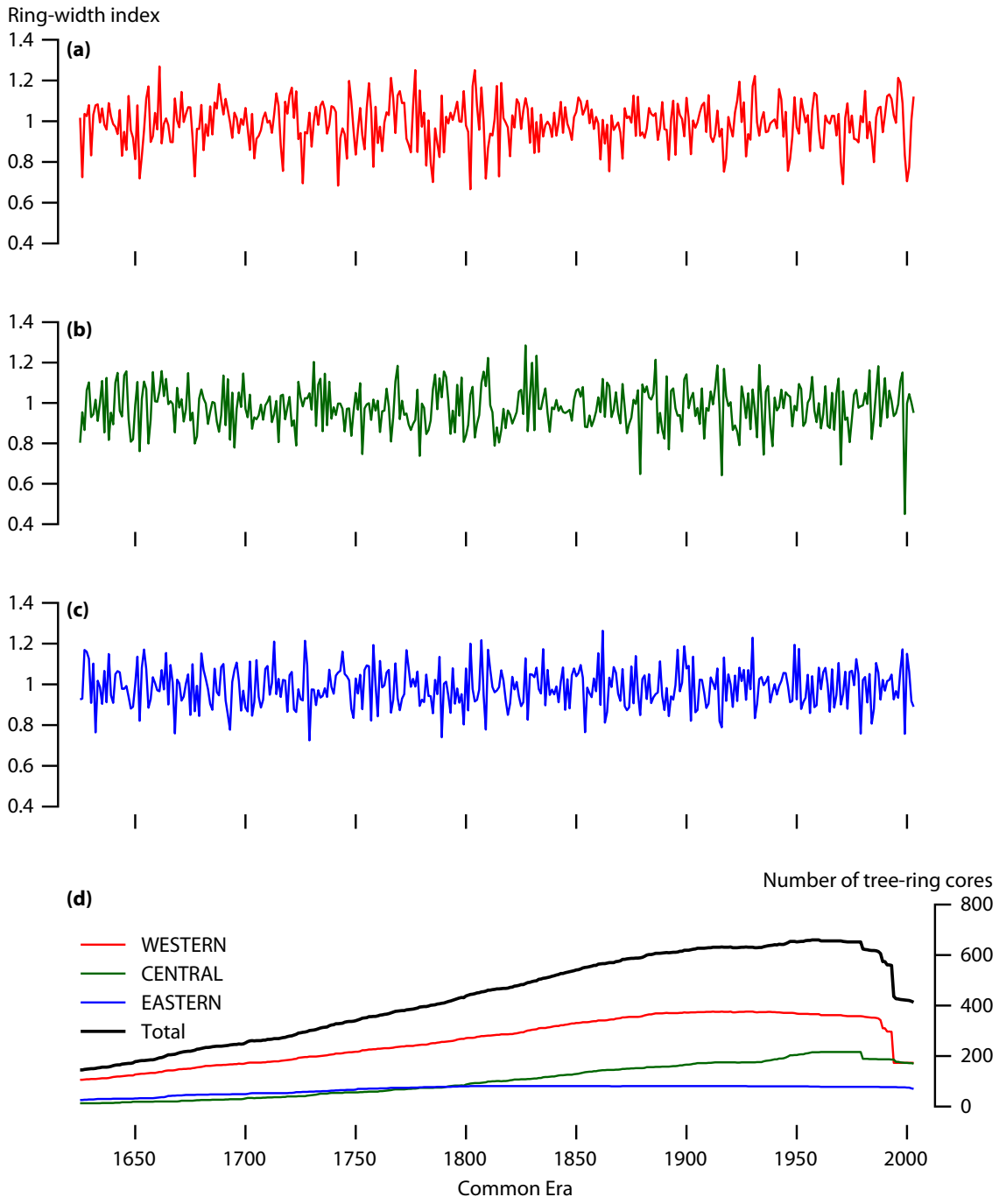

Figure 4.3 (a) WESTERN, (b) CENTRAL and (c) EASTERN composite chronologies and (d) the number of tree-ring series included in each composite. Only portions of the chronologies used in the Himalayan jet latitude reconstruction (1625-2003) are shown.

monotonic trends in HJL over the modern and pre-instrumental periods, as well as in the running variance over the reconstruction period.

4.4 Results and discussion

4.4.1 Himalayan jet latitude variability over the modern period (1948-2018)

Within the broader region that extends from north Africa to the Pacific, the latitudinal position of the STJ is most variable near the Himalayas (Figure 4.1a). In most springs, the Himalayan jet is anchored near its mean position at 29º N, but in some years (1956, 1971, 1984 and 1999) it moved substantially poleward, up to 37.5º N. During those years of extreme northerly displacements, the jet extended up to Kyrgyzstan and north-west China escaping the Himalayas and the Tibetan Plateau before re-acquiring its normal track and continuing over southeast China and farther east (Figure 4.1a). Conversely, the Himalayan jet did not make a single equatorward excursion during the modern period.

The HJL did not exhibit a significant linear trend during the modern period (M-K tau = 0.012, p-value = 0.88), which matches the observed behavior of the STJ over East Asia (Kuang & Zhang, 2005; Zhongda & Riyu, 2005). This lack of trend in STJ over Asia differs from the recent observed poleward displacements of other regional STJs, including those over the east Pacific and the Middle East (Fu & Lin, 2011; Maher et al., 2020; Strong & Davis, 2007) as well as the global mean STJs and Hadley Cell (Manney & Hegglin, 2018; Pena-Ortiz et al., 2013; Staten et al., 2018). However, these trends have been found to be season-specific and their magnitude depends on the data and metrics used (Adam et al., 2014; D'Agostino & Lionello, 2017; Grise et al., 2018). For instance, the expansion of the Hadley Circulation in the Northern Hemisphere has shown a

significant northward trend (1979-2014) in summer and fall, but not in winter or spring (Alfaro-Sánchez et al., 2018).

When the HJL is displaced northwards, most parts of central Asia experience anomalously hot and dry springs. The HJL is significantly ($p < 0.1$) negatively correlated with spring precipitation over much of the Himalayan foothills and plains in western Asia, including Afghanistan, Pakistan, and western and central India (see Appendix A: Figure S2a), but it is significantly positively correlated with spring temperature across all parts of central Asia, including the southern plains, the entire Himalayan range and the Tibetan Plateau (see Appendix A: Figure S2b). Similarly, during the four poleward excursions, spring precipitation was anomalously low over Afghanistan, Pakistan, western and central India, northern China and the eastern Himalayas of Bhutan and India (Figure 4.1b), whereas spring temperature was anomalously warm across most of central Asia (Figure 4.1c). These findings are consistent with high temperature and low precipitation anomalies observed in East Asia and North Africa associated with the poleward displacements of their respective regional STJs (Ambrosino et al., 2011; Gaetani et al., 2011; Kuang & Zhang, 2005; Schiemann et al., 2009; Wang et al., 2013; Zhao et al., 2014). The lack of significant correlations between the HJL and spring precipitation, as well as neutral precipitation composites across the high-altitude mountains and the Tibetan Plateau during the years of poleward excursions, might be caused by difficulties in representing hydroclimatic variability associated with such complex topography in the reanalysis and gridded products (Henn et al., 2018; Herrera et al., 2019; Hussain et al., 2017). Overall, our results support the concept that when the STJ is displaced poleward, storms are also allowed to shift farther north and warm tropical air

Table 4.1 Calibration and verification statistics for the Himalayan jet latitude reconstruction model.

Calibration period	R^2	R^2adj	Verification period	Correlation ($p < 0.001$)	Reduction of Error	Coefficient of Efficiency
Full period 1948-2003	47.6	44.6	-	-	-	-
First half 1948-1977	56.5	51.5	Second half 1978-2003	0.62	0.16	0.16
Second half 1974-2003	53.5	48.1	First half 1948-1973	0.45	0.21	0.21

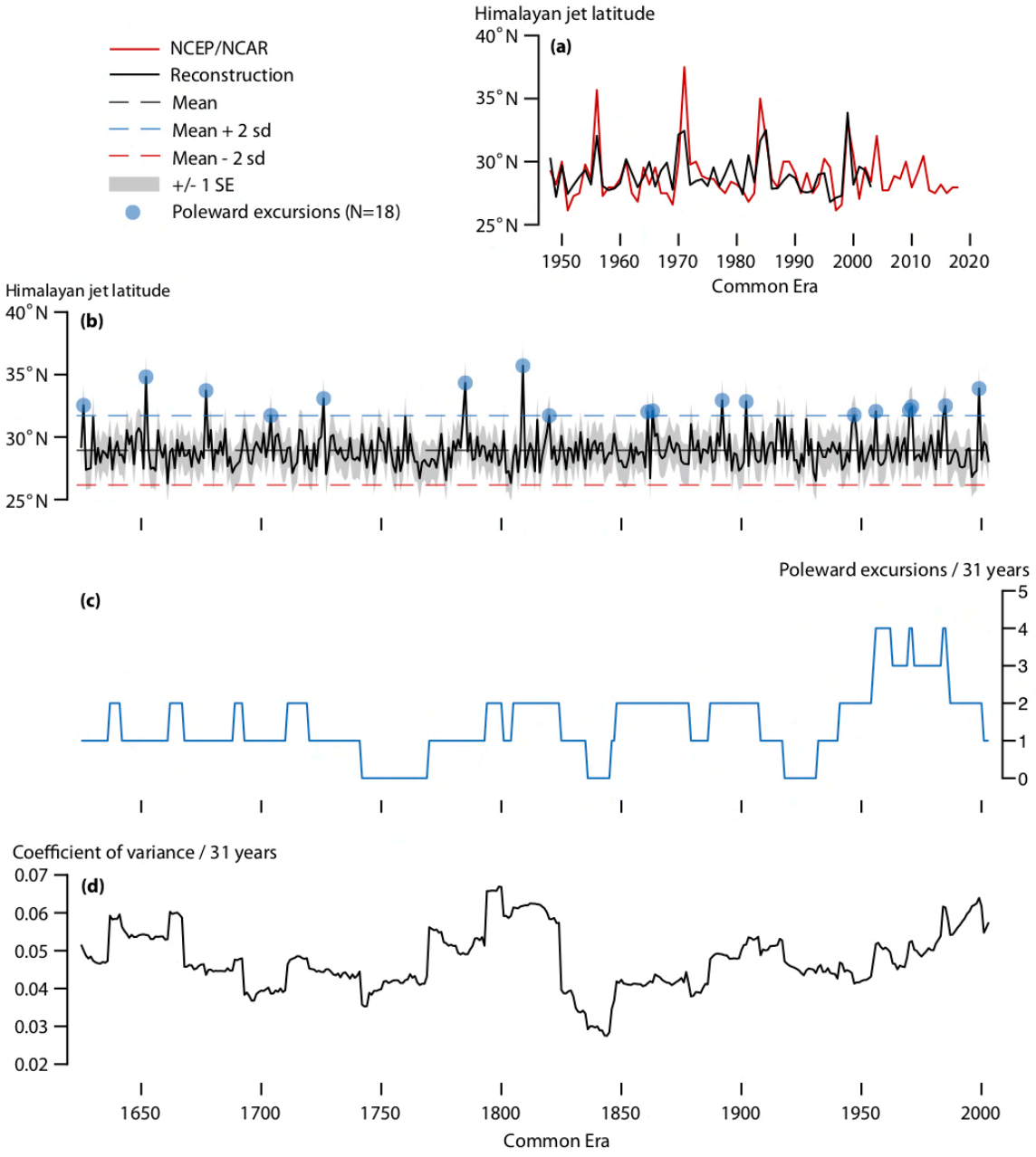

Figure 4.4 Multi-century reconstruction of the latitude of the spring Himalayan jet (HJL). (a) Comparison of NCEP/NCAR reanalysis-based (Kalnay et al., 1996; red line) and tree-ring based (black line) spring HJL (1948-2018). (b) HJL reconstruction (1625-2003; black line). The grey shading represents the standard error of estimate (+/- 1 SE) of the regression model. The dashed blue (red) line represents + (-) two standard deviations (sd) from the mean, which is marked by the dashed black line. The blue dots mark the years

of poleward HJL excursions (latitude greater than two standard deviations from the mean). (c) The number of poleward excursions and (d) coefficient of variance (standard deviation/mean) of the reconstructed HJL computed for a running 31-year window.

is able to advect into the higher latitudes, the combination of which makes the regions near the mean jet latitude drier than usual (Wang et al., 2013; Yin, 2005).

4.4.2 Pre-instrumental (1625-2003) Himalayan jet latitude variability

Our reconstruction model based on tree-ring chronologies explains 45% of the variance in observed spring HJL variability and is able to reproduce the four poleward Himalayan jet excursions in the modern period (Figure 4.4a). Both RE and CE verification statistics were positive, indicating the model's skill in reproducing interannual spring HJL variability (Table 4.1). We limit our reconstruction to the period 1625-2003, the period with adequate tree-ring sample replication to explain the population-level signal as judged by the Expressed Population Signal, a standard metric in dendroclimatology (Wigley et al., 1984; see Appendix A: Text S4).

Over the past four hundred years, we identified 13 cases of poleward HJL excursions (Figure 4.4b, Table 4.2), but no equatorward excursions. We found no significant linear trend in the mean HJL over the pre-instrumental period (M-K tau = 0.002, p-value = 0.95), but we did find a significant positive trend in HJL variance since 1850 (M-K tau = 0.487, $p < 0.0001$) that is most pronounced after 1950 (M-K tau = 0.65, $p < 0.0001$) (Figure 4.4d). The HJL variance also displayed a significantly positive trend from 1750-1800 (M-K tau = 0.57, $p < 0.0001$) and a negative trend from 1625-1750 (M-K tau = -0.499, $p < 0.0001$) and 1800-1850 (M-K tau = -0.625, $p < 0.0001$).

The poleward HJL excursions identified for the modern period are not thus not unprecedented over the past 400 years, but such displacements have become more common in recent decades, with the highest number of cases per century (seven) in the latter half of the 20th century (Figure 4.4c). The enhanced HJL variability since the 1950s

Table 4.2 Tree-ring reconstructed Himalayan jet latitudes (HJLs) during the poleward excursion years. Poleward excursions were identified when the latitude for any given year exceeded two standard deviations from the mean HJL over the reconstruction period.

Year	Himalayan jet latitude (reconstruction)
1626	32.534
1652	34.813
1677	33.716
1704	31.723
1726	33.079
1785	34.332
1809	35.703
1820	31.709
1861	32.011
1863	32.094
1892	32.931
1902	32.841
1947	31.764
1956	32.047
1970	32.149
1971	32.439
1985	32.5
1999	33.88

is consistent with the recent observed jet stream behavior elsewhere. Studies based on observations and models have demonstrated enhanced variability in the Northern Hemisphere midlatitude circulation and occurrence of extreme weather since the middle of the twentieth century and have related this to the anthropogenic climate change (Barnes & Polvani, 2013; Coumou et al., 2015; Francis & Vavrus, 2012; Mann et al., 2017). Tree-ring reconstructions have also shown that, like the HJL, latitudianl jet stream positions over East Asia, the North Pacific and the North Atlantic do not show long-term linear trends in their mean positions, but have exhibited unprecedented enhanced variance in recent decades (Trouet et al., 2018; Wright et al., 2015). Similar to our HJL results, the North Atlantic jet also experienced its highest number of positive extremes (poleward excursions) during the 20th century (Trouet et al., 2018).

Because interannual HJL variability is known to influence spring precipitation and temperature variability across central Asia (Hunt et al., 2018; Wang et al., 2013; Yin, 2005), we explored whether the broader region experienced drought during the years of poleward HJL excursions as identified in the reconstruction. For that purpose, we used the Monsoon Asia Drought Atlas (MADA), a tree-ring based reconstruction of a summer (June-July-August) drought metric (Cook et al., 2010), the Palmer Drought Severity Index (PDSI), that measures the status of soil moisture balance not only during summer, but also during earlier seasons or years (Palmer, 1965). During years of poleward HJL excursions (N=18; Table 4.2), much of west-central Asia experienced extreme summer drought (Figure 4.5). We acknowledge that most chronologies used in our reconstruction overlap with MADA tree-ring network, but there are also several independent tree-ring predictors from Kyrgyzstan and western China included in the MADA that show negative

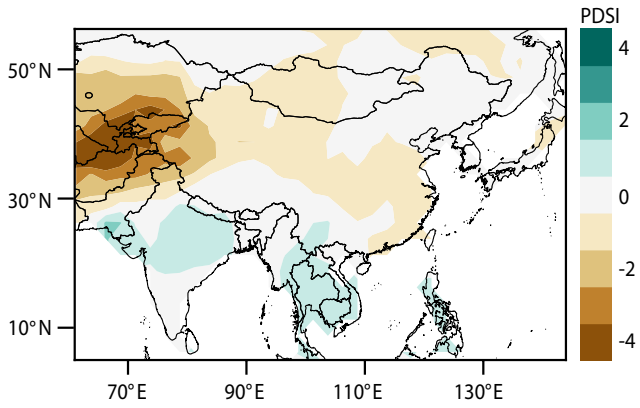

Figure 4.5 Map showing the composite summer (June-July-August) drought (Palmer Drought Severity Index, PDSI) index for monsoon Asia (Cook et al., 2010) associated with poleward excursions of the Himalayan subtropical jet , as reconstructed from tree rings.

PDSI values in those regions coincident with our poleward excursions. That agreement suggests that the northward HJL displacement might have pushed spring storms farther north than normal and created drought conditions that persisted until summer. The lack of drought in the central and eastern Himalayas during poleward HJL shifts might be related to the stronger effects of the western disturbances in the western Himalayas compared to their central and eastern counterparts (Dimri et al., 2015).

4.5 Conclusions

The position of the Himalayan subtropical jet during winter and spring is known to influence the region's climate by modulating storm tracks and meridional flow of warm tropical air (Hunt et al., 2018; Wang et al., 2013). In recent decades (post-1950), the Himalayan jet typically strikes immediately south of the Himalayas, but has also made rare poleward excursions. Our tree-ring reconstruction suggests that such HJL excursions are not unprecedented over the past four centuries, but that they have become more common in recent decades. We also show that the Himalayas experience hot and dry weather when the Himalayan jet moves north of the region. Based on these results, we suggest incorporating the HJL into forecasting models produced by meteorologists (Dimri & Mohanty, 2009; Joshi et al., 2017; Moore & Semple, 2004) to improve the accuracy of spring weather predictions in the Himalayas. Our reconstruction further suggests that the HJL has become increasingly variable, and therefore less reliable, in recent decades, which may pose a challenge to anticipating spring weather in the region.

Globally, the mean position of the subtropical jet stream has moved poleward in recent decades, and this general trend has held true for several regions (Archer & Caldeira, 2008; Manney & Hegglin, 2018; Strong & Davis, 2007). However, the mean

HJL shows no sign of following the same trajectory. This result, which could reflect the influence of land-ocean distribution (Hoskins & Valdes, 1990) and orographic effects (Held et al., 2002) confirms the unique character of the Himalayan jet in a global context. Because spring trends appear to be different for this region, it may be necessary to conduct season- and region-specific analysis of jet stream behavior, as recommended by prior studies (Grise et al., 2018; Maher et al., 2020, Belmecheri et al. 2017).

In recent decades, the HJL has shown more frequent poleward excursions and enhanced interannual variability. This behavior is unusual in the context of the past four centuries, but the drivers of that change are not known. Model-based studies have shown that the summer STJ over the larger Asian domain moved generally poleward during the Medieval Climate Anomaly due to a combination of several factors including an El Niño-like Pacific Ocean, warm Indian Ocean, large volcanic eruptions, and higher solar irradiance (Fallah et al., 2016; Jiang et al., 2020). Our multi-century HJL proxy could be used as a real-world target to compare against long model simulations, and thereby determine whether the apparent increase in the frequency of poleward excursions is due to natural climate variability or anthropogenic climate change.

4.6 Acknowledgements

Support for this work was provided by fellowships to Uday Thapa from the University of Minnesota's Graduate School and Department of Geography, Environment and Society and the Bell Museum of Natural History. This work also benefited from a Talle Family Research Award from the University of Minnesota's College of Liberal Arts.

References

Abiyu A, Mokria M, Gebrekirstos A, et al. (2018) Tree-ring record in Ethiopian church forests reveals successive generation differences in growth rates and disturbance events. *Forest Ecology and Management* 409: 835–844.

Adam O, Schneider T and Harnik N (2014) Role of changes in mean temperatures versus temperature gradients in the recent widening of the Hadley circulation. *Journal of Climate* 27:7450–7461.

Adhikari B, Di Falco S, Lovett JC, et al. (2004) Household characteristics and forest dependency: Evidence from common property forest management in Nepal. *Ecological Economics* 48: 245–257.

Agarwal A, Babel MS, Maskey S, et al. (2016) Analysis of temperature projections in the Koshi River Basin, Nepal. *International Journal of Climatology* 279: 266–279.

Agarwal, A., Babel, M.S., Maskey, S., et al. (2014) Analysis of future precipitation in the Koshi River basin, Nepal. *Journal of Hydrology* 513, 422–434.

Ahmed M and Zafar MU (2014) The status of tree-ring analysis in Pakistan. *Fuuast Journal of Biology* 4: 13–19.

Akhtar M, Ahmad N and Booij MJ (2008) The impact of climate change on the water resources of Hindukush-Karakorum-Himalaya region under different glacier coverage scenarios. *Journal of Hydrology* 355: 148–163.

Alfaro-Sánchez R, Nguyen H, Klesse S, et al. (2018) Climatic and volcanic forcing of tropical belt northern boundary over the past 800 years. *Nature Geoscience* 11: 933–938.

Allen CD, Macalady AK, Chenchouni H, et al. (2010) A global overview of drought and heat-induced tree mortality reveals emerging climate change risks for forests. *Forest Ecology and Management* 259: 660–684.

Altman J, Fibich P, Dolezal J, et al. (2014) TRADER: A package for tree ting analysis of disturbance events in R. *Dendrochronologia* 32: 107–112.

Alvarez-Uria P and Körner C (2007) Low temperature limits of root growth in deciduous and evergreen temperate tree species. *Functional Ecology* 21: 211–218.

Ambrosino C, Chandler RE and Todd MC (2011) Southern African monthly rainfall variability: An analysis based on generalized linear models. *Journal of Climate* 24: 4600–4617.

Anchukaitis KJ, Buckley BM, Cook ER, et al. (2010) Influence of volcanic eruptions on the climate of the Asian monsoon region. *Geophysical Research Letters* 37: 1-5.

Anderegg WRL, Schwalm C, Biondi F, et al. (2015) Pervasive drought legacies in forest ecosystems and their implications for carbon cycle models. *Science* 349: 528-532.

Applegate GB and Gilmour DA (1988) Biomass and productivity estimations for community forest management: A case study from the Hills of Nepal – I. Biomass and productivity of chir pine (Pinus roxburghii Sargent) plantations. *Biomass* 17: 115–136.

Archer CL and Caldeira K (2008) Historical trends in the jet streams. *Geophysical Research Letters* 35. doi: 10.1029/2008GL033614.

Aryal S, Bhuju DR, Kharal DK, et al. (2018) Climatic upshot using growth pattern of Pinus roxburghii from western Nepal. *Pakistan Journal of Botany* 50: 579–588.

Austin MP and Van Niel KP (2011). Improving species distribution models for climate change studies: Variable selection and scale. *Journal of Biogeography* 38: 1–8.

Babst F, Poulter B, Trouet V, et al. (2013) Site- and species-specific responses of forest growth to climate across the European continent. *Global Ecology and Biogeography* 22: 706–717.

Baral SK, Malla R and Ranabhat S (2009) Above-ground carbon stock assessment in different forest types of Nepal. *Banko Janakari* 19: 10–14.

Barnes EA and Polvani L (2013). Response of the midlatitude jets, and of their variability, to increased greenhouse gases in the CMIP5 models. *Journal of Climate* 26: 7117–7135.

Barton NP and Ellis AE (2009) Variability in wintertime position and strength of the North Pacific jet stream as represented by re-analysis data. *International Journal of Climatology* 29: 851–862.

Battipaglia G, Jaggi M, Saurer M, et al. (2008) Climatic sensitivity of δ18O in the wood and cellulose of tree rings: Results from a mixed stand of Acer pseudoplatanus L. and Fagus sylvatica L. *Palaeogeography Palaeoclimatoly Palaeoecology* 261: 193–202.

Beldring S and Vokso A (2012) Climate change impact on flow regimes of rivers in Bhutan and possible consequences for hydropower development. *Hydro Nepal: Journal of Water, Energy and Environment* 11: 67–68.

Belmecheri S, Babst F, Hudson AR, et al. (2017) Northern Hemisphere jet stream position indices as diagnostic tools for climate and ecosystem dynamics. *Earth Interactions* 21: 1-23.
Bhandari S, Gaire NP, Shah SK et al. (2019) A 307-year tree-ring SPEI reconstruction indicates modern drought in western Nepal Himalayas. *Tree-Ring Research,* 75: 73–85.
Bhattacharyya A and Shah SK (2009) Tree-ring studies in India past appraisal, present status and future prospects. *IAWA Journal* 30: 361–370.
Bhattacharyya A, Lamarche Jr VC and Hughes MK (1992) Tree-ring chronologies from Nepal. *Tree-Ring Bulletin* 52: 59–66.
Bhuju DR (2016) Nepal tree ring study updates. *Dendrochronologia* 38: 117.
Bhutiyani MR, Kale VS and Pawar NJ (2010) Climate change and the precipitation variations in the northwestern Himalaya: 1866-2006. *International Journal of Climatology* 30: 535–548.
Biemans H, Siderius C, Lutz AF, et al. (2019) Importance of snow and glacier meltwater for agriculture on the Indo-Gangetic Plain. *Nature Sustainability* 2: 594–601.
Birch JC, Thapa I, Balmford A, et al. (2014) What benefits do community forests provide, and to whom? A rapid assessment of ecosystem services from a Himalayan forest, Nepal. *Ecosystem Services* 8: 118–127.
Bocchiola D and Diolaiuti G (2013) Recent (1980-2009) evidence of climate change in the upper Karakoram, Pakistan. *Theoretical and Applied Climatology* 113: 611–641.
Bollasina MA, Ming Y and Ramaswamy V (2011) Anthropogenic aerosols and the weakening of the South Asian summer monsoon. *Science* 334: 502–505.
Bräuning A (2004) Tree-ring studies in the Dolpo-Himalya (western Nepal). In: Jansma, E., Bräuning, A., Schlesser (Eds.), *Proceedings of the DENDROSYMPOSIUM 2003. TRACE-Tree Rings in Archaelogy, Climatology and Ecology*, Utrecht. pp. 8–12.
Bretfeld M, Doerner JP and Franklin SB (2015) Radial growth response and vegetative sprouting of aspen following release from competition due to insect-induced conifer mortality. *Forest Ecology and Management* 347: 96–106.
Brienen RJW and Zuidema PA (2006) Lifetime growth patterns and ages of Bolivian rain forest trees obtained by tree ring analysis. *Journal of Ecology* 94: 481–493.
Briffa KR, Schweingruber FH, Jones PD, et al. (1998) Reduced sensitivity of recent tree-growth to temperature at high northern latitudes. *Nature* 391: 6678-6678.
Büntgen U, Frank D, Liebhold A, et al. (2009) Three centuries of insect outbreaks across the European Alps. *New Phytologist* 182: 929–941.
Camarero JJ, Bigler C, Carlos J, et al. (2011) Synergistic effects of past historical logging and drought on the decline of Pyrenean silver fir forests. *Forest Ecology and Management* 262: 759–769.
Camarero JJ, Sangüesa-Barreda G, Montiel-Molina C, et al. (2018) Past growth suppressions as proxies of fire incidence in relict Mediterranean black pine forests. *Forest Ecology and Management* 413: 9–20.
Cannon F, Carvalho LMV, Jones C, et al. (2017) The influence of tropical forcing on extreme winter precipitation in the western Himalaya. *Climate Dynamics* 48: 1213-1232.
Cannon F, Carvalho LMV, Jones C, et al. (2014) Multi-annual variations in winter westerly disturbance activity affecting the Himalaya. *Climate Dynamics* 44: 441–455.
Cannon F, Carvalho LMV, Jones C, et al. (2016) Winter westerly disturbance dynamics and precipitation in the western Himalaya and Karakoram: A wave-tracking approach. *Theoretical and Applied Climatology* 125: 27–44.
Central Bureau of Statistics (2012) *National Population and Housing Census 2011*. Central Bureau of Statistics (CBS), Kathmandu.
Chand N, Kerr GN and Bigsby H (2015) Production efficiency of community forest management in Nepal. *Forest Policy Economics* 50: 172–179.
Chave J, Rejou-Mechain J, Burgues A, et al. (2014) Improved allometric models to estimate the aboveground biomass of tropical trees. *Global Change Biology* 20: 3177-3190.
Chen F, Yuan Y, Yu S. et al. (2015) Influence of climate warming and resin collection on the growth of Masson pine (Pinus massoniana) in a subtropical forest, southern China. *Trees* 29: 1423–1430.
Chen J, Chen F, Feng S, et al. (2015) Hydroclimatic changes in China and surroundings during the Medieval Climate Anomaly and Little Ice Age: Spatial patterns and possible mechanisms. *Quaternary Science Reviews* 107: 98-111.

Chen X, Zhong Z and Lu W (2017) Association of the poleward shift of East Asian subtropical upper-level jet with frequent tropical cyclone activities over the Western North Pacific in summer. *Journal of Climate* 30: 5597–5603.
Cherubini P (2015) Enigmatic high-Asian tree rings: A postcard from the roof of the world (Kathmandu, Nepal). *Dendrochronologia* 34: 31-32.
Cleaveland MK, Stahle DW, Therrell MD, et al. (2003) Tree-ring reconstructed winter precipitation and tropical teleconnections in Durango, Mexico. *Climatic Change 59*: 369–388.
Cole-Dai J, Ferris D, Lanciki A, et al. (2009) Cold decade (AD 1810-1819) caused by Tambora (1815) and another (1809) stratospheric volcanic eruption. *Geophysical Research Letters* 36, L22703. doi:10.1029/2009GL040882.
Cole-Dai J, Mosley-Thompson E and Thompson LG (1997) Annually resolved southern hemisphere volcanic history from two Antarctic ice cores. *Journal of Geophysical Research* 102: 761-771.
Compo GP, Whitaker JS, Sardeshmukh PD et al. (2011) The Twentieth Century Reanalysis Project. *Quarterly Journal of the Royal Meteorological Society* 137: 1–28.
Cook ER (1987) The decomposition of tree-ring series for environmental studies. *Tree-Ring Bulletin 47*: 37-59.
Cook ER and Kairiukstis L (1990) *Methods of Dendrochronology: Applications in the Environmental Sciences.* Kluwer Academic Publishers, Dordrecht.
Cook ER and Krusic PJ (2008) Experimental reconstruction of large-scale summer monsoon drought over India and the Tibetan Plateau using tree rings from "High Asia". *Palaeobotanist* 57: 515-528.
Cook ER and Peters K (1981) The smoothing spline: A new approach to standardizing forest interior tree-ring width series for dendroclimatic studies. *Tree-Ring Bulletin* 41:45–55.
Cook ER, Anchukaitis KJ, Buckley BM, et al. (2010) Asian monsoon failure and megadrought during the last millennium. *Science* 328: 486-489.
Cook ER, Krusic PJ and Jones PD (2003) Dendroclimatic signals in long tree-ring chronologies from the Himalayas of Nepal. *International Journal of Climatology* 23: 707-732.
Cook ER, Krusic PJ, Anchukaitis KJ, et al. (2013a) Tree-ring reconstructed summer temperature anomalies for temperate East Asia since 800 CE. *Climate Dynamics* 41: 2957-2972.
Cook ER, Krusic PJ, and Jones PD (2003) Dendroclimatic signals in long tree-ring chronologies from the Himalayas of Nepal. *International Journal of Climatology* 23: 707–732.
Cook ER, Krusic PJ, Peters K, et al. (2017) *Program ARSTAN version 44.* https://www.ldeo.columbia.edu/tree-ring-laboratory/resources/software.
Cook ER, Meko DM, Stahle DW, et al., (1999) Drought reconstructions for the continental United States. *Journal of Climate* 12: 1145-1162.
Cook ER, Palmer JG, Ahmed M, et al. (2013b) Five centuries of upper Indus River flow from tree rings. Journal of Hydrology 486: 365-375.
Cook ER, Woodhouse CA, Eakin CM, et al. (2004) Long-term aridity changes in the western United States. *Science* 306: 1015-1018.
Copenheaver CA, Pokorski EA, Currie JE, et al. (2006) Causation of false ring formation in Pinus banksiana: A comparison of age, canopy class, climate and growth rate. *Forest Ecology and Management* 236: 348–355.
Corns IGW (1988) Compaction by forestry equipment and effects on coniferous seedling growth on four soils in the Alberta foothills. *Canadian Journal of Forest Research* 18: 75–84.
Coumou D, Lehmann J and Beckmann J (2015) The weakening summer circulation in the Northern Hemisphere mid-latitudes. *Science* 348: 324–327.
D'Agostino R and Lionello P (2017) Evidence of global warming impact on the evolution of the Hadley Circulation in ECMWF centennial reanalyses. *Climate Dynamics* 48: 3047–3060.
D'Arrigo RD and Jacoby GC (1991) A 1000-year record of winter precipitation from northwestern New Mexico, USA: A reconstruction from tree-rings and its relation to El Nino and the Southern Oscillation. *The Holocene* 1: 95–101.
Dangal SP, Das AK and Paudel SK (2017) Effectiveness of management interventions on forest carbon stock in planted forests in Nepal. *Journal of Environmental Management* 196: 511–517.
Dawadi B, Liang E, Tian L, et al. (2013) Pre-monsoon precipitation signal in tree rings of timberline Betula utilis in the central Himalayas. *Quaternary International* 283: 72-77.

De Micco V, Balzano A, Cufar K, et al. (2016) Timing of false ring formation in Pinus halepensis and Arbutus unedo in southern Italy: Outlook from an analysis of xylogenesis and tree-ring chronologies. *Frontiers in Plant Science* 7: 1–14.
Department of Forest Research and Survey (2006) *Thinning guidelines for Pinus patula and Pinus roxburghii (Nepali)*. DFRS Research Leaflet No 21. Department of Forest Research and Survey (DFRS), Kathmandu.
Deslauriers A, Sergio R and Tommaso A (2007) Dendrometer and intra-annual tree growth: What kind of information can be inferred? *Dendrochronologia* 25: 113-124.
Dhital YP, Kayastha RB and Shi J (2013) Soil bioengineering application and practices in Nepal. *Environmental Management* 51: 354–364.
Dimri AP and Mohanty UC (2009) Simulation of mesoscale features associated with intense western disturbances over western Himalayas. *Meteorological Applications* 16: 289–308.
Dimri AP, Niyogi D, Barros AP, et al. (2015) Western Disturbances: A review. *Reviews of Geophysics* 53: 225–246.
Dittmar C, Zech W and Elling W (2003) Growth variations of common beech (Fagus sylvatica L.) under different climatic and environmental conditions in Europe – A dendroecological study. *Forest Ecology and Management* 173: 63–78.
Dixit A (2009) Kosi embankment breach in Nepal: Need for a paradigm shift in responding to floods. *Economical and Political Weekly* 7: 70–78.
Donoghue DNM, Watt PJ, Cox NJ, et al. (2007) Remote sensing of species mixtures in conifer plantations using LiDAR height and intensity data. *Remote Sensing of Environment* 110: 509-522.
Druckenbrod DL, Pederson N, Rentch J, et al. (2013) A comparison of times series approaches for dendroecological reconstructions of past canopy disturbance events. *Forest Ecology and Management* 302: 23–33.
Du Y, Li T, Xie Z, et al. (2016). Interannual variability of the Asian subtropical westerly jet in boreal summer and associated with circulation and SST anomalies. *Climate Dynamics* 46: 2673–2688.
Duan K, Yao T and Thompson LG (2004) Low-frequency of southern Asian monsoon variability using a 295-year record from the Dasuopu ice core in the central Himalayas. *Geophysical Research Letters* 31: 28–31.
Duan K, Yao T and Thompson LG (2006) Response of monsoon precipitation in the Himalayas to global warming. *Journal of Geophysical Research Atmospheres* 111: 1–8.
Dukpa D, Cook ER, Krusic PJ, et al. (2018) Applied dendroecology informs the sustainable management of Blue Pine forests in Bhutan. *Dendrochronologia* 49: 89–93.
Dullinger S, Gattringer A, Thuiller W, et al. (2012) Extinction debt of high-mountain plants under twenty-first-century climate change. *Nature Climate Change* 2: 619–622.
Durre I, Vose RS and Wuertz DB (2006) Overview of the integrated global radiosonde archive. *Journal of Climate* 19: 53–68.
Durre I, Yin X, Vose RS, et al. (2018) Enhancing the data coverage in the integrated Global Radiosonde Archive. *Journal of Atmospheric and Oceanic Technology* 35: 1753–1770.
Elsen PR and Tingley MW (2015) Global mountain topography and the fate of montane species under climate change. *Nature Climate Change* 5: 5–10.
Eriksson M, Jianchu X, Shrestha AB, et al. (2009) *The Changing Himalayas: Impact of climate change on water resources and livelihoods un the greater Himalyas*. International Centre for Integrated Mountain Development (ICIMOD), Kathmandu.
Esper J, Frank DC, Wilson RJS, et al. (2007) Uniform growth trends among central Asian low and high elevation juniper tree sites. Trees-Structure and Function 21: 141-150.
Esper J, Schneider L, Smerdon JE, et al. (2015) Signals and memory in tree-ring width and density data. *Dendrochronologia* 35: 62-70.
Esper J, Schweingruber FH and Winiger M (2002) 1300 years of climatic history for Western Central Asia inferred from tree-rings. *The Holocene* 12: 267–277.
Esper J, St. George S, Anchukaitis K, et al. (2018) Large-scale, millennial-length temperature reconstructions from tree-rings. *Dendrochronologia* 50: 81–90.
Fallah B, Sodoudi S and Cubasch U (2016) Westerly jet stream and past millennium climate change in arid Central Asia simulated by COSMO-CLM model. *Theoretical and Applied Climatology* 124: 1079–1088.

Fernandes A, Rollinson CR, Kearney WS, et al. (2018) Declining radial growth response of coastal forests to hurricanes and Nor'easters. *Journal of Geophysical Research: Biogeosciences* 123: 832–849.
Figueira AMS, Miller SD, de Sousa CAD, et al. (2008) Effects of selective logging on tropical forest tree growth. *Journal of Geophysical Research* 113: doi: 10.1029/2007JG000577.
Francis JA and Vavrus SJ (2012) Evidence linking Arctic amplification to extreme weather in mid-latitudes. *Geophysical Research Letters* 39: 1–6.
Fritts HC (1971) Dendroclimatology and dendroecology. *Quaternary Research* 1: 419–449.
Fritts HC (1976) *Tree Rings and Climate*. Academic Press, London.
Fritts HC, Smith DG, Cardis JW, et al. (1965) Tree-ring characteristics along a vegetation gradient in northern Arizona. *Ecology* 46: 393-401.
Fu Q and Lin P (2011) Poleward shift of subtropical jets inferred from satellite-observed lower-stratospheric temperatures. *Journal of Climate* 24: 5597–5603.
Fu Q, Johanson CM, Wallace JM, et al. (2006) Enhanced mid-latitude tropospheric warming in satellite measurements. *Science* 312: 1179.
Fujii R and Sakai H (2002) Paleoclimatic changes during the last 2.5 myr recorded in the Kathmandu Basin, Central Nepal Himalayas. *Journal of Asian Earth Science* 20: 255-266.
Gaetani M, Baldi M, Dalu GA, et al. (2011) Jetstream and rainfall distribution in the Mediterranean region. *Natural Hazards and Earth System Sciences* 11: 2469–2481.
Gaire NP, Bhuju DR and Koirala M (2013) Dendrochronological studies in Nepal: Current status and future prospects. *Fuuast Journal of Biology* 3: 1-9.
Gaire NP, Bhuju DR, Koirala M, et al. (2017a) Tree-ring based spring precipitation reconstruction in western Nepal Himalaya since AD 1840. *Dendrochronologia* 42: 21-30.
Gaire NP, Dhakal YR, Lekhak HC, et al. (2011) Dynamics of Abies spectabilis in relation to climate change at the treeline ecotone in Langtang National Park. *Nepal Journal of Science and Technology* 12: 220-229.
Gaire NP, Dhakal YR, Shah SK, et al. (2019) Drought (scPDSI) reconstruction of trans-Himalayan region of central Himalaya using Pinus wallichiana tree-rings. *Palaeogeography Palaeoclimatoly Palaeoecology* 514: 251–264.
Gaire NP, Koirala M, Bhuju DR (2017b) Site- and species-specific treeline responses to climatic variability in eastern Nepal Himalaya. *Dendrochronologia* 41: 44–56.
Gaire NP, Koirala M, Bhuju DR, et al. (2014) Treeline dynamics with climate change at central Nepal Himalaya. *Climate of the Past* 10: 1277-1290.
Gao C, Robock A and Ammann C (2008) Volcanic forcing of climate over the past 1500 years: An improved ice core-based index for climate models. *Journal of Geophysical Research* 113(D23): D23111. http://doi.org/ 10.1029/2008JD010239.
Gauli AK and Hauser M (2011) Commercial management of non-timber forest products in Nepal's community forest user groups: who benefits? *International Forestry Review* 13: 35–45.
Gautam MR and Acharya K (2012) Streamflow trends in Nepal. Hydrological Sciences Journal 57: 344-357. Gayer E, Lave J, Pik R, et al. (2006) Monsoonal forcing of
Genova M, Leocadia C and Javier D (2014) Resin tapping in Pinus pinaster: Effects on growth and response function to climate. *European Journal of Forest Research* 133: 323–333.
Glaser B and Zech W (2005) Reconstruction of climate and landscape changes in a high mountain lake catchment in the Gorkha Himal, Nepal during the Late Glacial and Holocene as deduced from radiocarbon and compound-specific stable isotope analysis of terrestrial, aquatic and microbi. *Organic Geochemistry* 36: 1086–1098.
Glock W and Pearson GA (1937) *Principles and Methods of Tree-Ring Analysis*. Washington, DC: Carnegie. S
Goosse H, Guiot J, Mann ME, et al. (2012) The medieval climate anomaly in Europe: Comparison of the summer and annual mean signals in two reconstructions and in simulations with data assimilation. *Global and Planetary Change* 84-85: 35-47.
Government of Nepal (2014) *Nepal fifth national report on Convention on Biological Diversity*. Ministry of Forest and Soil Conservation, Kathmandu.
Gray KL and Hamann A (2013) Tracking suitable habitat for tree populations under climate change in western North America. *Climatic Change* 117: 289-303.
Grise KM, Davis SM, Staten PW, et al. (2018) Regional and seasonal characteristics of the recent expansion of the tropics. *Journal of Climate* 31: 6839–6856.

Hamed KH and Rao AR (1998). A modifier Mann-Kendall trend test for autocorrelated data. *Journal of Hydrology* 204: 182–196.
Hamid M, Khuroo AA, Charles B, et al. (2019) Impact of climate change on the distribution range and niche dynamics of Himalayan birch, a typical treeline species in Himalayas. *Biodiversity and Conservation* 28: 2345–2370.
Hannah DM, Kansakar SR, Gerrard a. J, et al. (2005) Flow regimes of Himalayan rivers of Nepal: Nature and spatial patterns. *Journal of Hydrology* 308: 18–32.
Harris I, Jones PD, Osborn TJ, et al. (2014) Updated high-resolution grids of monthly climatic observations - the CRU TS3.10 Dataset. *International Journal of Climatology* 34: 623–642.
He X, Burgess KS, Gao LM, et al. (2019) Distributional responses to climate change for alpine species of Cyananthus and Primula endemic to the Himalaya-Hengduan Mountains. *Plant Diversity* 41: 26–32.
Held IM, Ting M and Wang H (2002) Northern winter stationary waves: Theory and modeling. *Journal of Climate* 15: 2125–2144.
Henn B, Newman AJ, Livneh B, et al. (2018) An assessment of differences in gridded precipitation datasets in complex terrain. *Journal of Hydrology* 556: 1205–1219.
Herrera S, Kotlarski S, Soares PMM, et al. (2019) Uncertainty in gridded precipitation products: Influence of station density, interpolation method and grid resolution. *International Journal of Climatology* 39: 3717–3729.
Hoffer M and Tardif JC (2009) False rings in jack pine and black spruce trees from eastern Manitoba as indicators of dry summers. *Canadian Journal of Forest Research* 39: 1722–1736.
Holmes RL (1983) Computer-assisted quality control in tree-ring dating and measurement. *Tree-Ring Bulletin* 43: 69-78.
Holmes RL (1994) *Dendrochronology Program Library-User's Manual*. Tucson, AZ: University of Arizona.
Gayer E, Lave J, Pik R, et al. (2006) Monsoonal forcing of Holocene glacier fluctuations in Ganesh Himal (Central Nepal) constrained by cosmogenic 3He exposure ages of garnets. *Earth and Planetary Science Letters* 252: 275-288.
Hoorn C, Ohja T and Quade J (2000) Palynological evidence for vegetation development and climatic change in the Sub-Himalayan Zone (Neogene, Central Nepal). *Palaeogeography, Palaeoclimatology, Palaeoecology* 163: 133–161.
Hoskins BJ and Valdes PJ (1990) On the existence of storm-tracks. *Journal of Atmospheric Sciences* 47: 1854–1864.
Hoy A, Katel O, Thapa P, et al. (2016) Climatic changes and their impact on socio-economic sectors in the Bhutan Himalayas: an implementation strategy. *Regional Environmental Change* 16: 1401–1415.
Hunt KMR, Curio J, Turner AG, et al. (2018) Subtropical westerly jet influence on occurrence of western disturbances and Tibetan Plateau vortices. *Geophysical Research Letters* 45: 8629–8636.
Hussain S, Song X, Ren G, et al. (2017) Evaluation of gridded precipitation data in the Hindu Kush–Karakoram–Himalaya mountainous area. *Hydrological Sciences Journal* 62: 2393–2405.
Immerzeel W, van Beek LPH, Konz M, et al. (2012) Hydrological response to climate change in a glacierized catchment in the Himalayas. *Climatic Change* 110: 721–736.
Immerzeel WW and Bierkens MFP (2012) Asia's water balance. *Nature Geoscience* 5: 841–842.
Immerzeel WW, van Beek LPH and Bierkens MFP (2010) Climate change will affect the Asian Water Towers. *Science* 328: 1382–1385.
Jiang N, Yan Q and Wang, H (2020) Variation of the summer Asian westerly jet over the last millennium based on the PMIP3 simulations. *Holocene* 30: 332–343.
Jin R, Li Y, Long Q and Liu S (2018) The 200-hPa wind perturbation in the subtropical westerly over East Asia related to medium-range forecast of summer rainfall in China. *Journal of Meteorological Research* 32: 491–502.
Jones A (2000) Effects of cattle grazing on North American arid ecosystems: A quantitative review. *Western North American Naturalist* 60: 155–164.
Joshi JC, Kumar T, Srivastava S, et al. (2017) Optimisation of Hidden Markov Model using Baum–Welch algorithm for prediction of maximum and minimum temperature over Indian Himalaya. *Journal of Earths System Science* 126. doi: 10.1007/s12040-016-0780-0.
Joshi LM, Kotlia BS, Ahmad SM, et al. (2017) Reconstruction of Indian monsoon precipitation variability between 4.0 and 1.6 ka BP using speleothem δ18O records from the Central Lesser Himalaya,

India. *Arabian Journal of Geosciences* 10. doi:10.1007/s12517-017-3141-7
Kalnay E, Kanamitsu M, Kistler R, et al. (1996) The NCEP/NCAR 40-year reanalysis project. *Bulletin of the American Meteorological Society* 77: 437–472.
Kanel KR and Niraula DR (2004) Can rural livelihood be improved in Nepal through community forestry? *Banko Janakari* 14: 19–26.
Karki R, Hasson S, Schickhoff U, et al. (2017) Rising precipitation extremes across Nepal. *Climate* 5. doi:10.3390/cli5010004.
Karki R, Talchabhadel R, Aalto J, et al. (2015) New climatic classification of Nepal. *Theorotical and Applied Climatology*. doi: 10.1007/s00704-015-1549-0.
Kaushik P, Kaushik D and Khokra SL (2013) Ethnobotany and phytopharmacology of Pinus roxburghii Sargent: A plant review. *Journal of integrative medicine* 11: 371–376.
KC A and Thapa Parajuli RB (2014) Climate change and its impact on tourism in the Manaslu Conservation Area, Nepal. *Tourism Planning & Development* 12: 225–237.
KC B and Stainback GA (2012) Financial analysis of chir pine plantations for carbon offsets, timber and resin in Nepal. *Banko Janakari* 22: 3–10.
Kharal DK, Meilby H, Rayamajhi S, et al. (2014) Tree ring variability and climate response of Abies spectabilis along an elevation gradient in Mustang, Nepal. *Banko Janakari* 24: 3-13.
Kharal DK, Thapa UK, St George S, et al. (2017) Tree-climate relations along an elevational transect in Manang Valley, central Nepal. *Dendrochronologia* 41: 57–64.
Klippel L, St. George S, Ulf Büntgen, et al. (2020) Differing pre-industrial cooling trends between tree rings and lower-resolution temperature proxies. *Climate of Past* 16: 729-742.
Koch P, Wernli H and Davies HC (2006) An event-based jet-stream climatology and typology. *International Journal of Climatology* 26: 283–301.
Körner C and Paulsen J (2004) A world-wide study of high altitude treeline temperatures. *Journal of Biogeography* 31: 713–732.
Koteswaram P (1953) An analysis of the high tropospheric wind circulation over India in winter. *Indian Journal of Meteorology and Geophysics* 4: 13–21.
Koteswaram P and Parthasarathy S (1954) The mean jet stream over India in the pre-monsoon and post-monsoon seasons and vertical motions associated with subtropical jet streams. *Indian Journal of Meteorology and Geophysics* 5: 138–156.
Koteswaram P, Raman CRV and Parthasarathy (1953) The mean jet stream over India and Burma in winter. *Indian Journal of Meteorology and Geophysics* 4: 112-122.
Krusic P, Cook ER, Dukpa D, et al. (2015) Six hundred thirty-eight years of summer temperature variability over the Bhutanese Himalaya. *Geophysical Research Letters* 42: 2988–2994.
Kuang X and Zhang Y (2005) Seasonal variation of the East Asian subtropical westerly jet and Its association with the heating field over East Asia. *Advances in Atmospheric Sciences* 22: 831–840.
Kulkarni A, Patwardhan S, Kumar KK, et al. (2013) Projected climate change in the Hindu Kush–Himalayan region by using the high-resolution regional climate model PRECIS. *Mountain Research and Development* 33: 142–151.
Lammeranner W, Rauch HP and Laaha G (2005) Implementation and monitoring of soil bioengineering measures at a landslide in the middle mountains of Nepal. *Plant Soil* 278: 159–170.
Lamsal P, Kumar L, Atreya K, et al. (2018) Forest ecosystem services in Nepal: A retrospective synthesis, research gaps and implications in the context of climate change. *International Forestry Review* 20: 506–537.
Lang TJ and Barros AP (2004) Winter storms in the central Himalayas. Journal of the Meteorological Society of Japan *82*: 829-844.
Lemus-Lauzon I, Bhiry N, Arseneault D, et al. (2018) Tree-ring evidence of changes in the subarctic forest cover linked to human disturbance in northern Labrador (Canada). *Ecoscience* 25: 135–151.
Li D, Xiao Z and Zhao L (2019) Preferred solar signal and its transfer in the Asian–Pacific subtropical jet region. *Climate Dynamics* 52: 5173–5187.
Liang E, Dawadi B, Pederson N, et al. (2014) Is the growth of birch at the upper timberline in the Himalayas limited by moisture or by temperature? *Ecology* 95: 2453-2465.
Liu Y, Bao G, Song H, et al. (2009) Precipitation reconstruction from Hailar pine (Pinus sylvestris var. mongolica) tree rings in the Hailar region, Inner Mongolia, China back to 1865 AD. *Paleogeography, Paleoclimatology, Paleoecology* 282: 81-87.

Liu Y, Cai Q, Shi J, et al. (2005) Seasonal precipitation in the south-central Helan Mountain region, China, reconstructed from tree-ring width for the past 224 years. *Canadian Journal of Forest Research* 35: 2403-2412.
Lorimer CG and Frelich LE (1989) A methodology for estimating canopy disturbance frequency and intensity in dense temperatre forests. *Canadian Journal of Forest Research* 19: 651–663.
Lu J, Vecchi GA and Reichler T (2007) Expansion of the Hadley cell under global warming. *Geophysical Research Letters* 34. https://doi.org/10.1029/2006GL028443.
Luintel H, Bluffstone RA and Scheller (2018) The effects of the Nepal community forestry program on biodiversity conservation and carbon storage. *PLoS One* 13: 1–19.
Lutz AF, Immerzeel WW, Shrestha AB, et al. (2014) Consistent increase in High Asia's runoff due to increasing glacier melt and precipitation. *Nature Climate Change* 4: 587–592.
Maddison D (2001) In search of warmer climates? The impact of climate change on flows of British tourists. *Climatic Change* 49: 193–208.
Madhura RK, Krishnan R, Revadekar JV, et al. (2014) Changes in western disturbances over the Western Himalayas in a warming environment. *Climate Dynamics* 44: 1157–1168.
Mahagaonkar A, Wangchuk S, Ramanathan A, et al. (2017) Glacier environment and climate change in Bhutan-An overview. *Journal of Climate Change* 3: 1–10.
Mahat TBS, Griffin DM and Shepherd KR (1987) Human impacts on some forests of the middle hills of Nepal Part 3. Forests in the subsistence economy of Sindhu Palchok and Kabhre Palanchok. *Mountain Research and Development* 7: 53–70.
Maher P, Kelleher ME, Sansom PG, et al. (2020). Is the subtropical jet shifting poleward? *Climate Dynamics* 54: 1741–1759.
Mainali K, Shrestha BB, Sharma RK, et al. (2020) Contrasting responses to climate change at Himalayan treelines revealed by population demographics of two dominant species. *Ecology and Evolution* 10: 1209–1222.
Mall RK, Singh R, Gupta A, et al. (2006). Impact of climate change on Indian agriculture: A review. *Climatic Change*, *78*(2–4), 445–478.
Mani MS (1974) Biogeography of the Himalaya. In MS Mani (Ed.), *Ecology and Biogeography in India* (pp. 664–681). Dr W. Junk Publishers, The Hague.
Mann ME, Rahmstorf S, Kornhuber K, et al. (2017) Influence of anthropogenic climate change on planetary wave resonance and extreme weather events. *Scientific Reports* 7. https://doi.org/10.1038/srep45242
Mann ME, Zhang Z, Rutherford S, et al. (2009) Global signatures and dynamical origins of the Little Ice Age and Medieval Climate Anomaly. *Science* 326: 1256-1260.
Manney GL and Hegglin MI (2018) Seasonal and gegional variations of long-term changes in upper-tropospheric jets from reanalyses. *Journal of Climate* 31: 423–448.
Matalas NC (1962) Statistical properties of tree-ring data. *Hydrological Sciences Journal* 7: 39-47.
Maurer JM, Schaefer JM, Rupper S, et al. (2019) Acceleration of ice loss across the Himalayas over the past 40 years. *Science Advances* 5. doi: 10.1126/sciadv.aav7266.
McCarroll D and Loader NJ (2004) Stable isotopes in tree rings. *Quaternary Science Reviews* 23:771–801.
McMahon SM and Parker GG (2015) A general model of intra-annual tree growth using dendrometer bands. *Ecology and Evolution* 5: 243-254.
Meko DM, Touchan R and Anchukaitis KJ (2011) Seascorr: A MATLAB program for identifying the seasonal climate signal in an annual tree-ring time series. *Computers and Geosciences* 37: 1234–1241.
Melvin TM and Briffa KR (2008) A "signal-free" approach to dendroclimatic standardization. *Dendrochronologia* 26: 71-86.
Melvin TM, Briffa KR, Nicolussi K, et al. (2007) Time-varying response smoothing. *Dendrochronologia* 25: 65-69.
Miao J, Wang T and Wang H (2020) Interdecadal variations of the East Asian winter monsoon in CMIP5 preindustrial simulations. *Journal of Climate* 33: 559–575.
Miller JD, Immerzeel WW and Rees G (2012) Climate change impacts on glacier hydrology and river discharge in the Hindu Kush–Himalayas. *Mountain Research and Development* 32: 461–467.
Mishra Y, Nakamura T, Babel MS, et al. (2018) Impact of climate change on water resources of the Bheri River Basin, Nepal. *Water (Switzerland)* 10: 1–21.
Mölg T, Maussion F and Scherer D (2014) Mid-latitude westerlies as a driver of glacier variability in

monsoonal High Asia. *Nature Climate Change* 4: 68–73.
Moore GWK and Semple JL (2004) High Himalayan meteorology: Weather at the South Col of Mount Everest. *Geophysical Research Letters* 31. doi: 10.1029/2004GL020621
Moran-Ordonez A, Lahoz-Monfort J, Elith, J, et al. (2017) Evaluating 318 continental-scale species distribution models over a 60-year prediction horizon: What factors influence the reliability of predictions? *Global Ecology and Biogeography* 26: 371–384.
Myers N, Mittermiere R, Mittermiere C, et al. (2000) Biodiversity hotspots for conservation priorities. *Nature* 403: 853–858.
Nayava JL (1980). Rainfall in Nepal. *Himalayan Review* 12: 1–18.
Nepal SK (2000) Tourism in protected areas: The Nepalese Himalaya. *Annals of Tourism Research* 27: 661-681.
Nie Y, Sheng Y, Liu Q, et al. (2017). A regional-scale assessment of Himalayan glacial lake changes using satellite observations from 1990 to 2015. *Remote Sensing of Environment* 189: 1–13.
Novak K, Luis MD, Saz MA, et al. (2016) Missing rings in Pinus halepensis: The missing link to relate the tree-ring records to extreme climatic events. *Frontier in Plant Science* 7: 1-11.
Nowacki GJ and Abrams MD (1997) Radial-growth averaging criteria for reconstructing disturbance histories from pre-settlement-origin oaks. *Ecological Monographs* 67: 225–249.
Nyaupane GP and Chhetri N (2009) Vulnerability to climate change of nature-based tourism in the Nepalese Himalayas. *Tourism Geographies* 11: 95–119.
Ohsawa M, Shakya PR, Numata M, et al. (1986) Distribution and succession of west Himalayan forest types in the eastern part of the Nepal Himalaya. *Mountain Research and Development* 6: 143–157.
Ojha HR, Sulaiman VR, Sultana P, et al. (2014) Is South Asian agriculture adapting to climate change? Evidence from the Indo-Gangetic Plains. *Agroecology and Sustainable Food Systems* 38: 505–531.
Omelko A, Ukhvatkina O and Zhmerenetsky A (2016) Disturbance history and natural regeneration of an old-growth Korean pine-broadleaved forest in the Sikhote-Alin mountain range, southeastern Russia. *Forest Ecology and Management* 360: 221–234.
Oppenheimer C (2003) Climatic, environmental and human consequences of the largest known historic eruption: Tambora volcano (Indonesia) 1815. *Progress in Physical Geography* 2: 230-259.
Owen LA (2009) Latest Pleistocene and Holocene glacier fluctuations in the Himalaya and Tibet. *Quaternary Science Reviews* 28: 2150-2164.
PAGES 2k Consortium (2013) Continental-scale temperature variability during the past two millennia. Nature Geoscience 6: 339-346.
Pallardy SG (2010) *Physiology of Woody Plants*. Academic Press. San Diego.
Palmer WC (1965). *Meteorologucal Droughts*. *Research Paper* (Vol. 45). U.S. Department of Commerce, Weather Bureau Research.
Pandey S, Maraseni TN and Cockfield G (2014) Carbon stock dynamics in different vegetation dominated community forests under REDD+: A case from Nepal. *Forest Ecology and Management* 327: 40–47.
Pandit R and Bevilacqua E (2011) Forest users and environmental impacts of community forestry in the hills of Nepal. *Forest Policy and Economics* 13: 345-352.
Panta M, Kim K and Joshi C (2008) Temporal mapping of deforestation and forest degradation in Nepal: Applications to forest conservation. *Forest Ecology and Management* 256: 1587–1595.
Panthi, S., Bräuning, A., Zhou, Z., Fan, Z., 2017. Tree rings reveal recent intensified spring drought in the central Himalaya. Nepal. *Global and Planetary Change* 157: 26–34.
Papadopoulos AM (2013) Resin tapping history of an Aleppo pine forest in central Greece. *The Open Forest Science Journal* 6: 50–53.
Parobeková Z, Sedmáková D, Kucbel S, et al. (2016) Influence of disturbances and climate on high-mountain Norway spruce forests in the Low Tatra Mts. Slovakia. *Forest Ecology and Management* 380: 128–138.
Pearson RG and Dawson TP (2003) Predicting the impacts of climate change on the distribution of species: Are bioclimate envelope models useful? *Global Ecology and Biogeography* 12: 361–371.
Pena-Ortiz C, Gallego D, Ribera P, et al. (2013) Observed trends in the global jet stream characteristics during the second half of the 20th century. *Journal of Geophysical Research Atmospheres* 118: 2702–2713.

Petritan AM, Bouriaud O, Frank, DC, et al. (2017) Dendroecological reconstruction of disturbance history of an old-growth mixed sessile oak-beech forest. *Journal of Vegetation Science* 28: 117–127.
Piraino S, María E, Ariel M, et al. (2017) Anthropogenic disturbance impact on the stem growth of Prosopis flexuosa DC forests in the Monte desert of Argentina: A dendroecological approach. *Dendrochronologia* 42, 63–72.
Popescu SC (2007) Estimating biomass of individual pine trees using airborne lidar. *Biomass and* Bioenergy 31: 646-655.
Pradhan K (2009) *The Gorkha Conquests*. Kathmandu: Himal Books.
Pulido, M., Schnabel, S., Francisco, J., Contador, L., Lozano-parra, J., González, F., 2018. The impact of heavy grazing on soil quality and pasture production in rangelands of SE Spain. Land Degrad. Dev. 230, 219–230.
Rajbhandari R, Bhakta A and Wahid S (2017) Extreme climate projections over the transboundary Koshi River Basin using a high-resolution regional climate model. *Advances in Climate Change Research* 8: 199–211.
Rajbhandari R, Shrestha AB, Nepal S, et al. (2018) Projection of future precipitation and temperature change over the transboundary Koshi River basin using Regional Climate Model PRECIS. *Atmospheric and Climate Sciences* 8: 163–191.
Rana E, Thwaites R and Luck G (2017) Trade-offs and synergies between carbon, forest diversity and forest products in Nepal community forests. *Environmental Conservation* 44: 5–13.
Rayback SA, Shrestha KB and Hofgaard A (2017) Growth variable-specific moisture and temperature limitations in co-occurring alpine tree and shrub species, central Himalayas, Nepal. *Dendrochronologia* 44: 193–202.
Rydval M, Druckenbrod D, Anchukaitis KJ, et al. (2016) Detection and removal of disturbance trends in tree-ring series for dendroclimatology. *Canadian Journal of Forest Research* 46: 387–401.
Sano M, Furuta F, Kobayashi O, et al. (2005) Temperature variations since the mid-18th century for western Nepal, as reconstructed from tree-ring width and density of Abies spectabilis. *Dendrochronologia* 23: 83-92.
Sano M, Ramesh R, Sheshshayee M, et al. (2011) Increasing aridity over the past 223 years in the Nepal Himalaya inferred from a tree-ring d18O chronology. *The Holocene* 22: 809-817.
Sano M, Tshering P, Komori J, et al. (2013) May–September precipitation in the Bhutan Himalaya since 1743 as reconstructed from tree ring cellulose δ18O. *Journal of Geophysical Research: Atmospheres* 118: 8399-8410.
Schiemann R, Luthi D and Schar C (2009) Seasonality and interannual variability of the westerly jet in the Tibetan Plateau Region. *Journal of Climate* 22: 2940–2957.
Schlutz F and Zech W (2004) Palynological investigations on vegetation and climate change in the Late Quaternary of Lake Rukche area, Gorkha Himal, Central Nepal. *Vegetation History and Archeobotany* 13: 81-90.
Schmidt B (1993) Dendrochronological research in south Mustang. *Ancient Nepal* 130-133: 20-33.
Schmidt B, Wazny T, Malla K, et al. (1999) Chronologies for historical dating in high Asia/Nepal. In: Wimmer R and Vetter RE (eds) *Tree-Ring Analysis: Biological, Methodological and Environmental Aspects.* Wallingford: CAB International, 205-211.
Schongart J, Gribel R, da Fonseca-Jr S, et al. (2015) Age and growth patterns of Brazil nut trees (Bertholletia excelsa Bonpl.) in Amazonia. Brazil. *Biotropica* 47: 550–558.
Schreier H, Shah PB, Lavkulich LM, et al. (1994) Maintaining soil fertility under increasing land use pressure in the middle mountains of Nepal. *Soil Use and Management* 10: 137–142.
Schulman E (1941) Some propositions in tree-ring analysis. *Ecology* 22: 193-195.
Schwartz MW, Iverson LR, Prasad AM, et al. (2006) Predicting extinctions as a result of climate change. *Ecology* 87: 1611-1615.
Seidel DJ, Fu Q, Randel WJ, et al. (2007) Widening of the tropical belt in a changing climate Some. *Nature Geoscience* 1: 21–24.
Shah SK, Bhattacharyya A and Chaudhary V (2014) Streamflow reconstruction of Eastern Himalaya River, Lachen 'Chhu', North Sikkim, based on tree-ring data of Larix griffithiana from Zemu Glacier basin. *Dendrochronologia* 32: 97–106.
Shah SK, Mehrotra N and Bhattacharyya A (2014) Tree-ring studies from eastern Himalayas: Prospects and challenges. *Himalayan Research Journal* 2: 21–28.

Sharma A, Sharma L and Goyal (2018) A review on Himalayan pine species: Ethnopharmacological, phytochemical and pharmacological aspects. *Journal of Pharmacognosy* 10: 611–619.
Sharma J (2012) Social science engagement and political interregnum in Nepal. *Economic and Political Weekly* XLVII: 1-8.
Shea JM, Immerzeel WW, Wagnon P, et al. (2015) Modelling glacier change in the Everest region , Nepal Himalaya. *The Cryosphere* 9: 1105–1128.
Shreevastav BB, Tiwari KR and Mandal RA (2019) Flood scenario and its risk management, policy, practices in Nepal. *Annals of Ecology and Environmental Science* 3: 1–14.
Shrestha AB and Aryal R (2011) Climate change in Nepal and its impact on Himalayan glaciers. *Regional Environmental Change* 11: 65-77.
Shrestha AB, Bajracharya SR, Sharma AR, et al. (2017) Observed trends and changes in daily temperature and precipitation extremes over the Koshi river basin 1975- 2010. *International Journal of Climatology* 37: 1066-1083.
Shrestha AB, Wake CP, Dibb JE, et al. (2000) Precipitation fluctuations in the Nepal Himalaya and its vicinity and relationship with some large-scale climatological parameters. *International Journal of Climatology* 20: 317-327.
Shrestha AB, Wake CP, Mayewski PA, et al. (1999) Maximum temperature trends in the Himalaya and its vicinity: An analysis based on temperature records from Nepal for the period 1971-94. *Journal of Climate* 12: 2775-2786.
Shrestha KB, Hofgaard A and Vandvik V (2014) Recent treeline dynamics are similar between dry and mesic areas of Nepal, central Himalaya. *Journal of Plant Ecology*. doi: 10.1093/jpe/rtu035.
Shrestha KB, Kumar P and Bista R (2017b) Growth responses of Abies spectabilis to climate variations along an elevational gradient in Langtang National Park in the central Himalaya, Nepal. *Journal of Forestry Research*. doi: 10.1080/13416979.2017.1351508.
Shrestha ML (2000) Interannual variation of summer monsoon rainfall over Nepal and its relation to Southern Oscillation Index. *Meteorology and Atmospheric Physics* 75: 21–28.
Shrestha S, Bastola S, Babel MS, et al. (2007) The assessment of spatial and temporal transferability of a physically based distributed hydrological model parameters in different physiographic regions of Nepal. *Journal of Hydrology* 347: 153–172.
Shrestha S, Karky BS, Gurung A, et al. (2013) Assessment of carbon balance in community forests. *Small-scale Forestry* 12: 507–517.
Shrestha S, Shrestha M and Babel MS (2016) Modelling the potential impacts of climate change on hydrology and water resources in the Indrawati River Basin, Nepal. *Environmental Earth Sciences* 75: 1–13.
Shrestha UB and Shrestha BB (2019) Climate change amplifies plant invasion hotspots in Nepal. *Diversity and Distributions* 25: 1599–1612.
Sigdel M and Ikeda M (2010) Spatial and temporal analysis of drought in Nepal using standardized precipitation index and its relationship with climate indices. *Journal of Hydrology and Meteorology* 7: 59-74.
Sigdel SR, Dawadi B, Camarero JJ, et al. (2018a). Moisture-limited tree growth for a subtropical Himalayan conifer forest in western Nepal. *Forests* 9. doi: 10.3390/f9060340.
Sigdel SR, Wang F, Camarero JJ, et al. (2018b) Moisture-mediated responsiveness of treeline shifts to global warming in the Himalayas. *Global Change Biology* 24: 5549–5559.
Singh J, Yadav RR and Wilmking M (2009) A 694-year tree-ring based rainfall reconstruction from Himachal Pradesh, India. *Climate Dynamics* 33: 1149-1158.
Slivinski LC, Compo GP, Whitaker JS, et al. (2019) Towards a more reliable historical reanalysis: Improvements for version 3 of the Twentieth Century Reanalysis system. *Quarterly Journal of the Royal Meteorological Society* 145: 2876–2908.
Smith RGB and Brennan P (2006) First thinning in sub-tropical eucalypt plantations grown for high-value solid-wood products: A review. *Australian Forestry* 69: 305–312.
Song M, Zhou C and Ouyang H (2004) Distributions of dominant tree species on the Tibetan Plateau under current and future climate scenarios. *Mountain Research and Development* 24: 166–173.
St. George S (2014) An overview of tree-ring width records across the Northern Hemisphere. *Quaternary Science Reviews* 95: 132-150.
St. George S and Ault TR (2014) The imprint of climate within Northern Hemisphere trees. *Quaternary Science Reviews* 89: 1–4.

St. George S and Esper J (2019) Concord and discord among Northern Hemisphere paleotemperature reconstructions from tree rings. *Quaternary Science Reviews* 203: 278–281.
St. George S, Ault TR and Torbenson MCA (2013) The rarity of absent growth rings in Northern Hemisphere forests outside the American Southwest. *Geophysical Research Letters* 40: 3727-3731.
Stainton JDA (1972) *Forests of Nepal*. Hafner Publishing Company, New York.
Staten PW, Lu J, Grise KM, et al. (2018) Re-examining tropical expansion. *Nature Climate Change* 8: 768-775.
Stevans S (2003) Tourism and deforestation in the Mt. Everest region of Nepal. *The Geographical Journal* 169: 255-277.
Stevenson S, Overpeck JT, Fasullo J, et al. (2018). Climate variability, volcanic forcing, and last millennium hydroclimate extremes. *Journal of Climate* 3: 4309–4327.
Stocker TF, Qin D, Plattner GK, et al. (eds) (2013) *The Physical Science Basis*. Cambridge: Cambridge University Press, 4-29.
Stokes M and Smiley T (1968) *An Introduction to Tree Ring Dating*. University of Chicago Press, Chicago.
Stothers RB (1984) The great Tambora eruption in 1815 and its aftermath. *Science* 224: 1191-1198.
Strong C and Davis RW (2007) Winter jet stream trends over the Northern Hemisphere. *Quarterly Journal of the Royal Meteorological Society* 133: 2109–2115.
Suzuki E (1990) Dendrochronology in coniferous forests around Lake Rara, west Nepal. *The Botanical Magazine Tokyo* 103: 297-312.
Talchabhadel R, Karki R, Thapa BR, et al. (2018) Spatio-temporal variability of extreme precipitation in Nepal. *International Journal of Climatology* 38: 4296–4313.
Thapa UK and St. George S (2019) Detecting the influence of climate and humans on pine forests across the dry valleys of eastern Nepal's Koshi River basin. *Forest Ecology and Management* 440: 12–22.
Thapa UK, Shah SK, Gaire NP, et al. (2013) Influence of climate on radial growth of Abies pindrow in western Nepal Himalaya. *Banko Janakari* 23: 14–19.
Thapa UK, Shah SK, Gaire NP, et al. (2015) Spring temperatures in the far-western Nepal Himalaya since AD 1640 reconstructed from Picea smithiana tree-ring widths. *Climate Dynamics* 45: 2069-2081.
Thapa UK, St. George S and Trouet V. Increasingly frequent poleward excursions by the Himalayan subtropical jet. *Geophysical Research Letters*. Submitted.
Thapa UK, St. George S, Kharal DK, et al. (2017) Tree growth across the Nepal Himalaya during the last four centuries. *Progress in Physical Geography* 41: 478–495.
Thoms CA (2008) Community control of resources and the challenge of improving local livelihoods: A critical examination of community forestry in Nepal. *Geoforum* 39:1452–1465.
Tiwari A, Fan Z, Jump AS, et al. (2017) Gradual expansion of moisture sensitive Abies spectabilis forest in the Trans-Himalayan zone of central Nepal associated with climate change. *Dendrochronologia* 41: 34–43.
Trenberth KE, Dai A, van der Schrier G, et al. (2014) Global warming and changes in drought. *Nature Climate Change* 4: 3–8.
Trotsiuk V, Pederson N, Druckenbrod DL, et al. (2018) Testing the efficacy of tree-ring methods for detecting past disturbances. *Forest Ecology and Management* 425: 59–67.
Trouet V (2014). A tree-ring based late summer temperature reconstruction (AD 1675-1980) for the northeastern Mediterranean. *Radiocarbon* 56: S69-S78.
Trouet V, Babst F and Meko M (2018) Recent enhanced high-summer North Atlantic Jet variability emerges from three-century context. *Nature Communications* 9. doi:10.1038/s41467-017-02699-3
van der Maaten E, Mehl A, Wilmking M, et al. (2017) Tapping the tree-ring archive for studying effects of resin extraction on the growth and climate sensitivity of Scots pine. *Forest Ecosystems*. doi: 10.1186/s40663- 017-0096-9.
Veh G, Korup O and Walz A (2020) Hazard from Himalayan glacier lake outburst floods. *Proceedings of the National Academy of Sciences of the United States of America* 117: 907–912.
Vicente-Serrano SM, Begueria S and Lopez-Moreno JI (2010) A multiscalar drought index sensitive to global warming: the standardized precipitation evapotranspiration index. *Journal of Climate* 23: 1696–1718.

Vitali V, Brang P, Cherubini P, et al. (2016) Radial growth changes in Norway spruce montane and subalpine forests after strip cutting in the Swiss Alps. *Forest Ecology and Management* 364: 145–153.
Wahl ER, Zorita E, Trouet V, et al. (2019). Jet stream dynamics, hydroclimate, and fire in California from 1600 CE to present. *Proceedings of the National Academy of Sciences of the United States of America* 116: 5393–5398.
Wang W, Zhou W, Wang X., et al. (2013) Summer high temperature extremes in southeast China associated with the East Asian jet stream and circumglobal teleconnection. *Journal of Geophysical Research Atmospheres* 118: 8306–8319.
Whitney LF (1977) Relationship of the subtropical jet stream to severe local storms. *Monthly Weather Review* 105: 398–412.
Wigley TML, Briffa KR and Jones PD (1984) On the average value of correlated time series, with applications in dendroclimatology and hydrometeorology. *Journal of Climate and Applied Meteoriology* 23: 201–213.
Wilcox LJ, Hoskins BJ and Shine KP (2012) A global blended tropopause based on ERA data. Part II: Trends and tropical broadening. *Quarterly Journal of the Royal Meteorological Society* 138: 576–584.
Williams AP, Allen CD, Macalady AK, et al. (2012) Temperature as a potent driver of regional forest drought stress and tree mortality. *Nature Climate Change* 3: 292–297.
Wright WE, Guan BT, Tseng YH, et al. (2015) Reconstruction of the springtime East Asian Subtropical Jet and Western Pacific pattern from a millennial-length Taiwanese tree-ring chronology. *Climate Dynamics* 44: 1645–1659.
Xu J, Grumbine RE, Shrestha A, et al. (2009). The melting Himalayas: Cascading effects of climate change on water, biodiversity, and livelihoods. *Conservation Biology* 23: 520–530.
Yang B, Qin C, Wang J, et al. (2014) A 3,500-year tree-ring record of annual precipitation on the northeastern Tibetan Plateau. *Proceedings of the National Academy of Sciences* 25: 2903-2908.
Yin JH (2005) A consistent poleward shift of the storm tracks in simulations of 21st century climate. *Geophysical Research Letters* 32: 1–4.
Zhang SY, Chauret G, Swift DE, et al. (2006) Effects of precommercial thinning on tree growth and lumber quality in a jack pine stand in New Brunswick, Canada. *Canadian Journal of Forest Research* 36: 945–952.
Zhang Y and Chen J (2017) Characterizing the winter concurrent variation patterns of the subtropical and polar-front jets over East Asia. *Journal of Meteorological Research* 31: 160–170.
Zhao S, Pederson N, D'Orangeville L, et al. (2019) The International Tree-Ring Data Bank (ITRDB) revisited: Data availability and global ecological representativity. *Journal of Biogeography* 46: 355–368.
Zhao Y, Wang MZ, Huang AN, et al. (2014) Relationships between the West Asian subtropical westerly jet and summer precipitation in northern Xinjiang. *Theoretical and Applied Climatology* 116: 403–411.
Zhongda L and Riyu LU (2005) Interannual meridional displacement of the East Asian upper-tropospheric jet stream in summer. *Advances in Atmospheric Sciences* 22: 199–211.

Appendix A: Supporting Information for CHAPTER 4

Contents of this file

Introduction

Texts S1 to S4

Figures S1 to S7

Tables S1

Introduction

This supplementary information provides details of the reanalysis and tree-ring data used to reconstruct the latitude of the spring Himalayan jet (Himalayan jet latitude or HJL, hereafter) presented in Chapter 4. In Text S1, we explain why we chose the National Centers for Environmental Prediction-National Center for Atmospheric Research (NCEP/NCAR) reanalysis data (Kalnay et al., 1996) to calculate the HJL. We also explain our strategy to screen tree-ring chronologies for reconstruction and the relationships between them and HJL (Text S2). In text S3, we discuss how we produce the composite tree-ring chronologies used in the reconstruction. Text S4 justifies the length of reconstruction (1625-2003). Figures S1 to S5 support assertions we made on the use of different reanalysis products and Figure S6 shows the network of tree-ring chronologies that passed the climate sensitivity test and the strength of association with the HJL. We also include a plot showing inter-chronology correlations among the tree-ring chronologies that passed the screening criteria that were used to reconstruct the HJL back to 1625 (Figures S7). Table S1 provides the details of 23 tree-ring chronologies from the Himalayan region used in the reconstruction.

Text S1. On the choice of reanalysis data

We calculated the HJL using three reanalysis databases: NCEP/NCAR (Kalnay et al., 1996), 20th Century Version 2 (20C V2, Compo et al., 2011), and 20th Century Version 3 (20C V3, Slivinski et al., 2019). These three databases contain globally gridded monthly values at 2.5° × 2.5°, 2° × 2°, and 1° × 1° resolutions for the periods of 1948-2018, 1851-2014, and 1836-2015, respectively. We identified the latitude of the subtropical jet for each longitudinal grid cell as the latitude of the maximum average spring (March-May) wind speed at 200mb geopotential height, and we calculated the HJL for each year by averaging the latitudes for all longitudes within the Himalayan corridor (70-95°E). This same method was applied for all three data sources (Figure S1).

The HJLs computed from the three data sources are significantly positively correlated ($p < 0.01$) with each other over the period of overlap, but the strength of association between any two HJL time series is not strong ($r < 0.6$ for any pair; Figure S1) compared to other regions. For example, the same parameter computed from the NCEP/NCAR and 20C Reanalysis datasets has correlation coefficients above 0.9 in the North Atlantic region (Trouet et al., 2018). The 20th Century Reanalysis covers a much longer time period than the NCEP/NCAR, which is desirable to cross-validate tree-ring reconstructions, but both 20C V2 and 20C V3 are unrealistically variable prior to 1950. Estimates of jet stream positions prior to 1920 have been criticized due to the decline in station density and measurement quality (Alfaro-Sánchez et al., 2018; Trouet et al., 2018). We, therefore, truncated each index to retain only HJL values after 1920.

Next, we compared the three HJL time series with regional climate variables to see whether the higher-resolution reanalysis database performs better in capturing the spatial extent of the HJL's effect on temperature and precipitation. Regardless of data source, the HJL showed similar effects on regional temperature and precipitation: it is significantly positively correlated with temperature across much of central Asia and significantly negatively correlated with precipitation south of the Himalayas in western and central Asia for any period of comparison (Figures S2, S3, S4). None of the HJL time series showed significant correlations with precipitation in the core Himalayas, which might be due to the challenges in representing hydroclimatic variability associated with complex topography in the reanalysis and gridded data (Henn et al., 2018; Herrera et al., 2019; Hussain et al., 2017).

Fifty-eight tree-ring chronologies from the Himalayan region passed climate sensitivity screening with a significant positive correlation with spring precipitation and/or a significant negative correlation with spring temperature (Figure S6, Text S2). Only 23 of these chronologies, however, were significantly correlated with the NCEP/NCAR-derived spring HJL and even fewer, 10 or 6 chronologies, with the 20C V2- and V3-derived HJL, respectively (Figure S5).

In sum, even though the 20th Century Reanalysis extends back to the middle of the 19th century, in the Himalayas, the usable length of the 20C does not appear to exceed the available length of NCEP/NCAR database (1948-present). Regardless of reanalysis data type used, the HJL showed similar spatial correlations with spring climate. Meteorologists have predominantly used the

NCEP/NCAR reanalysis database over other databases to characterize the modern-time behavior of the subtropical jet stream over east Asia (Chen et al., 2017; Du et al., 2016; Jin et al., 2018; Li et al., 2019; Zhang & Chen, 2017). In our tests, a higher number of tree-ring chronologies (that are sensitive to the same aspects of climate influenced by the HJL) captured year-to-year variability of the NCEP/NCAR-derived HJL than the two versions of 20 C products. Considering these factors, we use the NCEP/NCAR-derived HJL as our target for reconstruction.

Text S2. On tree-ring chronologies used to reconstruct the Himalayan jet latitude

Our initial pool contained 143 tree-ring width chronologies from Pakistan, India, Nepal, and Bhutan where climate is influenced by the HJL. The majority of tree-ring records were derived from the International Tree-Ring Data Bank (Zhao et al., 2019) and six chronologies were previously produced by the authors (Thapa & St. George, 2019). Individual studies producing these records report that tree growth at most of the sites across the Himalayan region are sensitive to moisture balance during winter and/or spring (Bhandari et al., 2019 and references therein; Cook et al., 2013b; Esper et al., 2007). Because spring climate in the region is influenced by the HJL (Hunt et al., 2018; Figures 4.1bc, S2, S3, S4), Himalayan tree-ring width chronologies could be potentially used as proxy for that aspect of regional circulation.

For the purpose of our study, we retained only those chronologies from the initial network that had (i) significant ($p < 0.1$) positive correlations with regional

spring (March-May) precipitation and or significant negative correlations with spring temperature and (ii) significant ($p < 0.1$) negative correlations with the HJL. From the initial network, 58 tree-ring chronologies passed the first screening (Figure S6a). Most (50 out of 58) chronologies were negatively correlated with the HJL (Figure S6b), but only 23 records had correlation values significant at 0.1 level, which we used in the final reconstruction (Figure 4.2a, Table S1). The signs of the correlations between each of the three composite tree-ring chronologies and spring climate variables (Figure 4.2b-g) correspond to those between the HJL and the same climate variables (Figure S2). When the Himalayan jet moves north, the region is both hotter and drier (Figures 4.1bc and S2), and that combination negatively affects tree growth, justifying the negative correlations between the HJL and tree-ring width chronologies.

Text S3. On the creation of regional composite tree-ring chronologies

Based on the locations and degree of coherence (Figures 4.2a and S7), we clustered the 23 chronologies that passed the screening criteria in three groups from west to east across the Himalayas, and created three regional composite chronologies: WESTERN (16 chronologies from Pakistan and western India), CENTRAL (four chronologies from Nepal), and EASTERN (three chronologies from Bhutan). Each composite chronology was developed by combining all individual ring-width series from each contributing site chronology within that region (Alfaro-Sánchez et al., 2018; Trouet 2014, Figure 4.3). Each individual ring-width series was detrended to remove age-related trends using cubic smoothing splines with 50% frequency cut-off at 100 years, and then three

regional composite chronologies were produced by averaging all detrended series for each region using robust biweight means (Cook & Peters, 1981).

Text S4. On the length of the Himalayan jet latitude reconstruction

We developed a HJL reconstruction for the period of 1625-2003 based on tree-ring sample depth in the composite chronologies. The three regional chronologies have adequate sample replication to explain the population-level signal for the period 1215-2006 (WESTERN), 1760-2012 (CENTRAL), and 1625-2006 (EASTERN) as judged by the commonly used but general metric, Expressed Population Signal (Wigley et al., 1984). We applied a stepwise linear regression model of the three regional chronologies against the modern spring HJL, but only WESTERN and EASTERN composites were retained for reconstruction. Because the number of individual tree-ring series contributing to the EASTERN composite dropped substantially after 2003 (from seventy to eight, Figure 4.3), the most recent (post-2003) years were excluded from the reconstruction. Finally, we restricted our reconstruction for 1625-2003, the period common to WESTERN and EASTERN composites.

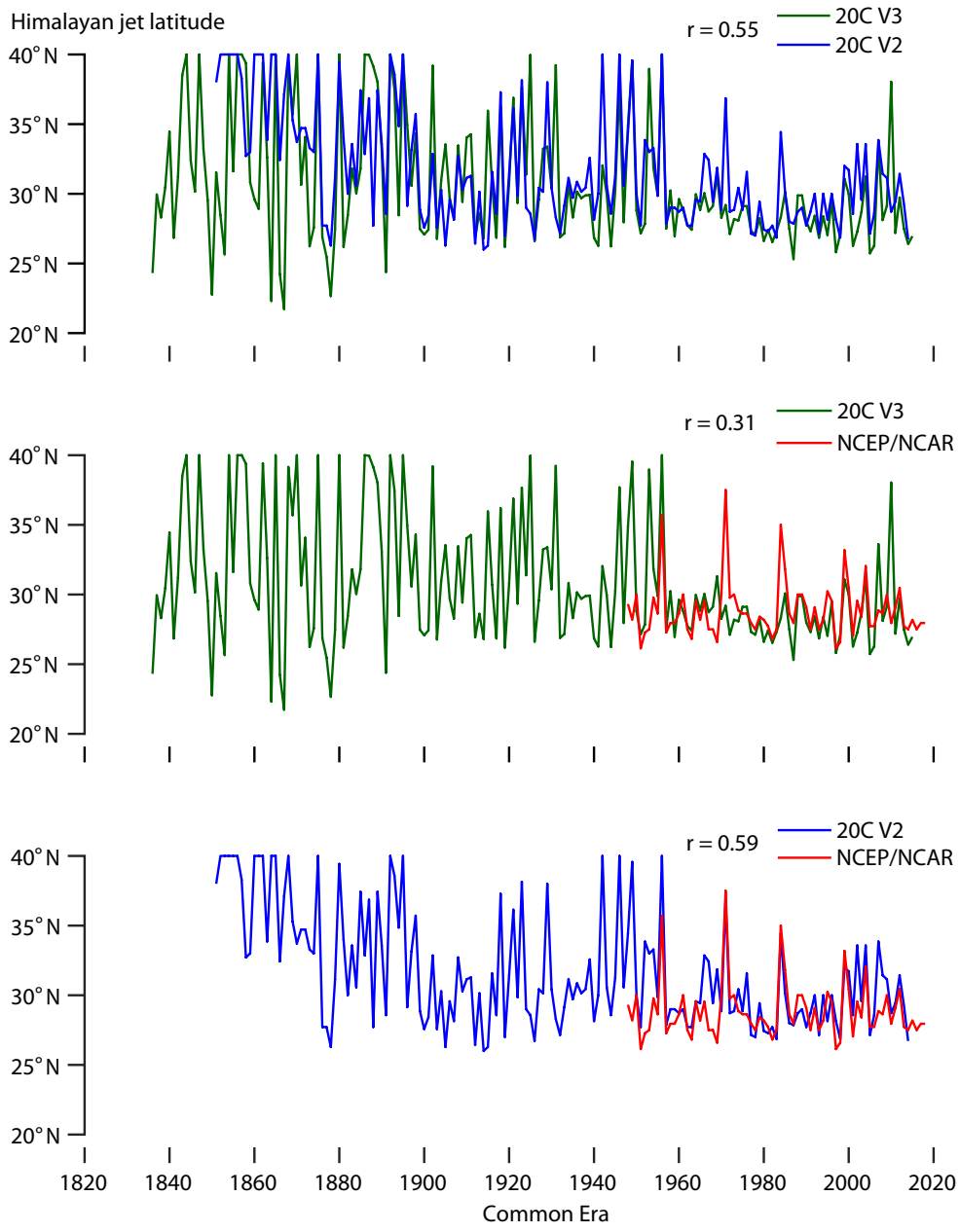

Figure S1. Time-series comparisons of the Himalayan jet latitudes (HJLs) calculated using three reanalysis databases: 20th Century Version 3 (20C V3, green; Slivinski et al., 2019), 20th Century Version 20C V2, blue; Compo et al., 2011), and National Centers for Environmental Prediction/National Center for Atmospheric Research (NCEP/NCAR, red; Kalnay et al., 1996). Correlation coefficients (r, $p < 0.01$) between each pair of time series are also displayed.

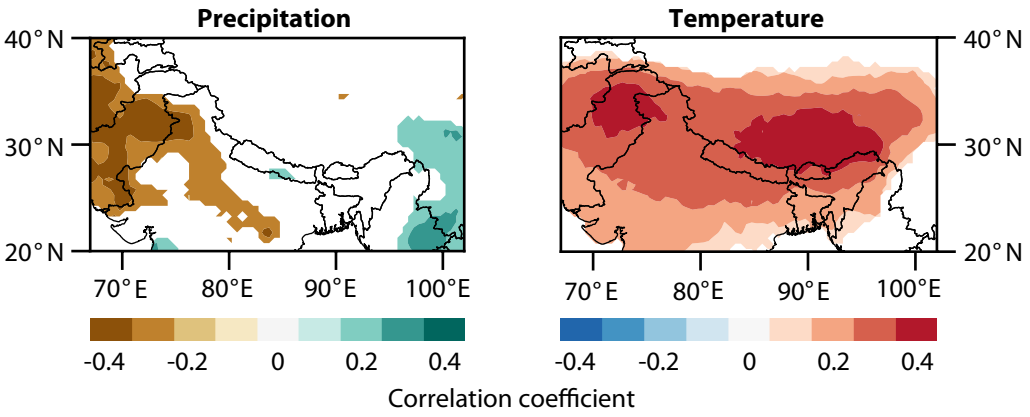

Figure S2. Maps showing correlations between the NCEP/NCAR-derived HJL and CRU TS4.03 spring (March-May) climate (Harris et al., 2014) over the 1948 to 2018 period: (left) precipitation and (right) temperature. Only significant correlations ($p < 0.1$) are shaded.

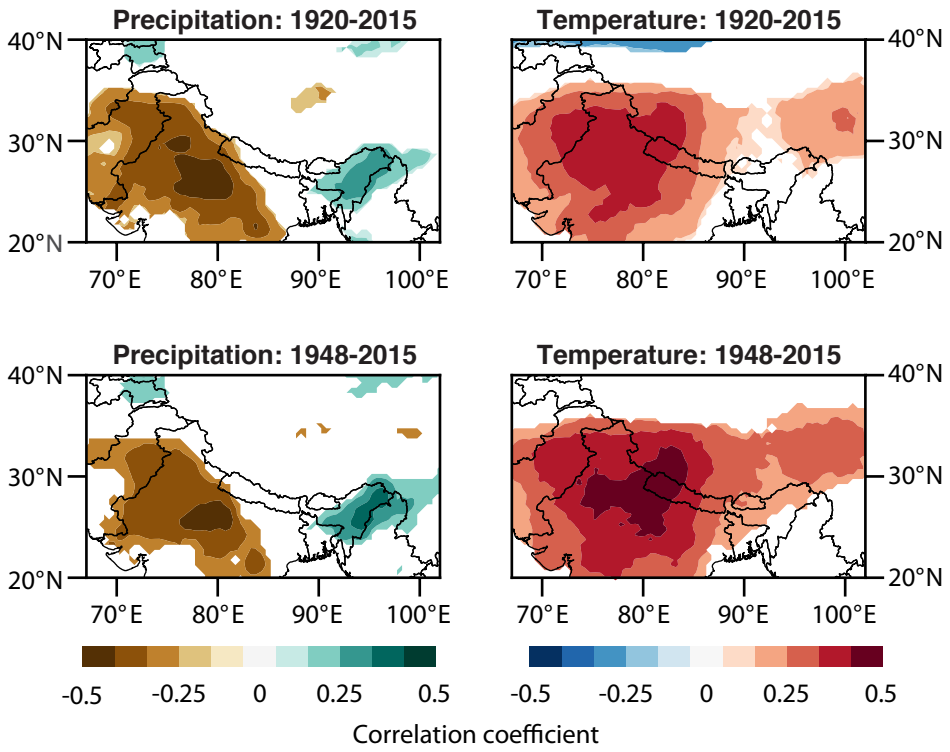

Figure S3. Maps showing correlations between the 20C V3 reanalysis-derived HJL and CRU TS4.03 spring climate (Harris et al., 2011): (left) precipitation and (right) temperature during two intervals (top: 1920-2015, bottom: 1948-2015). Only significant correlations ($p < 0.1$) are shaded.

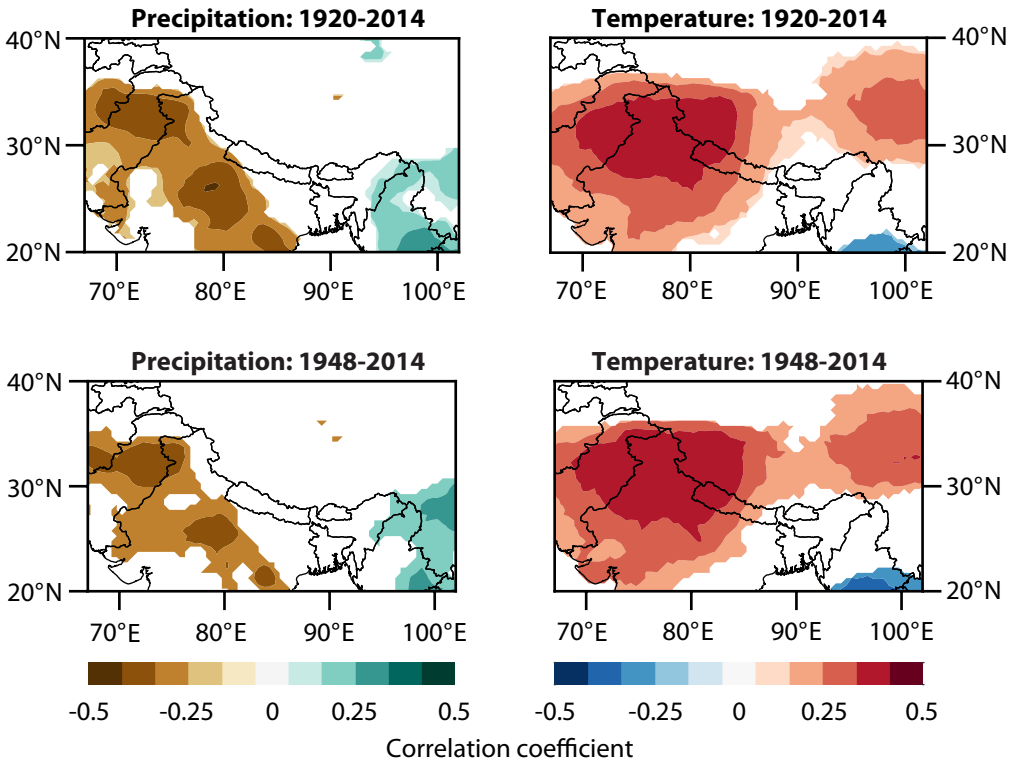

Figure S4. Maps showing correlations between the 20C V2 reanalysis-derived HJL and CRU TS4.03 spring climate (Harris et al., 2014): (left) precipitation and (right) temperature during two intervals (top: 1920-2014, bottom: 1948-2014). Only significant correlations ($p < 0.1$) are shaded.

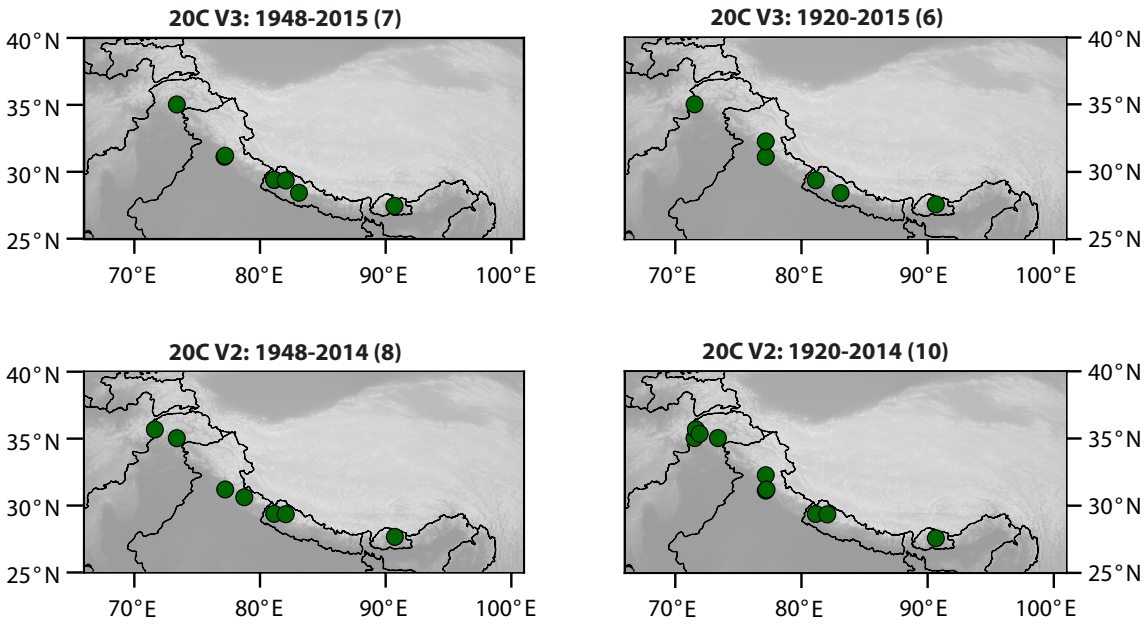

Figure S5. Maps showing the locations of tree-ring chronologies that passed both screening criteria as described in Text S2 for the two versions of 20C Reanalysis data. Each chronology is sensitive to the same aspect of spring climate that is influenced by the Himalayan jet latitude (HJL), and also significantly correlated with the HJL calculated using the two versions of 20C Reanalysis data for different time intervals (top: 20C V3 for 1948-2015 & 1920-2015; bottom: 20C V2 for 1948-2014 & 1920-2014).

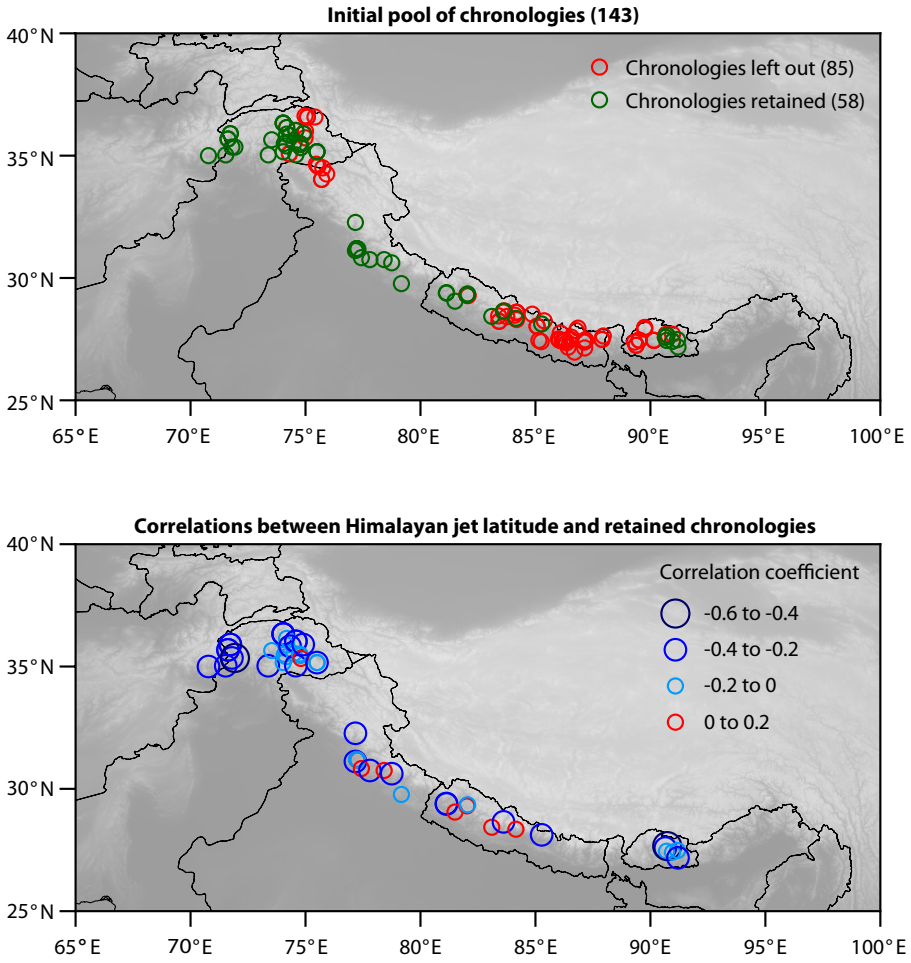

Figure S6. Top: Locations of our initial pool of 143 tree-ring chronologies. Chronologies that passed the initial climate sensitivity test (those that were significantly and positively correlated with local spring precipitation and/or significantly and negatively correlated with local spring temperature) are marked in green. Tree-ring records that did not satisfy either criteria are marked in red and were excluded from further analysis. Bottom: Correlation coefficients between the NCEP/NCAR-derived Himalayan jet latitude (HJL) and each of the retained chronologies. Only those 23 chronologies that were significantly correlated ($p < 0.1$) with the HJL target were included as potential predictors in our reconstruction model

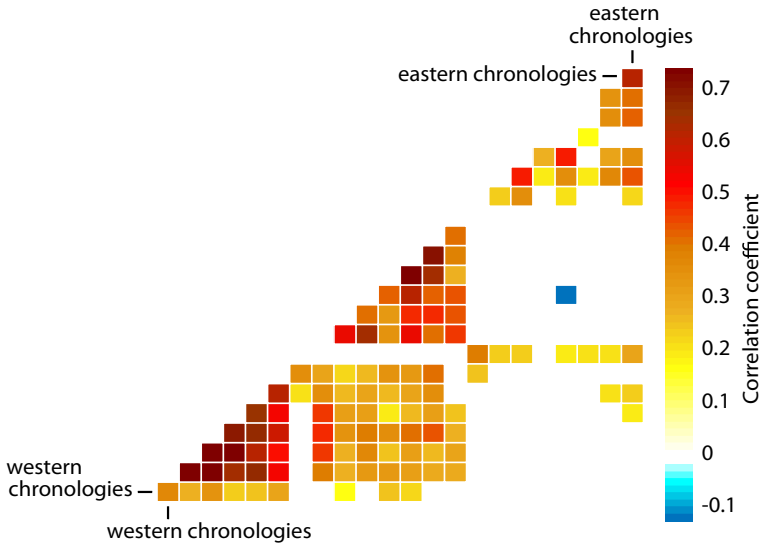

Figure S7. Matrix of inter-chronology correlations for all pairs of 23 tree-ring chronologies used in the Himalayan jet latitude reconstruction. Correlations are calculated for the period of overlap between each pair of chronologies, and only those values significant at 0.1 level are shaded.

Table S1. Metadata of the tree-ring width chronologies used in the Himalayan jet latitude (HJL) reconstruction. These 23 chronologies are sensitive to the same aspects of spring climate that are influenced by the HJL and correlated significantly with the HJL target.

Site code	Species	Site name	Lat (N)	Lon (E)	Elevation (m)	Reference
paki037	PCSM	Sheshan, Pakistan	35.03	71.53	2530	Cook et al., (2013b)
paki020	CDDE	Kalash Valley, Pakistan	35.68	71.63	NaN	PAGES 2k Consortium (2013)
paki021	PIGE	Kalash Valley, Pakistan	35.68	71.63	NaN	PAGES 2k Consortium (2013)
paki022	CDDE	Chitral-Gol NP, Pakistan	35.9	71.73	NaN	PAGES 2k Consortium (2013)
paki023	PIGE	Chitral-Gol NP, Pakistan	35.9	71.73	NaN	PAGES 2k Consortium (2013)
paki040	CDDE	Zairat Chitral, Pakistan	35.35	71.8	NaN	ITRDB
paki027	CDDE	Islam Baiky, Pakistan	35.35	71.93	NaN	PAGES 2k Consortium (2013)
paki032	ABPI	Murree-Ayubia, Pakistan	35.03	73.38	NaN	Cook et al., (2013b)
paki006	JUSP	Pakistan high Cha2	36.33	74.03	3500	Esper et al., (2007)
paki007	JUSP	Pakistan high Cha3	36.33	74.03	3900	Esper et al., (2007)
paki005	JUSP	Pakistan low Cha1	36.33	74.03	2700	Esper et al., (2007)
paki024	PCSM	Chera Gilgit, Pakistan	35.033	74.58	NaN	PAGES 2k Consortium (2013)
paki001	JUSP	Bagrot 1, Pakistan	36.03	74.58	3100	Esper et al., (2007)
paki002	JUSP	Bagrot 2, Pakistan	36.03	74.58	3300	Esper et al., (2007)
paki014	JUSP	Pakistan low Sat1	35.16	75.5	3300	Esper et al., (2007)
indi013	CDDE	Manali, India	32.27	77.17	2000	ITRDB
bhw009	ABPI	Khaptad, Nepal	29.38	81.13	3000	Thapa et al., (2013)
bhw010	PCSM	Khaptad, Nepal	29.4	81.13	2700	Thapa et al., (2015)
bhw023	ABSB	Mustang, Nepal	28.65	83.61	2700	Kharal et al., (2014)
nepa029	TSDU	Langtang, Nepal	28.12	85.27	2670	Cook et al., (2003)
bt005	TSDU	Tshele Pang, Bhutan	27.45	90.15	NaN	Cook et al., (2010)
bt001	TSDU	Gaytsha, Bhutan	27.58	90.65	NaN	Cook et al., (2010)
bt002	TSDU	Naspey, Bhutan	27.66	90.73	NaN	Cook et al., (2010)

Note: ABPI: *Abies pindrow*; ABSB: *Abie spectabilis*; CDDE: *Cedrus Deodara*; JUSP: *Juniperus* spp. PCSM: *Picea smithiana*; PIGE: *Pinus geradiana*; TSDU: *Tsuga dumosa*.